New therapeutic targets in the intrinsic apoptotic pathway in neuroblastoma

Lamers, Fieke

Publication date
2012
Document Version
Final published version

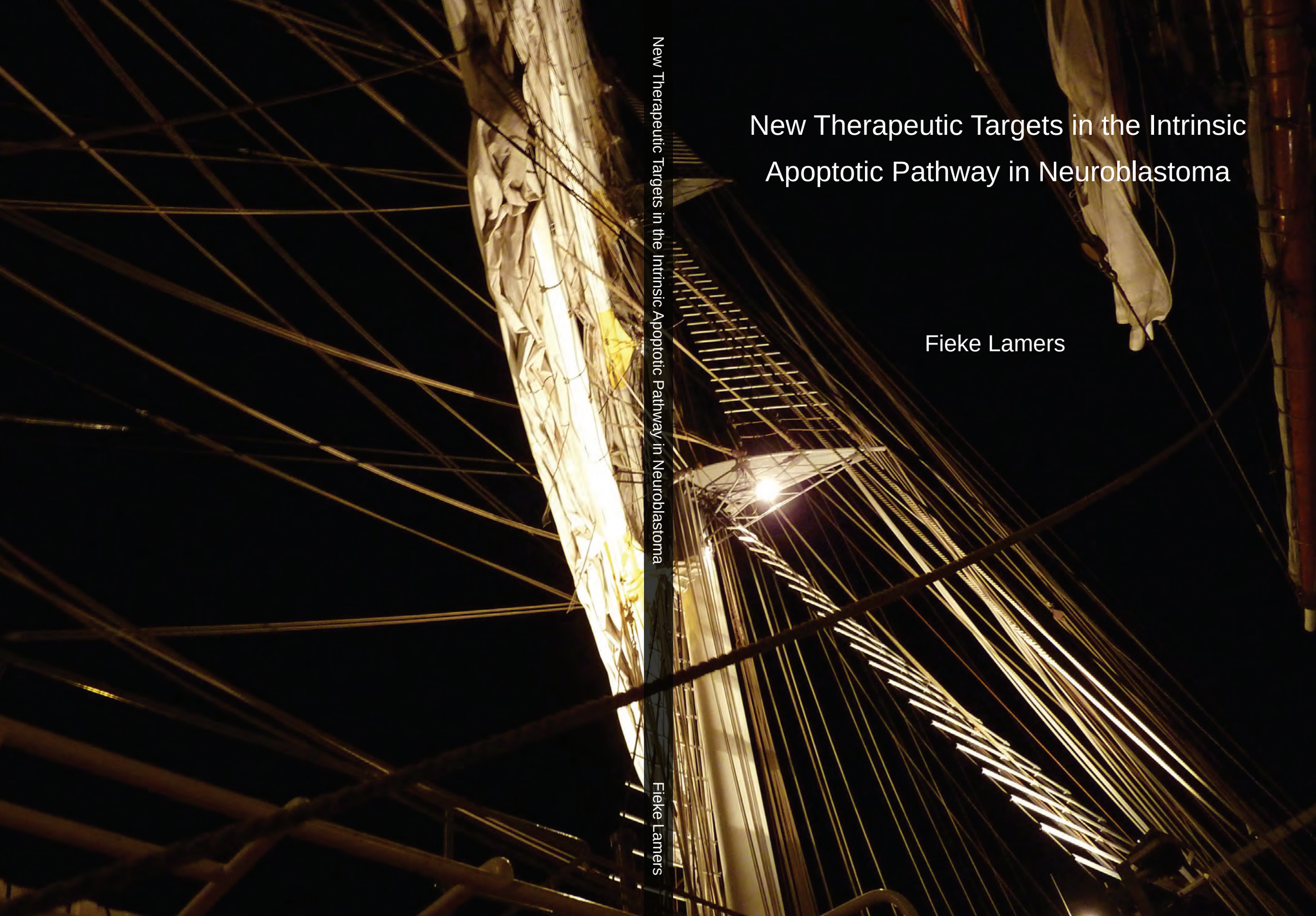

New Therapeutic Targets in the Intrinsic Apoptotic Pathway in Neuroblastoma

Fieke Lamers

New Therapeutic Targets in the Intrinsic Apoptotic Pathway in Neuroblastoma

Fieke Lamers

New Therapeutic Targets in the Intrinsic Apoptotic Pathway in Neuroblastoma

Fieke Lamers

New Therapeutic Targets in the Intrinsic Apoptotic Pathway in Neuroblastoma

The research presented in this thesis was performed at the Department of Oncogenomics at the Academic Medical Center of the University of Amsterdam.

The research presented in this thesis was financially supported by the department of Oncogenomics, the Academic Medical Center Amsterdam, the University of Amsterdam, Top Institute Pharma, KiKa foundation, the Netherlands Cancer Foundation and the Tom Voûte fonds.

Publication of this thesis was financially supported by the department of Oncogenomics, the Academic Medical Center Amsterdam, the Tom Voûte fonds, Millipore, Clean Air and Beun de Ronde.

Layout: Eelco Roos, Department of Clinical Genetics, AMC
Printed by: CPI Wöhrmann Print Service
ISBN: 978-94-6203-040-4

New Therapeutic Targets in the Intrinsic Apoptotic Pathway in Neuroblastoma

ACADEMISCH PROEFSCHRIFT

ter verkrijging van de graad van doctor

aan de Universiteit van Amsterdam

op gezag van de Rector Magnificus

prof.dr. D.C. van den Boom

ten overstaan van een door het college voor promoties

ingestelde commissie,

in het openbaar te verdedigen in de Aula der Universiteit

op vrijdag 15 juni 2012, te 11:00 uur

door

Sophia Gerharda Maria Lamers

geboren te Zwolle

Promotiecommissie:

Promotores:	**Prof.dr. H.N. Caron**
	Prof.dr. R. Versteeg
Co-promotor:	**dr. J.J. Molenaar**
Overige leden:	**Prof.dr. A. Eggert**
	Prof.dr. J.P. Medema
	Prof.dr. D.J. Richel
	Prof.dr. R. Pieters
	Prof.dr. S. Fulda
	Dr. A.C. Verschuur

Faculteit der Geneeskunde

Contents

1

Introduction

1. Neuroblastoma

1.1 Symptoms and diagnosis

Neuroblastoma are tumors that originate from the embryonal precursor cells of the sympathetic nervous system in early childhood. This tumor can arise anywhere throughout the sympathetic nervous system and the tumors are very heterogeneous in site, symptoms and outcome. Most neuroblastoma are localized in the abdomen (65%) of which the adrenal gland is the most common primary site with a prevalence of at least 30% of the tumors, followed by abdominal, thoracic, cervical and pelvic sympathetic ganglia (fig. 1). Neuroblastoma may metastasize to the lymph nodes, bone marrow, bone, liver and skin. Paraspinal located tumors tend to invade the neuronal foramina and can cause compression of the spinal cord. Bone metastases tend to appear in the orbit and therefore periorbital ecchymosis is a classical sign of disseminated neuroblastoma. About half of the patients presents with evidence of metastatic disease, ranging from loco regional spread in lymph nodes to distant metastases. Children with metastases mostly have extensive tumor burden and are very ill. About 5% of the patients are infants with a phenotype of small tumors that metastasize to skin, liver and bone marrow that tend to disappear spontaneously without treatment.[1-4]

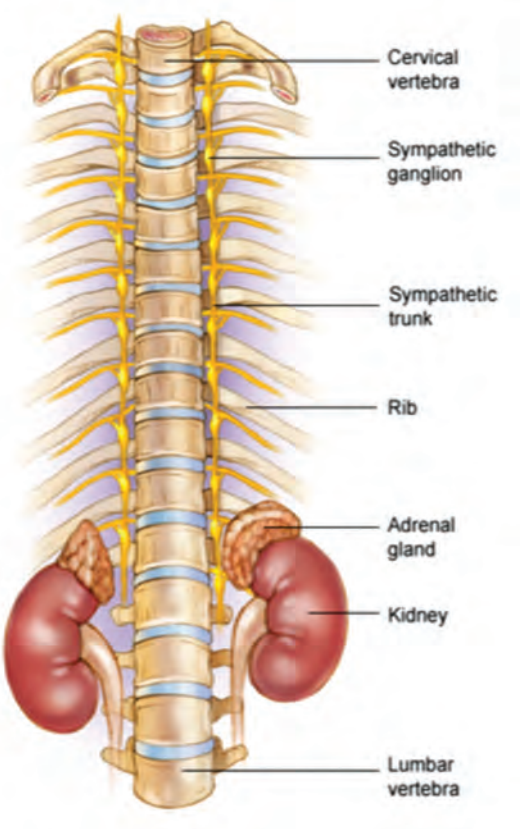

Fig 1. Common regions of primary neuroblastoma localization (www.cancer.net; American Society of Clinical Oncology)

Neuroblastoma diagnosis requires either a positive histological analysis or evidence of neuroblastoma cells in the bone marrow with positive catecholamines in the urine.[1-4] A diagnostic tool is the Metaiodobenzylguanidine (MIBG) scan. MIBG is a neurotransmitter-like substance that can be radioactively labeled with ^{131}I for treatment or ^{123}I for diagnostics. The compound

is actively transported into the cell by the norepinephrine transporter, which is specifically expressed in 90% of the neuroblastoma tumors.[5-8]

1.2 Tumor biology

Neuroblastic tumors typically show a lack of differentiation and therefore histological markers of early developmental lineages can still be seen in the tumor.[1,3,4] The classification of neuroblastic tumors into ganglioneuroma, ganglioneuroblastoma or neuroblastoma is based on the proportion of neural type cells (neuroblasts and ganglion cells) and Schwann type cells. Neuroblastoma are the most undifferentiated and the most aggressive of the neuroblastic tumors. These can be classified as differentiating, poorly differentiated and the most aggressive undifferentiated. Neuroblastoma are composed almost entirely of neuroblasts which appear as small round blue cells. The ganglioneuroblastoma contain neuroblasts with a more mature appearance that are clustered in small foci surrounded by Schwannian stroma. Ganglioneuroma are predominantly composed of Schwann cells with mature ganglion cells.[9]

1.3 Risk stratification

Tumors are staged according to the International Neuroblastoma Staging System (INSS). Stage 1, 2 and 3 represent regional tumors with or without positive lymph nodes. Stage 4 tumors have distant metastases. The specific subgroup of stage 4S tumors is reserved for patients less than 1 year of age with dissemination limited to skin, liver and/or bone marrow.[3] Stage 1-3 neuroblastoma have an excellent prognosis, but the majority of patients with stage 4 tumors die. The word ‘staging’ suggests that each neuroblastoma starts as a stage 1 tumor, which can progress to a high stage tumor. If so, early diagnosis and treatment of neuroblastoma would result in lower incidence of high stage tumors. However, in large population screening programs where young infants were screened for catecholamines in the urine, more children were diagnosed with low stage neuroblastoma but the screening did not have any effect on the incidence of high stage neuroblastoma.[10,11] Only screening in older infants resulted in diagnosis of more neuroblastoma with genetic unfavorable markers. However, this did not result in a significantly decreased mortality either.[12] Therefore, it seems that the different stages of neuroblastoma are in fact different types of neuroblastoma tumors that cannot change into one another.

Risk stratification is based on tumor stage according to the INSS, age of the patient and genetic risk factors such as MYCN amplification and deletion of 1p (fig. 2). In Europe all neuroblastoma and ganglioneuroblastoma are included in the treatment protocols

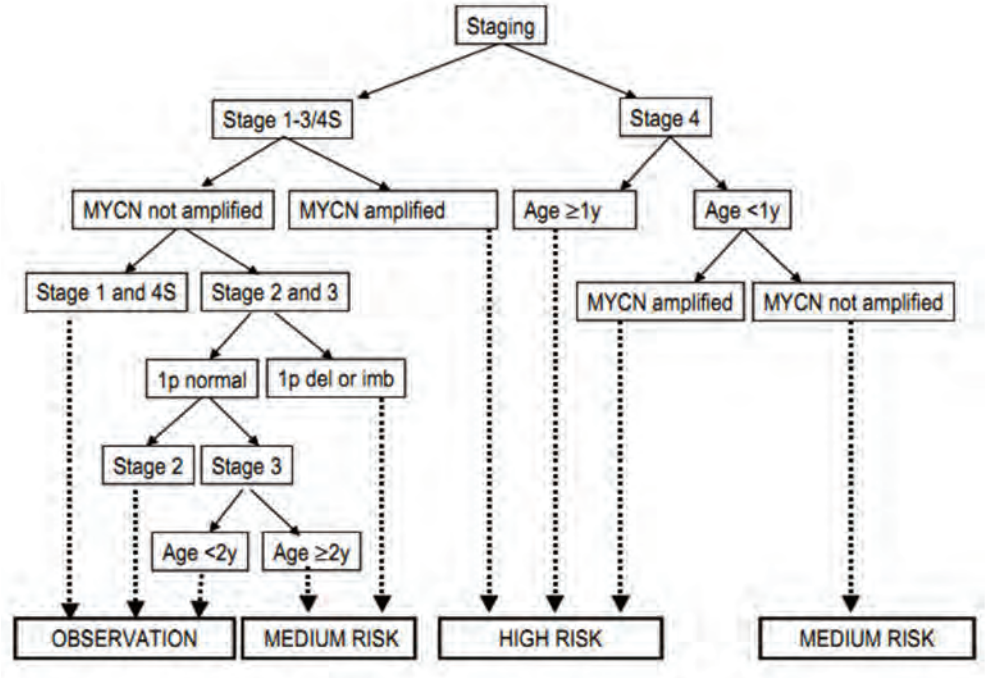

Fig 2. INSS risk stratification according to the German Neuroblastoma Trial, NB2004. Risk stratification is based on the combination of the four markers: tumor stage, patient age at diagnosis, status of MYCN and status of chromosome 1p36. (http://protiv-raka.org/wp-content/uploads/2011/02/protokol_neuroblastoma.pdf)

for malignant neuroblastoma. Ganglioneuroma on the other hand are classified as a benign disease and are not included.[1,3] Recently several high throughput methods have shown additional value in risk stratification. Specifically Comparative Genomic Hybridization adds critical prognostic information to conventional markers and will be included in future treatment stratification.[13] Also the development of Whole Genome Sequencing can give a lot of information about individual tumors and may therefore be an interesting tool for personalized medicine.

1.4 Prognosis and Therapy

Patients with low-risk tumors can be treated by surgery alone and have a very good prognosis. However, patients with high risk disease are treated with intensive chemotherapy, surgery and high-dose myeloablative therapy to eradicate minimal residual disease. Despite this extensive treatment, children with high stage neuroblastoma have a poor prognosis with 35% overall survival. Even though neuroblastoma is a very rare disease with 30 to 40 new patients in the Netherlands

every year, it is still the second cause of cancer related death in children. The Dutch Childhood Oncology Group (DCOG) Neuroblastoma Disease Committee has launched a new treatment protocol in 2007, which is based on the German Pediatric Oncology Group (GPOG) treatment strategy (fig. 3) [14,15]. In the Dutch protocol twice radioactive ^{131}I-MIBG treatment was added up front to the German high risk protocol [6,7]. After initial radiation 3 cycles N5 chemotherapy (cisplatinum, etoposide, vindesine) and 3 cycles N6 chemotherapy (vincristine, dacarbazine, ifosfamide, doxorubicin) are given. Resection is performed if substantial tumor remains after induction therapy. This resection should be attempted after the 4th or 6th chemotherapy cycle. After

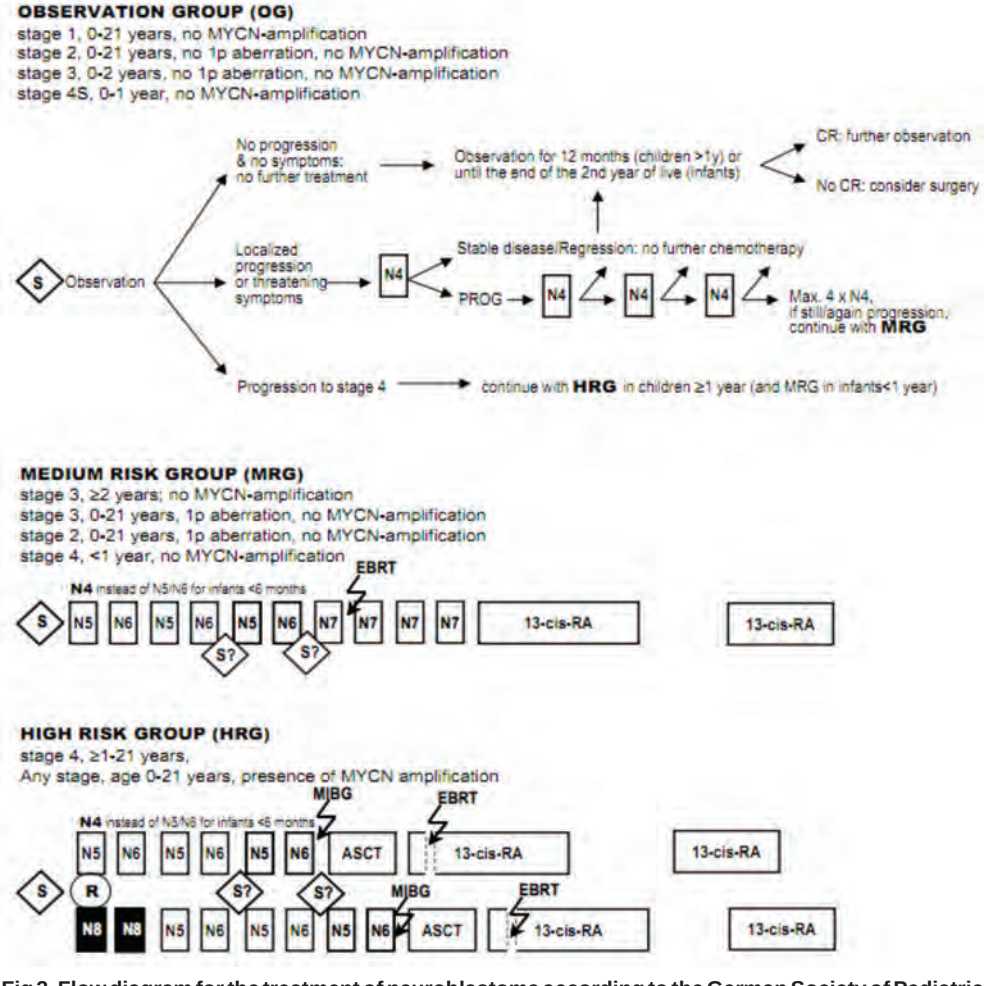

Fig 3. Flow diagram for the treatment of neuroblastoma according to the German Society of Pediatric Oncology and Hematology (GPOH) study NB2004. (S = surgery, R = randomization, N4/5/6/7/8 = chemotherapy cycles, MIBG = MIBG treatment, EBRT = external beam radiation therapy, 13-cis-RA = 13-cis-retinoic acid). (http://protiv-raka.org/wp-content/uploads/2011/02/protokol_neuroblastoma.pdf)

the primary induction therapy and surgery a myeloablative high-dose-chemotherapy with melphalan, etoposide and carboplatin is given, followed by autologous stem cell reinfusion. Finally retinoic acid is given in 6 cycles followed by a short break and 3 more cycles (fig. 3) [14,15].

1.5 Common genetic aberrations

Various types of genetic aberrations occur in neuroblastoma. DNA content aberrations are very frequent and divide neuroblastoma into two categories: near-diploid and hyper-diploid. Hyper-diploid tumors are thought to have defects in mitosis, associated with whole chromosome gains and losses. These tumors tend to be less aggressive. In contrast, more malignant neuroblastoma show chromosomal rearrangements and unbalanced translocations. These tumors maintain their diploid DNA content. Near-diploid as well as hyper-diploid tumors have gains or losses, only in the near-diploid tumors these events concern chromosome arms or regions while hyper-diploid tumors tend to have gains or losses of whole chromosomes.[1]

Gain in neuroblastoma is most frequently found in chromosome 17. The 17q arm is gained in almost all high stage neuroblastoma. Because breakpoints vary, gain from 17q21 to the telomere suggests a dosage effect of several genes in that region.[1,16] One of the candidate tumor driving genes is *BIRC5* (Survivin), which will be discussed in this thesis. Partial loss is most frequently seen in chromosome 1p and 11q. Both are associated with poor prognosis but only 1p deletions are strongly correlated with *MYCN* amplification. For chromosome 1 the Smallest Region of Overlap (SRO) is located at 1p36 in which several potential tumor suppressor genes have been identified. On chromosome 11 the SRO is located around 11q23, but no tumor suppressor genes in this region have been identified yet.[1,2,16]

The chromosome 2p arm also shows frequent gain. This region encompasses *MYCN* and *ALK*, the two best known oncogenes in neuroblastoma. *MYCN* is amplified in 20% of neuroblastoma, which strongly correlates with a bad prognosis. The Myc oncogene family members, *MYC* (c-Myc), *MYCN* and *MYCL*, are transcription factors that are involved in cell growth through protein synthesis, transcriptional regulation of ribosomal RNA processing, cell adhesion and tumor invasion [1-4,17]. The other oncogene on 2p is *ALK* (anaplastic lymphoma kinase), a receptor tyrosine kinase involved in neuronal differentiation. Potentially activating *ALK* mutations located in the kinase domain were recently found in 6-10% of the neuroblastoma. In most cases of familiar neuroblastoma and in a few cases of sporadic neuroblastoma *ALK* was mutated.[18-23] A correlation was found between *ALK* mutations and high stage tumors.[19] Moreover, when *ALK* was also over-expressed or amplified, the correlation

to a poor outcome was stronger.[23]

In addition, the *PHOX2B* homeobox transcription factor, which functions in the differentiation of the sympatho-adrenal lineage, was found to be sporadically mutated.[24] Studies indicate that this mutation can be one of the possible defects in cell maturation and differentiation that may be cancer predisposing.[24,25] The functional consequences are still being studied.

1.6 New neuroblastoma therapies

Until a few years ago the survival of high stage neuroblastoma patients was 20%.The first more specific neuroblastoma targeting compounds are currently implemented in treatment protocols and have started to improve survival rates. The first one is an antibody treatment targeting GD2. Recently, randomized phase 3 clinical trials using the anti-GD2 antibody ch14.18 alternating with cycles of GM-CSF or interleukin-2 showed a significant improvement in 2-year event-free survival in the immunotherapy group.[4,26-29] ^{131}I-MIBG is another neuroblastoma specific therapy that is currently being used for neuroblastoma treatment. It showed to be effective in newly diagnosed, high risk neuroblastoma patients with a large tumor mass and a high uptake and storage of the radio-pharmaceutical [6,7].

Targeted therapies, specific for genes with a role in neuroblastoma tumors, aim at *ALK* and *AURKA*. *AURKA* has been identified as a potential target for therapy. The gene was found to be sporadically amplified in neuroblastoma and showed an extensive over-expression. Moreover, a synthetic lethal-like relation with *MYCN* was found.[30] A clinical phase I/II trial in neuroblastoma patients with the AURKA inhibiting small molecule MLN8237 is ongoing. (http://clinicaltrials.gov) Since the identification of *ALK* as a potential tumor-driving gene in neuroblastoma, ALK targeting compounds have been extensively tested in vitro and in vivo. At this time, Crizotinib (Pfizer) is the most successfully developed compound. Crizotinib is currently in phase I/II clinical trial in neuroblastoma patients [20,31]. Mutated genes are found to be the most interesting genes to target in cancer therapy. However, besides *ALK*, no other genes were frequently mutated in neuroblastoma[32], and it seems that copy number defects are more likely to be of major importance in the development of neuroblastoma. Therefore, the best option in neuroblastoma is to target pathways, and for this thesis we chose the intrinsic apoptotic pathway as a drug target.

2. Apoptosis

The most widely used classification of mammalian cell death recognizes three types: apoptosis, necrosis and autophagy. Apoptosis is programmed cell death, which will be explained in more detail further on in this paragraph. Cells that undergo necrosis are characterized by cell and organelle swelling or rupture of surface membranes with spillage of intracellular contents. The compromise of organellar membranes allows proteolytic enzymes to escape from lysosomes, enter the cytosol, and cause cell demolition. Autophagy is a process in which cells generate energy and metabolites by digesting their own organelles and macromolecules.[33] One of the hallmarks of cancer is the mechanism by which tumors evade apoptosis.[34] This is the focus of this thesis and it will be further explained in the next paragraphs.

2.1 Morphology of apoptosis

Activation of the apoptotic cascade results in shrinking of the cell and its nucleus. Cytoskeletal proteins are cleaved by aspartate-specific proteases, and thereby subcellular components collapse. Other characteristic features are chromatin condensation and nuclear fragmentation. Unlike in necrosis, the plasma membranes remain intact and participate in the process of apoptosis. DNA fragments and other small particles such as organelles and bits of cytoplasm, are enclosed by a membrane to form the so called ‘apoptotic bodies’. These apoptotic bodies are engulfed by macrophages and thereby apoptotic cells are removed from the tissue without an inflammatory response. This is unlike necrosis, where the cell membrane becomes leaky so that its contents are released into the surrounding tissue, causing inflammation.[33]

2.2 Extrinsic apoptosis pathway

An apoptotic signal from outside the cell can induce members of the Tumor Necrosis Factor (TNF) superfamily to bind the receptors on the cell membrane (TRAIL, TNFR, DR4, DR5 and FAS). This initiates the formation of the multiprotein death-inducing signaling complex, which triggers the catalytic activity of CASP8. CASP8 can activate CASP3 directly, resulting in apoptosis, or it can activate the mitochondrial (intrinsic) apoptotic pathway via cleavage of tBID, which eventually also results in CASP3 cleavage and apoptosis (fig. 4). The NF-κB pathway is also regulated by cell death receptors. After activation by the receptors, signaling to IKK proceeds either through the canonical or through the non-canonical pathway, which results in activation of NF-κB and transcription of both pro-death and pro-survival target genes.[33,35-37]

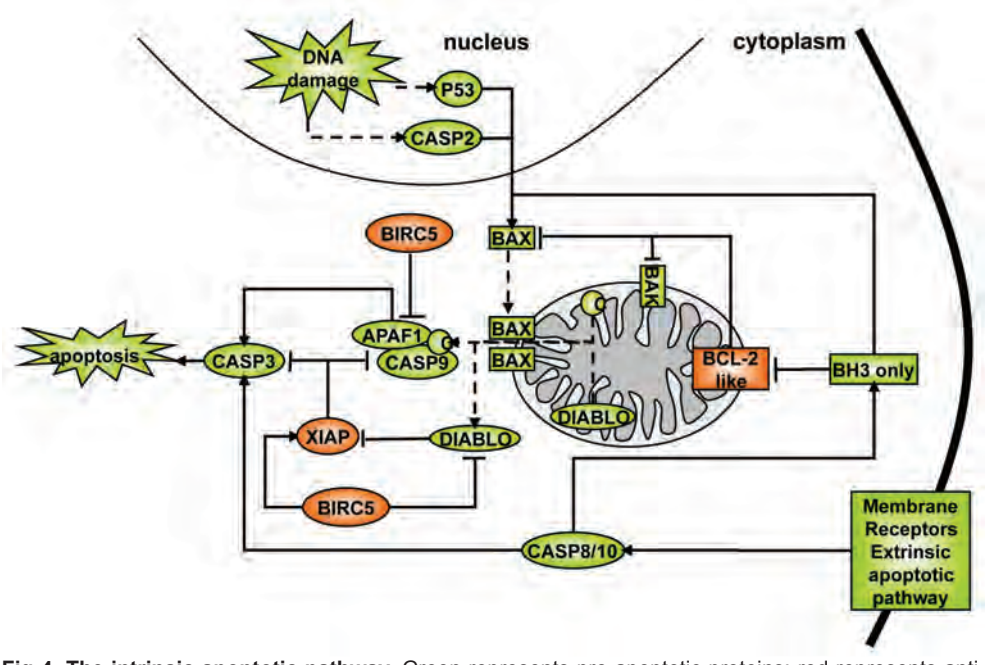

Fig 4. The intrinsic apoptotic pathway. Green represents pro-apoptotic proteins; red represents anti-apoptotic proteins.

2.3 Intrinsic apoptosis pathway

The intrinsic or mitochondrial apoptotic pathway can be activated after an apoptotic signal from inside the cell. Initiators include increased intracellular reactive oxygen species, DNA damage, the unfolded protein response, and the deprivation of growth factors.[33,35] Upon an apoptotic signal the mitochondrial permeability is increased by BAX and BAK. These proteins form complexes with themselves and thereby form pores in the membrane of the mitochondria through which pro-apoptotic proteins such as Cytochrome C and DIABLO are released. When released to the cytoplasm Cytochrome C forms a complex with APAF1 and inactive pro-CASP9. This complex is called the apoptosome. By the formation of this complex CASP9 is activated, which activates cleavage of CASP7 and CASP3. The other protein released from the mitochondria is DIABLO which can bind and antagonize 'Inhibitor of Apoptosis Proteins' (IAPs).[33,35] Release of Cytochrome C and DIABLO from the mitochondria is regulated by the BCL2 family proteins. These proteins have at least one of the four BCL2 homology (BH) domains. Anti-apoptotic members of the BCL2 family include BCL2, MCL1, BCL2L1, BCL2L2, BCL2A1 and BCL2L10 and have all four BH domains. These proteins are located on the outer mitochondrial membrane where they bind to BAX and BAK (both multi-domain members of the BCL2 family),

resulting in inhibition of pore formation and thereby preventing the release of caspase activating proteins from the mitochondria into the cytosol. There are two types of pro-apoptotic members of the BCL2 family, also called BH3-only proteins. One set of proteins (BBC3, BCL2L11 and BID) can either induce BAX and BAK or bind to the anti-apoptotic BCL2 family members and thereby inhibit them. The other set of proteins (PMAIP1, BAD, BIK, HRK, BMF and BCL2L14) can only inhibit the anti-apoptotic BCL2 family members.[33,35,38]

Another important group of apoptosis inhibitors are the IAPs, defined by the presence of a baculovirus IAP repeat (BIR) protein domain.[39] BIRC2 and BIRC3 can suppress TNFα stimulated cell death by preventing formation of the TNFR1 pro-apoptotic signaling complex. They can also regulate the NF-κB pathway by ubiquitination of NF-κB-inducing kinase (NIK).[40,41] BIRC6 can induce ubiquitination and degradation of DIABLO.[42-44] BIRC5 can bind and inhibit DIABLO functionally by blocking its BIR-domain or it can bind and stabilize XIAP, another IAP. This results in inhibition of caspase activation and apoptosis.[45-47] In addition BIRC5 has a function in the nucleus. BIRC5 was found to be a chromosomal passenger protein that forms a complex with CDCA8 (Borealin), AURKB (Aurora Kinase B) and INCENP by which it regulates microtubule dynamics at the kinetochores. If the microtubule-kinetochore dynamics are disturbed, mitotic catastrophe occurs. This results in P53 and CASP2 activation after which the mitochondrial apoptotic pathway is activated (fig. 4) [48-52].

2.4 Apoptosis and neuroblastoma

The apoptotic pathway is often deregulated in neuroblastoma. Mutations of the established tumor suppressor *TP53* do occur in tumors that relapse after treatment. However, *TP53* mutations are very rare in primary neuroblastoma.[1,2,53] TP53 is shown to be functionally inactivated through sequestration in the cytoplasm in undifferentiated neuroblastoma.[1,2] Also, the p53/MDM2/p14^{ARF} pathway is often inactivated by *MDM2* amplification or p14^{ARF} inactivation specifically in *MYCN* amplified cells. MDM2-p53 antagonist Nutlin-3 resulted in TP53-mediated growth arrest and apoptosis in these cells.[54,55] Recent studies also showed convincingly that miR-380-5p suppresses *TP53* and that it is associated with a poor outcome in patients with *MYCN* amplification. Treatment with miR-380-5p antagonist induced p53-dependent cell death in neuroblastoma cells and decreased tumor growth in vivo.[56,57]

CASP8 is hypermethylated and thereby inactive in some neuroblastoma resulting in an inactive extrinsic apoptotic pathway.[1,16] *BIRC5* is highly expressed in neuroblastoma, which correlates to a bad prognosis.[58-61] Also, the expression of

BCL2 is often increased in neuroblastoma tumors and cell lines.[62,63] BIRC5 and BCL2 are both found to be good potential targets for therapy for which compounds are clinically available.[55,58-65] However, no consistent genomic aberrations in the intrinsic apoptotic pathway in neuroblastoma are known.

3. Drug development

3.1 Mechanism of currently used cytostatics

Neuroblastoma are the second cause of cancer related death in children. In children that survive, over 70% suffer from severe side effects of the therapy. Currently used cytostatics in neuroblastoma treatment are aspecific compounds with severe toxic effects on normal cells as well [1,3,14]. Because of the lack of efficacy and the extended toxicity it is necessary to find more specific targeted compounds which will affect neuroblastoma tumor cells and leave normal cells unharmed. We follow a standardized preclinical procedure that will be further clarified in the coming paragraphs (fig. 5).

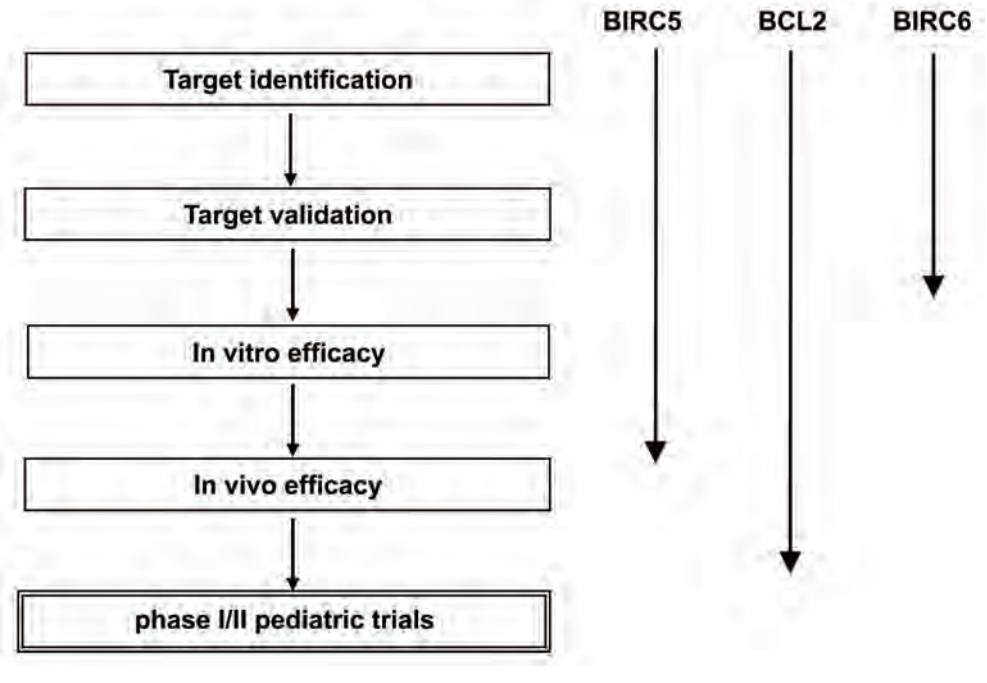

Fig 5. Flow diagram of the preclinical steps in drug development research. The projects of this thesis are presented on the right with arrows.

3.2 Target identification

Target gene selection is based on identification of aberrations in DNA and mRNA expression in neuroblastoma tumor samples. In addition correlations of expression levels and DNA aberrations to clinical properties are used as selection criteria. For that purpose, a large series of neuroblastoma samples were analyzed using various high throughput assays. To analyze these high-throughput data Jan Koster and colleagues have designed the bioinformatic platform R2. Affymetrix mRNA profiles of 143 neuroblastoma and 24 neuroblastoma cell lines, array CGH and SNP array data of 110 neuroblastoma tumors and 24 cell lines have been generated in our lab and can be analyzed by R2.[66-68] Moreover, we can compare our data with public available profiles of over 25,000 tumor samples of 50 different tumor types. R2 facilitates an integrated analysis and allows identification of important regulatory pathways. This platform has been used extensively for this thesis. Recently we sequenced the complete genomes of 87 primary neuroblastoma.[32,69]

3.3 Target validation

The next step in targeted drug development is the validation of a gene or pathway as drug target in neuroblastoma cell line systems. We have used a panel of 24 neuroblastoma cell lines and 6 primary neuroblastoma cultures with diverse genetic properties such as *MYCN* amplification and *ALK* mutations.[70-72] In these models the expression levels of potential drug targets are manipulated. Silencing is mainly performed using the RNA interference technique. We used plasmids that express short hairpin RNA molecules combined with a lentiviral transfection system (Sigma TRC). In addition we use a stable doxycycline inducible lentiviral system if knock down of a certain gene is studied in more detail [73]. Over-expression analysis is studied with a lentiviral stable inducible plasmid with a Tet operator system (Invitrogen). If knock-down or over-expression of a certain target gene leads to a significant phenotype like apoptosis or differentiation, further analysis is performed using targeted compounds.

3.4 In vitro and in vivo compound efficacy

Preferably, targeted compounds are selected that have already passed Phase I/II clinical trials in adults. Phase I trials in children are difficult to establish and pharmaceutical companies are reluctant to test targeted compounds solely for development in children. The core questions in this phase of research are whether this compound induces apoptosis at low concentrations and whether apoptosis is caused by specifically interfering with the gene or protein of interest. These findings can also lead to the identification of biomarkers of efficacy that can be used in further

clinical development of the compound in neuroblastoma. We test if the compound works specifically against the tumor and not against normal tissue by using non-malignant fibroblasts. Finally we test if the compound works synergistically with the currently used cytostatics. After this, the compound is considered for testing in mouse models. For this we use a neuroblastoma xenograft model, in which a classical cell line or primary culture of neuroblastoma tumors is implanted subcutaneously in both flanks of the mice. Serial transplantation improves the reproducibility of the model. Mice are treated with the compound of interest and tumor growth is measured. If a compound is found to be effective in vitro and in vivo and the mechanism of action is validated, the next step is to test the compound in Phase I/II clinical trial.

4. Drug targets in the intrinsic apoptotic pathway

In this thesis, we identified and validated two targets in the intrinsic apoptosis pathway that can be inhibited by new compounds that are currently in Phase I/II clinical trial in adults.

In chapter 2 and 3 we identified BIRC5 as a potential target for therapy. We found BIRC5 to be highly expressed in neuroblastoma compared to normal tissues and other kinds of cancer and this high expression correlated to a bad prognosis. Validation of BIRC5 as a target revealed that its function in the chromosomal passenger complex is of major importance in neuroblastoma cells and knock down of BIRC5 by shRNA induced apoptosis via mitotic catastrophe. We validated the efficacy of a novel small molecule BIRC5 inhibitor, YM155. YM155 inhibited BIRC5 specifically and induced apoptosis in most neuroblastoma cell lines. However a subset of cell lines was resistant to YM155, which was caused by high ABCB1 expression. This ‘Multi Drug Resistance pump’ can be inhibited by cyclosporine or ABCB1 shRNA prior to treatment with YM155, which sensitized the resistant cell lines. We concluded that YM155 is an effective BIRC5 inhibitor in vitro.

Chapter 4 describes BCL2 as a new target for neuroblastoma therapy. Affymetrix micro-array expression data revealed that BCL2 is highly expressed in neuroblastoma tumors. Most neuroblastoma cell lines however, did not have this high expression except for KCNR and SJNB12, which we both used as a model. These cell lines were found to undergo massive apoptosis after BCL2 knockdown by shRNA or inhibition by ABT263, a small molecule BCL2 inhibitor. ABT263 also had an anti-tumor effect in a neuroblastoma mouse model. Combination assays of ABT263 with cytostatics that are regularly used in neuroblastoma patients revealed strong synergistic effects.

Validation of BIRC6 in chapter 5 gave us potential future opportunities for therapy, since knockdown of this gene resulted in increased DIABLO protein levels, inducing apoptosis. However, compounds directly targeting BIRC6 are currently not yet available.
Both YM155 and ABT263 are currently under evaluation for Phase I/II clinical trial in neuroblastoma patients with a relapse.

1

References

1. Brodeur, G.M., Neuroblastoma: Biological insights into a clinical enigma. Nature Reviews Cancer, 2003; 3: 203-216.
2. Janoueix-Lerosey, I., Schleiermacher, G., and Delattre, O., Molecular pathogenesis of peripheral neuroblastic tumors. Oncogene, 2010; 29: 1566-1579.
3. Maris, J.M., Hogarty, M.D., Bagatell, R., and Cohn, S.L., Neuroblastoma. Lancet, 2007; 369: 2106-2120.
4. Maris, J.M., Medical Progress: Recent Advances in Neuroblastoma. New England Journal of Medicine, 2010; 362: 2202-2211.
5. Boubaker, A. and Delaloye, A.B., Nuclear medicine procedures and neuroblastoma in childhood - Their value in the diagnosis, staging and assessment of response to therapy. Quarterly Journal of Nuclear Medicine, 2003; 47: 31-40.
6. de Kraker, J., Hoefnagel, K.A., Verschuur, A.C., van Eck, B., van Santen, H.M., and Caron, H.N., Iodine-131-metaiodobenzylguanidine as initial induction therapy in stage 4 neuroblastoma patients over 1 year of age. European Journal of Cancer, 2008; 44: 551-556.
7. Dubois, S.G. and Matthay, K.K., Radiolabeled metaiodobenzylguanidine for the treatment of neuroblastoma. Nuclear Medicine and Biology, 2008; 35: S35-S48.
8. Taggart, D., Dubois, S., and Matthay, K.K., Radiolabeled metaiodobenzylguanidine for imaging and therapy of neuroblastoma. Quarterly Journal of Nuclear Medicine and Molecular Imaging, 2008; 52: 403-418.
9. Shimada, H., Ambros, I.M., Dehner, L.P., Hata, J., Joshi, V.V., and Roald, B., Terminology and morphologic criteria of neuroblastic tumors - Recommendations by the International Neuroblastoma Pathology Committee. Cancer, 1999; 86: 349-363.
10. Kaneko, Y., Kanda, N., Maseki, N., Nakachi, K., Takeda, T., Okabe, I. et al, Current Urinary Mass-Screening for Catecholamine Metabolites at 6 Months of Age May be Detecting Only A Small Portion of High-Risk Neuroblastomas - A Chromosome and N-Myc Amplification Study. Journal of Clinical Oncology, 1990; 8: 2005-2013.
11. Murphy, S.B., Cohn, S.L., Craft, A.W., Woods, W.G., Sawada, T., Castleberry, R.P. et al, Do Children Benefit from Mass-Screening for Neuroblastoma - Consensus Statement from the American-Cancer-Society Workshop on Neuroblastoma Screening. Lancet, 1991; 337: 344-346.
12. Kerbl, R., Urban, C.E., Ambros, I.M., Dornbusch, H.J., Schwinger, W., Lackner, H. et al, Neuroblastoma mass screening in late infancy: Insights into the biology of neuroblastic tumors. Journal of Clinical Oncology, 2003; 21: 4228-4234.
13. Janoueix-Lerosey, I., Schleiermacher, G., Michels, E., Mosseri, V., Ribeiro, A., Lequin, D. et al, Overall Genomic Pattern Is a Predictor of Outcome in Neuroblastoma. Journal of Clinical Oncology, 2009; 27: 1026-1033.
14. Berthold, F. and Hero, B., Neuroblastoma - Current drug therapy recommendations as part of the total treatment approach. Drugs, 2000; 59: 1261-1277.
15. Berthold, F., Hero, B., Kremens, B., Handgretinger, R., Henze, G., Schilling, F.H. et al, Long-term results and risk profiles of patients in five consecutive trials (1979-1997) with stage 4 neuroblastoma over 1 year of age. Cancer Letters, 2003; 197: 11-17.
16. van Noesel, M.M. and Versteeg, R., Pediatric neuroblastomas: genetic and epigenetic 'Danse Macabre'. Gene, 2004; 325: 1-15.
17. Meyer, N. and Penn, L.Z., MYC - TIMELINE Reflecting on 25 years with MYC. Nature Reviews Cancer, 2008; 8: 976-990.
18. Chen, Y.Y., Takita, J., Choi, Y.L., Kato, M., Ohira, M., Sanada, M. et al, Oncogenic mutations of ALK kinase in neuroblastoma. Nature, 2008; 455: 971-U56.
19. De Brouwer, S., De Preter, K., Kumps, C., Zabrocki, P., Porcu, M., Westerhout, E.M. et al, Meta-analysis of Neuroblastomas Reveals a Skewed ALK Mutation Spectrum in Tumors with MYCN Amplification. Clinical Cancer Research, 2010; 16: 4353-4362.
20. George, R.E., Sanda, T., Hanna, M., Frohling, S., Luther, W., Zhang, J.M. et al, Activating mutations in ALK provide a therapeutic target in neuroblastoma. Nature, 2008; 455: 975-978.
21. Janoueix-Lerosey, I., Lequin, D., Brugieres, L., Ribeiro, A., de Pontual, L., Combaret, V. et al, Somatic and germline activating mutations of the ALK kinase receptor in neuroblastoma. Nature, 2008; 455: 967-U51.
22. Mosse, Y.P., Laudenslager, M., Longo, L., Cole, K.A., Wood, A., Attiyeh, E.F. et al, Identification of

ALK as a major familial neuroblastoma predisposition gene. Nature, 2008; 455: 930-U22.
23. Schulte, J.H., Bachmann, H.S., Brockmeyer, B., DePreter, K., Oberthur, A., Ackermann, S. et al, High ALK Receptor Tyrosine Kinase Expression Supersedes ALK Mutation as a Determining Factor of an Unfavorable Phenotype in Primary Neuroblastoma. Clinical Cancer Research, 2011; 17: 5082-5092.
24. van Limpt, V., Schramm, A., Lakeman, A., van Sluis, P., Chan, A., van Noesel, M. et al, The Phox2B homeobox gene is mutated in sporadic neuroblastomas. Oncogene, 2004; 23: 9280-9288.
25. Raabe, E.H., Laudenslager, M., Winter, C., Wasserman, N., Cole, K., LaQuaglia, M. et al, Prevalence and functional consequence of PHOX2B mutations in neuroblastoma. Oncogene, 2008; 27: 469-476.
26. Gilman, A.L., Ozkaynak, M.F., Matthay, K.K., Krailo, M., Yu, A.L., Gan, J. et al, Phase I Study of ch14.18 With Granulocyte-Macrophage Colony-Stimulating Factor and Interleukin-2 in Children With Neuroblastoma After Autologous Bone Marrow Transplantation or Stem-Cell Rescue: A Report From the Children's Oncology Group. Journal of Clinical Oncology, 2009; 27: 85-91.
27. Simon, T., Hero, B., Faldum, A., Handgretinger, R., Schrappe, M., Niethammer, D. et al, Consolidation treatment with chimeric anti-GD2-antibody ch14.18 in children older than 1 year with metastatic neuroblastoma. Journal of Clinical Oncology, 2004; 22: 3549-3557.
28. Yamane, B.H., Hank, J.A., Albertini, M.R., and Sondel, P.M., The development of antibody-IL-2 based immunotherapy with hu14.18-IL2 (EMD-273063) in melanoma and neuroblastoma. Expert Opinion on Investigational Drugs, 2009; 18: 991-1000.
29. Yu, A.L., Gilman, A.L., Ozkaynak, M.F., London, W.B., Kreissman, S.G., Chen, H.X. et al, Anti-GD2 Antibody with GM-CSF, Interleukin-2, and Isotretinoin for Neuroblastoma. New England Journal of Medicine, 2010; 363: 1324-1334.
30. Otto, T., Horn, S., Brockmann, M., Eilers, U., Schuttrumpf, L., Popov, N. et al, Stabilization of N-Myc Is a Critical Function of Aurora A in Human Neuroblastoma. Cancer Cell, 2009; 15: 67-78.
31. Ardini, E., Magnaghi, P., Orsini, P., Galvani, A., and Menichincheri, M., Anaplastic Lymphoma Kinase: Role in specific tumours, and development of small molecule inhibitors for cancer therapy. Cancer Letters, 2010; 299: 81-94.
32. Molenaar, J.J., Koster, J., Zwijnenburg, D.A., van Sluis, P., Valentijn, L.J., van der Ploeg, I. et al, Whole genome sequencing of neuroblastoma identifies defects in neuritogenesis genes. 2012. Nature . Ref Type: In Press
33. Hotchkiss, R.S., Strasser, A., Mcdunn, J.E., and Swanson, P.E., Mechanisms of Disease Cell Death. New England Journal of Medicine, 2009; 361: 1570-1583.
34. Hanahan, D. and Weinberg, R.A., Hallmarks of Cancer: The Next Generation. Cell, 2011; 144: 646-674.
35. Danial, N.N. and Korsmeyer, S.J., Cell death: Critical control points. Cell, 2004; 116: 205-219.
36. Hayden, M.S. and Ghosh, S., Shared principles in NF-kappaB signaling. Cell, 2008; 132: 344-362.
37. Kasperczyk, H., La Ferla-Bruhl, K., Westhoff, M.A., Behrend, L., Zwacka, R.M., Debatin, K.M. et al, Betulinic acid as new activator of NF-kappa B: molecular mechanisms and implications for cancer therapy. Oncogene, 2005; 24: 6945-6956.
38. Yip, K.W. and Reed, J.C., Bcl-2 family proteins and cancer. Oncogene, 2008; 27: 6398-6406.
39. LaCasse, E.C., Mahoney, D.J., Cheung, H.H., Plenchette, S., Baird, S., and Korneluk, R.G., IAP-targeted therapies for cancer. Oncogene, 2008; 27: 6252-6275.
40. Varfolomeev, E., Blankenship, J.W., Wayson, S.M., Fedorova, A.V., Kayagaki, N., Garg, P. et al, IAP antagonists induce autoubiquitination of c-IAPs, NF-kappa B activation, and TNF alpha-dependent apoptosis. Cell, 2007; 131: 669-681.
41. Fulda, S., Inhibitor of Apoptosis (IAP) Proteins: Novel Insights into the Cancer-Relevant Targets for Cell Death Induction. Acs Chemical Biology, 2009; 4: 499-501.
42. Hao, Y.Y., Sekine, K., Kawabata, A., Nakamura, H., Ishioka, T., Ohata, H. et al, Apollon ubiquitinates SMAC and caspase-9, and has an essential cytoprotection function. Nature Cell Biology, 2004; 6: 849-860.
43. Martin, S.J., An Apollon vista of death and destruction. Nature Cell Biology, 2004; 6: 804-806.
44. Qiu, X.B. and Goldberg, A.L., The membrane-associated inhibitor of apoptosis protein, BRUCE/Apollon, antagonizes both the precursor and mature forms of Smac and caspase-9. Journal of Biological Chemistry, 2005; 280: 174-182.
45. Dohi, T., Okada, K., Xia, F., Wilford, C.E., Samuel, T., Welsh, K. et al, An IAP-IAP complex inhibits apoptosis. Journal of Biological Chemistry, 2004; 279: 34087-34090.

46. Song, Z.Y., Yao, X.B., and Wu, M., Direct interaction between survivin and Smac/DIABLO is essential for the anti-apoptotic activity of survivin during taxol-induced apoptosis. Journal of Biological Chemistry, 2003; 278: 23130-23140.
47. Zangemeister-Wittke, U. and Simon, H.U., An IAP in action - The multiple roles of survivin in differentiation, immunity and malignancy. Cell Cycle, 2004; 3: 1121-1123.
48. Castedo, M., Perfettini, J.L., Roumie, T., Andreau, K., Medema, R., and Kroemer, G., Cell death by mitotic catastrophe: a molecular definition. Oncogene, 2004; 23: 2825-2837.
49. Castedo, M., Perfettini, J.L., Roumier, T., Valent, A., Raslova, H., Yakushijin, K. et al, Mitotic catastrophe constitutes a special case of apoptosis whose suppression entails aneuploidy. Oncogene, 2004; 23: 4362-4370.
50. Lens, S.M.A., Wolthuis, R.M.F., Klompmaker, R., Kauw, J., Agami, R., Brummelkamp, T. et al, Survivin is required for a sustained spindle checkpoint arrest in response to lack of tension. Embo Journal, 2003; 22: 2934-2947.
51. Lens, S.M.A., Rodriguez, J.A., Vader, G., Span, S.W., Giaccone, G., and Medema, R.H., Uncoupling the central spindle-associated function of the chromosomal passenger complex from its role at centromeres. Molecular Biology of the Cell, 2006; 17: 1897-1909.
52. Ruchaud, S., Carmena, M., and Earnshaw, W.C., The chromosomal passenger complex: One for all and all for one. Cell, 2007; 131: 230-231.
53. Rausch, T., Jones, D.T., Zapatka, M., Stutz, A.M., Zichner, T., Weischenfeldt, J. et al, Genome Sequencing of Pediatric Medulloblastoma Links Catastrophic DNA Rearrangements with TP53 Mutations. Cell, 2012; 148: 59-71.
54. Van Maerken, T., Speleman, F., Vermeulen, J., Lambertz, I., De Clercq, S., De Smet, E. et al, Small-molecule MDM2 antagonists as a new therapy concept for neuroblastoma. Cancer Research, 2006; 66: 9646-9655.
55. Gamble, L.D., Kees, U.R., Tweddle, D.A., and Lunec, J., MYCN sensitizes neuroblastoma to the MDM2-p53 antagonists Nutlin-3 and MI-63. Oncogene, 2011.
56. Eggert, A. and Schulte, J.H., A small kiss of death for cancer. Nature Medicine, 2010; 16: 1079-1081.
57. Swarbrick, A., Woods, S.L., Shaw, A., Balakrishnan, A., Phua, Y., Nguyen, A. et al, miR-380-5p represses p53 to control cellular survival and is associated with poor outcome in MYCN-amplified neuroblastoma. Nature Medicine, 2010; 16: 1134-U113.
58. Adida, C., Berrebi, D., Peuchmaur, M., Reyes-Mugica, M., and Altieri, D.C., Anti-apoptosis gene, survivin, and prognosis of neuroblastoma. Lancet, 1998; 351: 882-883.
59. Islam, A., Kageyama, H., Takada, N., Kawamato, T., Takayasu, H., Isogai, E. et al, High expression of Survivin, mapped to 17q25, is significantly associated with poor prognostic factors and promotes cell survival in human neuroblastoma. Oncogene, 2000; 19: 617-623.
60. Lamers, F., Schild, L., Koster, J., Versteeg, R., Caron, H., and Molenaar, J., Targeted BIRC5 silencing using YM155 causes cell death in neuroblastoma cells with low ABCB1 expression. European Journal of Cancer, 2011.
61. Lamers, F., van der Ploeg, I., Schild, L., Ebus, M.E., Koster, J., Hansen, B.R. et al, Knockdown of Survivin (BIRC5) causes Apoptosis in Neuroblastoma via Mitotic Catastrophe. Endocrine Related Cancer, 2011;18(6):657-68
62. Goldsmith, K.C. and Hogarty, M.D., Targeting programmed cell death pathways with experimental therapeutics: opportunities in high-risk neuroblastoma. Cancer Letters, 2005; 228: 133-141.
63. Goldsmith, K.C., Lestini, B.J., Gross, M., Ip, L., Bhumbla, A., Zhang, X. et al, BH3 response profiles from neuroblastoma mitochondria predict activity of small molecule Bcl-2 family antagonists. Cell Death and Differentiation, 2010; 17: 872-882.
64. Fulda, S. and Debatin, K.M., Apoptosis pathways in neuroblastoma therapy. Cancer Letters, 2003; 197: 131-135.
65. Lamers, F., Schild, L., den Hartog, I.J.M., Ebus, M.E., Westerhout, E.M., Ora I. et al, Targeted BCL2 inhibition effectively inhibits Neuroblastoma tumor growth. European Journal of Cancer. 2012, In Press
66. Garman, K.S., Nevins, J.R., and Potti, A., Genomic strategies for personalized cancer therapy. Human Molecular Genetics, 2007; 16: R226-R232.
67. Pinkel, D. and Albertson, D.G., Array comparative genomic hybridization and its applications in cancer. Nature Genetics, 2005; 37: S11-S17.
68. Quackenbush, J., Current concepts - Microarray analysis and tumor classification. New England

Journal of Medicine, 2006; 354: 2463-2472.
69. Meyerson, M., Gabriel, S., and Getz, G., Advances in understanding cancer genomes through second-generation sequencing. Nature Reviews Genetics, 2010; 11: 685-696.
70. Molenaar, J.J., Ebus, M.E., Koster, J., van Sluis, P., van Noesel, C.J.M., Versteeg, R. et al, Cyclin D1 and CDK4 activity contribute to the undifferentiated phenotype in neuroblastoma. Cancer Research, 2008; 68: 2599-2609.
71. Molenaar, J.J., Ebus, M.E., Geerts, D., Koster, J., Lamers, F., Valentijn, L.J. et al, Inactivation of CDK2 is synthetically lethal to MYCN over-expressing cancer cells. Proceedings of the National Academy of Sciences of the United States of America, 2009; 106: 12968-12973.
72. Morozova, O., Vojvodic, M., Grinshtein, N., Hansford, L.M., Blakely, K.M., Maslova, A. et al, System-Level Analysis of Neuroblastoma Tumor-Initiating Cells Implicates AURKB as a Novel Drug Target for Neuroblastoma. Clinical Cancer Research, 2010; 16: 4572-4582.
73. van de Wetering, M., Oving, I., Muncan, V., Fong, M.T.P., Brantjes, H., van Leenen, D. et al, Specific inhibition of gene expression using a stably integrated, inducible small-interfering-RNA vector. Embo Reports, 2003; 4: 609-615.

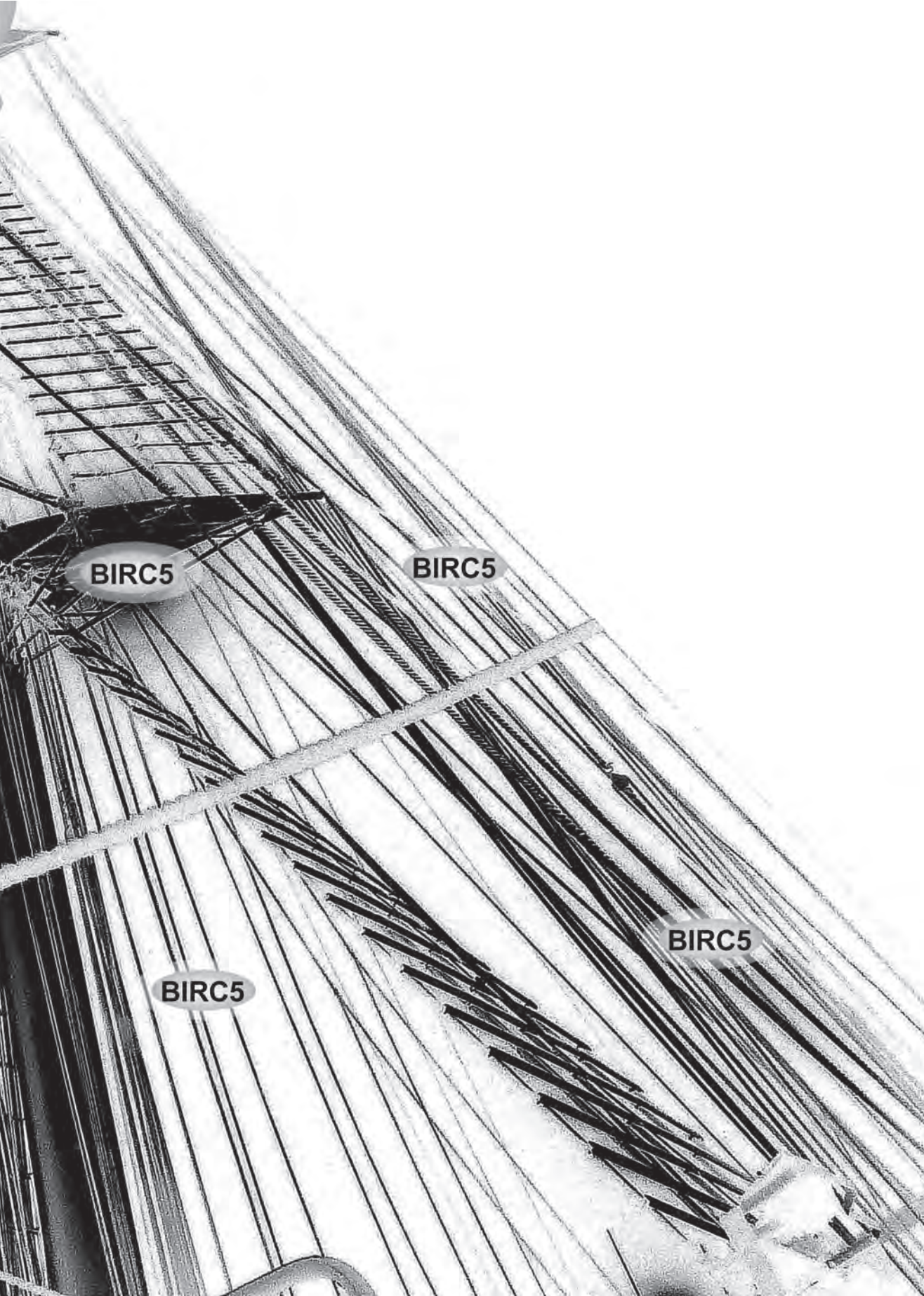
BIRC5
BIRC5
BIRC5
BIRC5

2

Knockdown of Survivin (BIRC5) Causes Apoptosis in Neuroblastoma via Mitotic Catastrophe

Knockdown of Survivin (BIRC5) Causes Apoptosis in Neuroblastoma via Mitotic Catastrophe

2

Fieke Lamers MSc[1], Ida van der Ploeg[1], Linda Schild[1], Marli E. Ebus[1], Jan Koster, PhD[1], Bo R. Hansen, PhD[2], Troels Koch, PhD[2], Rogier Versteeg PhD[1], Huib N. Caron PhD, MD[3], Jan J. Molenaar PhD, MD[1, 3]

[1] Department of Oncogenomics, Academic Medical Center, University of Amsterdam, Meibergdreef 15, PO box 22700, 1105 AZ Amsterdam, The Netherlands. [2] Santaris Pharma A/S, Kogle Allé 6, DK-2970 Hørsholm, Denmark. [3] Department of Pediatric Oncology, Emma Kinderziekenhuis, Academic Medical Center, University of Amsterdam, the Netherlands

Abstract

BIRC5 (Survivin) is one of the genes located on chromosome arm 17q in the region that is often gained in neuroblastoma. BIRC5 is a protein in the intrinsic apoptotic pathway that interacts with XIAP and DIABLO leading to CASP3 and CASP9 inactivation. BIRC5 is also involved in stabilizing the microtubule-kinetochore dynamics. Based on Affymetrix mRNA expression data, we here show that *BIRC5* expression is strongly up-regulated in neuroblastoma compared to normal tissues, adult malignancies and non malignant fetal adrenal neuroblasts. The over-expression of *BIRC5* correlates with an unfavorable prognosis independent of the presence of 17q gain. Silencing of *BIRC5* in neuroblastoma cell lines by various antisense molecules resulted in massive apoptosis as measured by PARP cleavage and FACS analysis. As both the intrinsic apoptotic pathway and the chromosomal passenger complex can be therapeutically targeted, we investigated in which of them BIRC5 exerted its essential anti-apoptotic role. Immunofluorescence analysis of neuroblastoma cells after BIRC5 silencing showed formation of multinucleated cells indicating mitotic catastrophe, which leads to apoptosis via TP53 and CASP2. We show that BIRC5 silencing indeed resulted in activation of TP53 and we could rescue apoptosis by CASP2 inhibition. We conclude that BIRC5 stabilizes the microtubules in the chromosomal passenger complex in neuroblastoma and that the apoptotic response results from mitotic catastrophe, which makes BIRC5 an interesting target for therapy.

Introduction

Neuroblastoma are pediatric tumors that originate from the embryonal precursor cells of the sympathetic nervous system. *MYCN* amplification, gain of 17q and deletion of 1p are frequently occurring genetic abnormalities in neuroblastoma and all correlate with a bad prognosis. Risk stratification is based on tumor stage according to the 'International Neuroblastoma Staging System' (INSS), age of the patient and genetic risk factors as *MYCN* amplification and deletion of 1p. Patients with low-risk tumors can be treated by surgery alone and have a very good prognosis. However, patients with high risk disease are treated with intensive chemotherapy, surgery and high-dose myeloablative therapy to eradicate minimal residual disease. Despite extensive treatment, children with high stage neuroblastoma have a poor prognosis with 20 to 35% overall survival.[1-3]

Chromosome 17q is gained in the majority of neuroblastoma and *BIRC5* (Survivin) is one of the genes located in the SRO (Smallest Region of Overlap) of 17q. BIRC5 is a member of the family of Inhibitor of Apoptosis Proteins (IAPs), which correlates to a bad prognosis.[4,5] It functions in the intrinsic apoptotic pathway and it is released from the mitochondria into the cytosol after cell death stimuli, where it can interact with HBXIP, XIAP or DIABLO. If the BIRC5-HBXIP complex is formed, it binds and inhibits CASP9 (Caspase-9), thus preventing apoptosome formation and CASP3 (Caspase-3) cleavage. If BIRC5 is not bound to HBXIP, it can form a complex with and stabilize XIAP, an IAP that inhibits CASP3 cleavage. BIRC5 can also bind and inactivate DIABLO (SMAC), a pro-apoptotic protein that binds and inhibits XIAP.[6-9]

More recent studies showed a second function of BIRC5 outside the intrinsic apoptotic pathway. BIRC5 was found to be a chromosomal passenger protein that forms a complex with CDCA8 (Borealin), AURKB (Aurora Kinase B) and INCENP by which it regulates microtubule dynamics at the kinetochores. Independent of the chromosomal passenger complex, BIRC5 can stabilize the microtubules by binding directly to them.[10-12] If the microtubule-kinetochore dynamics are disturbed, mitotic catastrophe occurs. This results in TP53 and CASP2 (Caspase-2) activation after which the mitochondrial apoptotic pathway is activated.[13,14] *BIRC5* has five isoforms, generated by alternative splicing. Three variants are anti-apoptotic (*BIRC5, BIRC5 ΔEx3, BIRC5 3B)* and two variants may be pro-apoptotic (*BIRC5 2B* and *BIRC5 2α*).[15,16]

We hypothesized that over-expression of *BIRC5*, observed in high risk neuroblastoma tumors, is involved in preventing apoptosis. Analysis of Affymetrix expression data showed that *BIRC5* is over-expressed in neuroblastoma compared to various normal tissues, adult tumors and compared to its tissue of origin (fetal adrenal medulla). High expression of *BIRC5* in neuroblastoma correlated to a bad prognosis independently of 17q-gain. Targeted inhibition of BIRC5 in neuroblastoma cell lines resulted in a strong induction of apoptosis. We analyzed whether this results from a role of BIRC5 in the intrinsic apoptotic pathway or a role in the chromosomal passenger complex. We did not detect an interaction between BIRC5 and DIABLO or XIAP. BIRC5 silencing resulted in multinucleated cells as shown by immunofluorescence and inhibition of CASP2 could rescue these cells from apoptosis. Also TP53 was activated after BIRC5 silencing. These data strongly suggest that apoptosis after *BIRC5* knockdown is caused by mitotic catastrophe.

Methods

Patient Material

The neuroblastic tumor panel used for Affymetrix microarray analysis contains 88 neuroblastoma samples. All samples were derived from primary tumors of untreated patients. Material was obtained during surgery and immediately frozen in liquid nitrogen.

RNA extraction and Affymetrix profiling

For profiling total RNA of neuroblastoma cell lines and tumors was extracted using Trizol reagent (Invitrogen) according to the manufacturer's protocol. RNA concentration was determined using the NanoDrop ND-1000 and quality was determined using the RNA 6000 Nano assay on the Agilent 2100 Bioanalyzer (Agilent Technologies). For Affymetrix Microarray analysis, fragmentation of RNA, labeling, hybridization to HG-U133 Plus 2.0 microarrays and scanning was carried out according to the manufacturer's protocol (Affymetrix Inc.). The expression data were normalized with the MAS5.0 algorithm within the GCOS program of Affymetrix. Target intensity was set to 100 (α1=0.04 and α2 0.06). If more than one probe set was available for one gene the probe set with the highest expression was selected, considered that the probe set was correctly located on the gene of interest. Public available neuroblastoma datasets we used were of Delattre[17] and Lastowska (geo ID: gse13136). Public available datasets were used for comparing neuroblastoma with

normal tissues (Roth dataset, geo ID: gse3526) and adult tumors (EXPO dataset, geo ID: gse2109). For the comparison between neuroblastoma and adrenal neuroblasts a public available dataset of 18 neuroblastoma (13 high stage neuroblastoma and 5 low stage neuroblastoma), 3 samples of the adrenal cortex and 3 samples of adrenal neuroblasts were used.[18] The correlation between BIRC5 expression and prognosis and the difference in expression between neuroblastoma and other tumors or normal tissue was analyzed using the bioinformatic platform R2.

Tissue array

Paraffin-embedded tumors were cut into 4-µm sections, mounted on aminoalkylsaline-coated glass slides, and dried overnight at 37°C. Sections were dewaxed in xylene and graded ethanol, and endogenous peroxidase was blocked in a 0.3% H2O2 solution in 100% methanol. Subsequently, the slides were rinsed thoroughly in distilled water and pretreated with a boiling procedure for 10 minutes in 10/1 mM Tris/EDTA pH 9 in an autoclave. After rinsing in distilled water and PBS, slides were incubated with primary antibody against BIRC5 (abcam, ab469). Slides were incubated for 1 hour in room temperature in a 1:5000 solution (diluted in an antibody diluent). Slides were then blocked with a postantibody blocking (Power Vision kit, ImmunoLogic) 1:1 diluted in PBS for 15 minutes, followed by a 30-minute incubation with poly–horseradish peroxidase (HRP)–goat α mouse/rabbit IgG (Power Vision kit, ImmunoLogic) 1:1 diluted in PBS. Chromogen and substrate were 3,3′-diaminobenzidine (DAB) and peroxide (1% DAB and 1% peroxide in distilled water). Nuclear counterstaining was done with hematoxylin. After dewatering in graded ethanol and xylene, slides were coated with glass. As a negative control we used liver tissue.

Cell lines

SHEP-21N was grown in RPMI-1640 medium (GIBCO) supplemented with 10% fetal calf serum, 4 mM l-glutamine, 100 µg/ml streptomycin and 100 U/ml penicillin. The other cell lines were grown in Dulbecco Modified Eagle Medium (DMEM), supplemented with 10% fetal calf serum, 10 mM L-glutamine, 10 U/ml penicillin, Non Essential Amino Acids (1x) and 10 µg/ml streptomycin. Cells were maintained at 37 ˚C under 5% CO_2. For primary references of these cell lines, see Molenaar et al.[19]

EZN-3042 and transfection procedures

Cells were transfected 24 hours after plating in 10-30% confluence. The Locked Nucleic Acid-Antisense Oligonucleotide (LNA-ASO; provided by Santaris Pharma) was dissolved in PBS and was transfected with Lipofectamin 2000 (invitrogen)

following manufacturer's procedures. The sequence of the BIRC5 LNA-ASO (EZN-3042) used was: CTCAatccatggCAGc. The sequence of Scrambled LNA-ASO (EZN-3046) was: CGCAgattagaaACCt. The LNA nucleotids are depicted in capitals; the small letters represent DNA nucleotids. Dose efficacy curves were made to calculate the IC50 levels (concentration drug needed for 50% cell survival).

Lentiviral shRNA production and transduction

Lentiviral particles were produced in HEK293T cells by cotransfection of lentiviral vector containing the short hairpin RNA (shRNA) with lentiviral packaging plasmids pMD2G, pRRE and pRSV/REV using FuGene HD. Supernatant of the HEK293T cells was harvested at 48 and 72 hours after transfection, which was purified by filtration and ultracentrifuging. The concentration was determined by a p24 ELISA.

Cells were plated in a 10% confluencey. After 24 hours cells were transduced with lentiviral BIRC5 shRNA (Sigma, TRCN0000073720) in various concentrations (Multiplicity of infection (MOI): 0.5 - 3). SHC-002 shRNA (non-targeting shRNA: CAACAAGATGAAGAGCACCAA) was used as a negative control. 24 hours after transduction medium was refreshed and puromycin was added to determine the efficacy of transduction. Protein was harvested 72 hours after transduction and analyzed by Western blot. Cells were harvested 48 and 72 hours after transfection for FACS analysis.

Compounds

ZM447439, a small molecule AURKB inhibitor, was dissolved in DMSO with a concentration of 100 mM for stock solution. For synergy assays a concentration series was made from 0 – 6250 nM.

CASP2 inhibition

24 hours after plating IMR32 cells in 10% confluence, Z-Val-Asp(OMe)-Val-Ala-Asp(OMe)-FMK (ZVDVAD-FMK , a widely used CASP2 inhibitor; R&D systems) was added to the cells following manufacturer's protocol in concentrations between 10 and 50 µM. The cells were transduced with BIRC5 shRNA at the same time. Both immunofluorescence and the MTT assay were performed 48 hours after treatment.

MTT-assay

Cells were plated in a 10-30% confluence in a 96-well plate and transfected after 24 hours with EZN-3042 and EZN-3046 as described above. 48 hours after transfection, 10 µl of Thyazolyl blue tetrazolium bromide (MTT, Sigma M2128) was added. After 4-6 hours of incubation 100 µl of 10% SDS, 0.01 M HCl was added to stop the

reaction. The absorbance was measured at 570 nm and 720 nm using a platereader (biotech). The IC50 (concentration drug needed for 50% cell viability reduction) was calculated using concentration vector curves. The Combination Index (CI) was calculated by the Chou Talalay method[20] using the CalcuSyn software.

RT-PCR

SKNBE cells were harvested 24 hours after transfection with EZN-3042. For RNA extraction Trizol reagent (invitrogen) was used according to the manufacturer's protocol and the RNA concentration was determined using the NanoDrop ND-1000. cDNA was made from 1 µg of the extracted RNA with 12.5 pM t12 primer in mQ at 70 ºC for 10 minutes. A mix was added with final concentrations of 2 mM MgCl2, 0.5 mM dNTP, 1x Fs-buffer and superscript III (Invitrogen, 100 U) in mQ. The reaction was performed at 50 ºC for 60 minutes and 70 ºC for 15 minutes. The primers (Biolegio) used for PCR of BIRC5 were: Forward: 5'-GCATGGGTGCCCCGACGTTG-3', Reverse: 5'-GCTCCGGCCAGAGGCCTCAA-3'. RT-PCR reactions were performed in a final concentration of: 312.5x diluted cDNA, 1 ng/µl forward primer and reverse primer and 2x diluted reddymix (ABgene) in mQ. After activation of Taq at 94 ºC, PCR followed with 35 cycles of denaturation at 95 ºC for 1 minute, annealing at 50 ºC for 1 minute and extension at 72 ºC for 2 minutes with a final extension at 72 ºC for 5 minutes. Equal volumes of PCR products were electrophoresed through a 1 % agarose gel in TBE-buffer.

Western Blotting

24 hours after transfection with EZN-3042, attached and floating cells were harvested on ice. Cells were lysated with Laemmlibuffer (20% glycerol, 4% SDS, 100mM Tris HCl pH 6.8 in mQ). Protein was quantified with RC-DC protein assay (Bio-Rad). Lysates were separated on a 10 % SDS-Page gel and electroblotted on a transfer membrane (Millipore, IPFL00010). Blocking and incubation were performed in 2.5 - 5% ELK in TBS using standard procedures. Primary antibodies used were BIRC5 rabbit polyclonal (abcam ab469), PARP mouse monoclonal (BD-biosciences, 556494), P53 (Neomarkers, BP53-12), and β-actin mouse monoclonal (abcam, ab6276). The secondary antibodies used were a secondary sheep anti-mouse or anti-rabbit horseradish peroxidase linked antibody (Amersham) or secondary antibodies provided by LI-COR. Proteins were visualized using an ECL detection kit (Amersham), or with the Odyssey bioanalyzer (LI-COR).

FACS analysis

24 and 48 hours after transfection with EZN-3042 both the attached and the floating cells were fixed with 100% ethanol at -20 ºC. After fixing, the cells were stained with 0.05 mg/ml propidium iodide and 0.05 mg/ml RNAse A in PBS. After 1 hour incubation, DNA content of the nuclei was analyzed using a fluorescence activated cell sorter. A total of 20,000 nuclei per sample were counted. The cell cycle distribution and apoptotic sub G1 fraction was determined using Flowjo version 7.2.2.

Co-immunoprecipitation

Cells were untreated or treated with ABT263 (Toronto Research Chemicals) at IC50 levels (4.4 μM for IMR32 and 7.9 μM for SKNSH). Cells were lysed in a buffer containing 150 mM NaCl, 50 mM Hepes, 5 mM EDTA, 0.3% NP-40, 10 mM β-glycerophosphate, 6% glycerol, protease inhibitors (Complete mini, Roche) and Phosphatase inhibitors (5 mM NaF, 1 mM Na2VO3). Antibodies used for IP were BIRC5 rabbit monoclonal (Cell Signaling, 2808) and DIABLO rabbit monoclonal (abcam, ab-32023). Negative controls were flag (Cell signaling, 2368) and protein without antibody. Other negative controls were for every antibody a sample without protein (data not shown). Protein-G agarose beads (Roche) and antibody have been incubated for pre-coupling overnight after which lysate was added and incubated overnight. Immunocomplexes were washed, heated at 95ºC for 10 minutes and put on a gel for Western blot. Primary antibodies used were rabbit polyclonal anti-BIRC5, rabbit monoclonal anti-XIAP (Cell signaling, 2045) and rabbit monoclonal anti-DIABLO. Blots were incubated overnight with primary antibodies, after which a one hour incubation step with anti-rabbit IgG was performed followed by incubation with the secondary antibody that was provided by LI-COR.

Immunofluorescence

Cells were grown on glass slides in 6-well plates. Cells were fixed with 4% paraformaldehyde in PBS 48 hours after treatment. We used mouse anti-α tubulin (1:1000, Sigma) as a primary antibody and goat anti-mouse (Alexa, A11029) for secondary antibody. Antibodies were dissolved in 5% ELK in PBS/0.2% tween-20. Slides were stained with DAPI (1:1000) in vectashield (Vector Laboratories). At least 5 pictures were made per slide and quantified for number of aberrant cells. Significance between groups was calculated using the Student's T-test.

Results

BIRC5 expression in neuroblastoma tumors

BIRC5 is up-regulated in several kinds of tumors and is widely investigated as a drug target.[21] We therefore evaluated the in vivo expression of *BIRC5* mRNA in neuroblastoma series analyzed by Affymetrix arrays. We used the R2 bioinformatics platform for data analysis (see methods). First, we analyzed the expression of *BIRC5* in 3 independent neuroblastoma data sets of different research groups comprising 88, 64 and 33 tumors. We also analyzed the *BIRC5* expression in various normal tissues and adult tumor types. Neuroblastoma have a significantly increased expression of *BIRC5* compared to normal tissues and also compared to various adult tumor types which are known to have increased *BIRC5* expression (fig 1a). Many neuroblastoma originate in the adrenal medulla, which largely consists of cells from the adrenal sympathetic neuronal lineage. *BIRC5* expression in high stage neuroblastoma tumors was also strongly increased compared to the fetal neuroblasts in normal adrenal tissue (fig 1b) and a higher *BIRC5* expression was found in high stage neuroblastoma than in stage 1, 2 and 4s tumors (fig 1c). We analyzed the prognostic value of *BIRC5* in our series of 88 neuroblastoma used for expression profiling and as expected we found that a high *BIRC5* expression correlated with a worse patient outcome (the lowest P-value of 6.8×10^{-7} was observed at a cut-off expression value of 400) (fig 1d). The poor prognosis was also significant independent of chromosome 17q gain ($p = 4.0 \times 10^{-3}$ in tumors with 17q gain, data not shown). To verify if the *BIRC5* RNA expression is representative for BIRC5 protein expression we performed immunohistochemistry on 39 tumor samples and divided them in three groups based on BIRC5 protein staining. We compared this to the BIRC5 RNA expression of these tumors and found a significant correlation (fig 1e).

Apoptosis of neuroblastoma cell lines after BIRC5 knockdown

To assess the role of *BIRC5* in neuroblastoma, we silenced *BIRC5* expression in neuroblastoma cell lines by various methods. We first used a BIRC5 Locked Nucleic Acid-Antisense Oligonucleotide (LNA-ASO) that targets the coding sequence of exon 4 of *BIRC5* (EZN-3042). LNA bases contain a methylene bridge that connects the 2'-oxygen of the ribose with the 4'-carbon, which makes it more stable than a regular oligonucleotide and suitable for therapeutic application.[22,23] LNA-ASO binds to RNA, prevents transcription and activates RNAse H resulting in cleavage of the target RNA molecule [24,25]. We used a panel of ten neuroblastoma cell lines, which all expressed relatively high BIRC5 expression as established by Affymetrix profiling

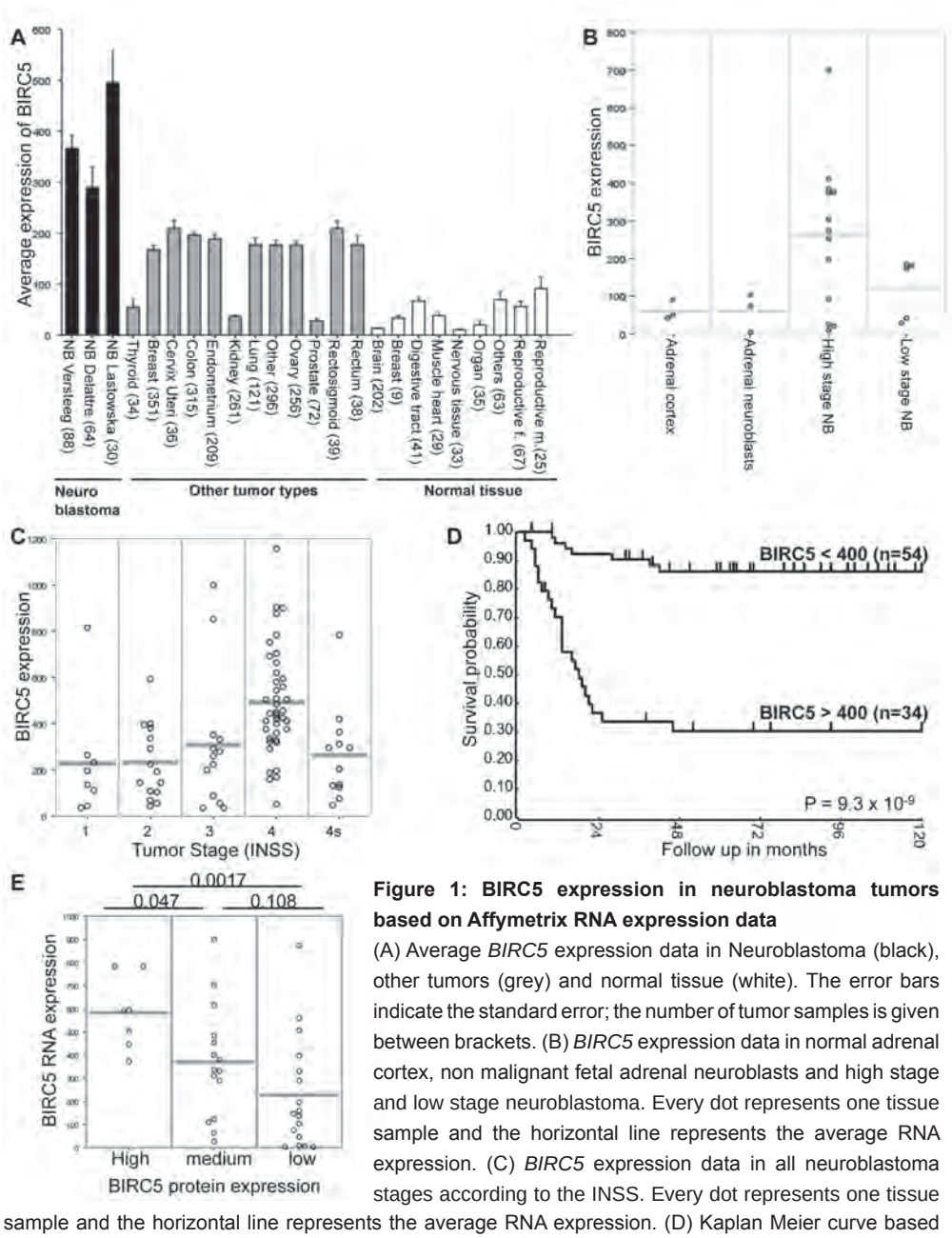

Figure 1: BIRC5 expression in neuroblastoma tumors based on Affymetrix RNA expression data

(A) Average *BIRC5* expression data in Neuroblastoma (black), other tumors (grey) and normal tissue (white). The error bars indicate the standard error; the number of tumor samples is given between brackets. (B) *BIRC5* expression data in normal adrenal cortex, non malignant fetal adrenal neuroblasts and high stage and low stage neuroblastoma. Every dot represents one tissue sample and the horizontal line represents the average RNA expression. (C) *BIRC5* expression data in all neuroblastoma stages according to the INSS. Every dot represents one tissue sample and the horizontal line represents the average RNA expression. (D) Kaplan Meier curve based on the survival data of 88 neuroblastoma tumors. The expression cutoff is 400. The upper line represents the survival curve of patients with low *BIRC5* expression and the lower line represents the survival curve of patients with high *BIRC5* expression. The logrank P-value is shown in the graph. (E) *BIRC5* RNA expression data are represented by the Y-axis. The three groups of protein expression are represented by the X-axis. Every dot is one tumor sample and the horizontal line shows the average RNA expression. The P-values are depicted above the graph.

	MYCN ampl	LOH 1p	17q gain	Survivin expression	IC50 EZN-3042 (nM)	IC50 EZN-3046 (nM)
SHEP 21N	Y	N	Y	1142	3	>50
IMR32	Y	Y	Y	2052	3	>50
SK-N-BE	Y	Y	Y	676,5	9	>50
TR14	Y	Y	Y	858	22	>50
SJNB10	Y	Y		1210	40	>50
SJNB-8	Y	Y	Y	1208	45	>50
SK-N-AS	N	N	Y	1044	46	>50
NGP-c4	Y	Y		1423	128	>250
SK-N-FI	N	N	Y	730	164	>250
SJNB-6	Y	Y	Y	1943	166	>250

Table 1: The IC50 (concentration drug needed for 50% less cell viability) of all neuroblastoma cell lines of the panel for EZN-3042 compared and the control EZN-3046 was determined by MTT assays. The occurrence of the most important genetic aberrations in neuroblastoma is also shown in this table.

(table 1). We determined the sensitivity of neuroblastoma cell lines for EZN-3042 by MTT assays. The IC50 (concentration drug needed for 50% cell viability reduction) of EZN-3042 determined by dose efficacy curves varied from 2 to 170 nM (fig 2a, table 1). No correlation between sensitivity to EZN-3042 and genetic aberrations or *BIRC5* expression levels in neuroblastoma cell lines was found (table 1).

For further analysis of EZN-3042 we used for each cell line its own IC50 value as a concentration. We analyzed the specific knock-down of *BIRC5* RNA after treatment of the cells with EZN-3042 by RT-PCR. The main transcript of *BIRC5* is clearly expressed in SKNBE and is reduced after EZN-3042 treatment. Furthermore, low levels of the alternative splice variants *BIRC5 2B* and *BIRC5 ΔEx3* were detected. All three variants were strongly silenced (fig 2b). We subsequently analyzed the effect of EZN-3042 for all ten neuroblastoma cell lines by Western blot. EZN-3042 treatment strongly reduced *BIRC5* expression in all cell lines and showed an increase of the PARP cleavage product of 80 kD, confirming an apoptotic response (fig 2c).

To exclude that the apoptotic response was caused by an off-target effect of EZN-3042, we also used lentivirally mediated shRNA silencing. The mode of action of shRNA differs from LNA-ASO, as shRNAs are cleaved by the cellular machinery into siRNA that can bind to the RNA-induced silencing complex (RISC), which in turn can bind and cleave the target mRNA.[26] The lentivirally delivered shRNA (which targeted another sequence in BIRC5 than EZN-3042) also down-regulated BIRC5 expression and induced PARP cleavage in the IMR32 cell line, while a control lentivirus (SHC002) did not affect BIRC5 levels (fig 2c right).

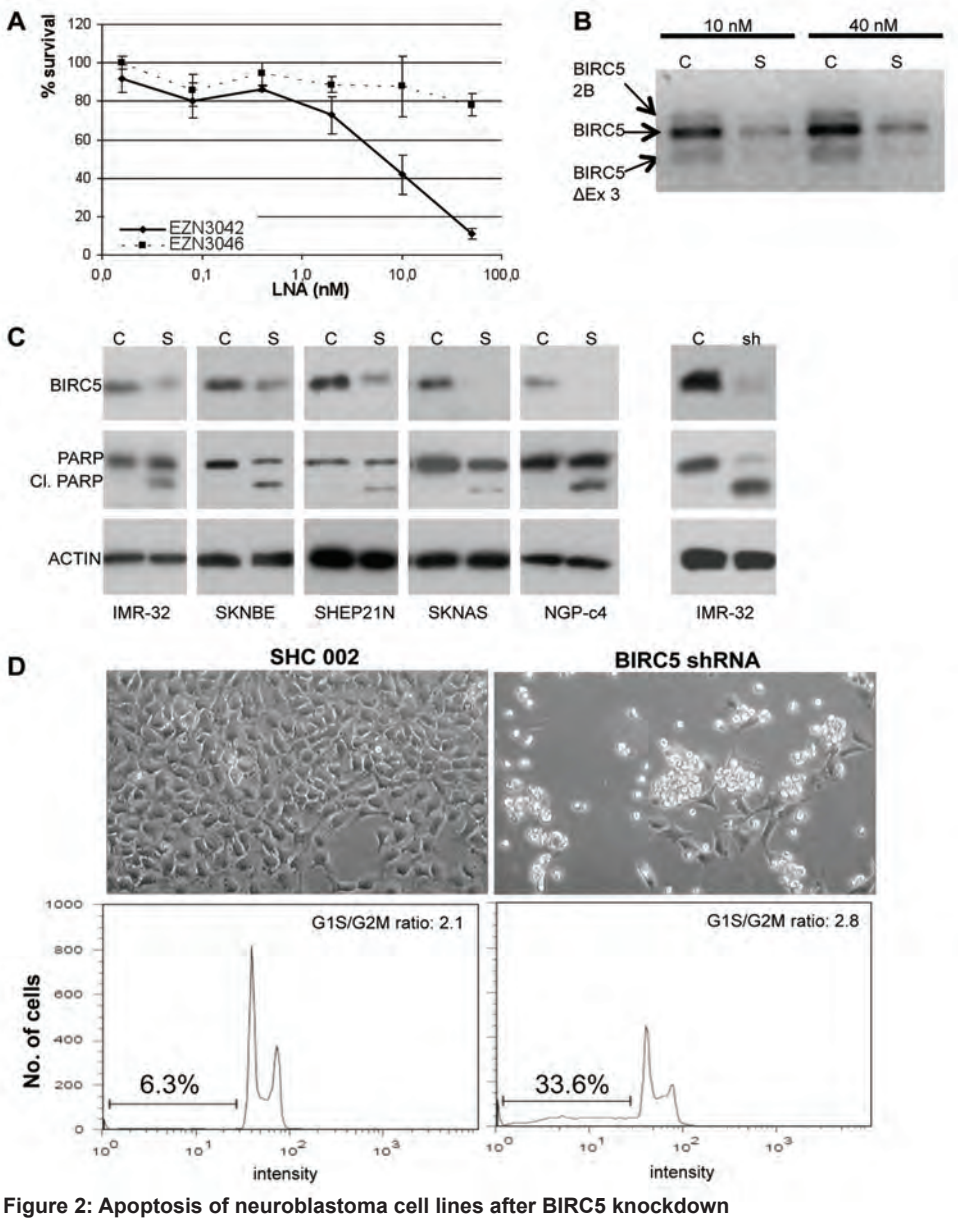

Figure 2: Apoptosis of neuroblastoma cell lines after BIRC5 knockdown

(A) The curve of cell viability determined by an MTT-assay after transfection of SKNBE with EZN-3042 and EZN-3046 (control). Cell viability is represented on the Y-axis and the EZN-3042 concentration in nM is represented on the X-axis. (B) RT-PCR of BIRC5 expression on RNA level after treatment of SKNBE with EZN-3042 (S) and EZN-3046 (control: C). Three bands are shown, which represent different BIRC5 isoforms. (C) Western blot of BIRC5 expression after treatment with EZN-3042 (S) or BIRC5 shRNA (sh). The Western blot was incubated with BIRC5, PARP and Actin. (D) FACS analysis of IMR32 after treatment with BIRC5 shRNA. Pictures were made of the cells that were harvested for FACS analysis. The Y-axes of the graphs represent the number of events and the X-axes represent the size of the particles detected. Apoptosis is shown by the sub G1-peak.

To validate the apoptotic response of BIRC5 knockdown and to analyze the effect on the cell cycle distribution we performed FACS analysis. After transduction of IMR32 with BIRC5 shRNA, the sub G1 fraction showed a more than a 5 fold increase from 6.3 to 33.6%, while the cell cycle distribution remained the same (fig 2d). Also after treatment of NGP-c4, SKNAS and IMR32 with EZN-3042, the sub G1 fractions increased with 19%, 28% and 22% respectively above the baseline levels (<7%), without a change in cell cycle distribution (data not shown). We conclude that silencing of BIRC5 results in a strong apoptotic response in neuroblastoma cells.

Anti-apoptotic effect of BIRC5 is mediated by its role in the chromosomal passenger complex

BIRC5 has been shown to inhibit the intrinsic apoptotic pathway via direct interaction with XIAP and DIABLO, but it can also stabilize the microtubules at the kinetochores. The mode of action of BIRC5 is relevant when it is used as a drug target, as this may predict synergistic effects with other targeted drugs. We therefore analyzed the binding partners of BIRC5 protein in IMR32 cells by co-immunoprecipitation. Immunoprecipitation of protein lysates with a BIRC5 antibody did not reveal co-immunoprecipitation of XIAP or DIABLO. As a positive control, we also performed immunoprecipitation of the same lysates with an antibody to DIABLO, which showed a clear co-immunoprecipitation of XIAP (fig 3a, left). DIABLO is located in the mitochondria in non-apoptotic cells which could explain the negative IP results between DIABLO and BIRC5. To confirm that BIRC5 is not bound to DIABLO in an apoptotic state, we induced apoptosis by addition of ABT263, an established BCL2 inhibitor. No interaction between BIRC5 and DIABLO was seen (fig 3a, right) which confirms our previous conclusion. Although these negative results do not formally exclude interaction of BIRC5 with DIABLO or XIAP, it suggests that alternative mechanisms are involved.

To demonstrate whether the anti-apoptotic function of BIRC5 in neuroblastoma cells is mediated by its role in the chromosomal passenger complex, we further analyzed IMR32 cells after silencing of BIRC5. We first performed immunofluorescence analyses of cells. IMR32 cells became large after shRNA mediated BIRC5 silencing and showed an increase in the number of micronuclei (fig 3b, panel 1, 2 and 4; P = 0.02). This suggested a disturbance of normal DNA segregation during mitosis, which could lead to the apoptotic response by mitotic catastrophe. Apoptosis after this process is mediated by activation of CASP2 and P53.[13,14] We reasoned that inhibition of CASP2 could rescue cells from mitotic catastrophe induced apoptosis,

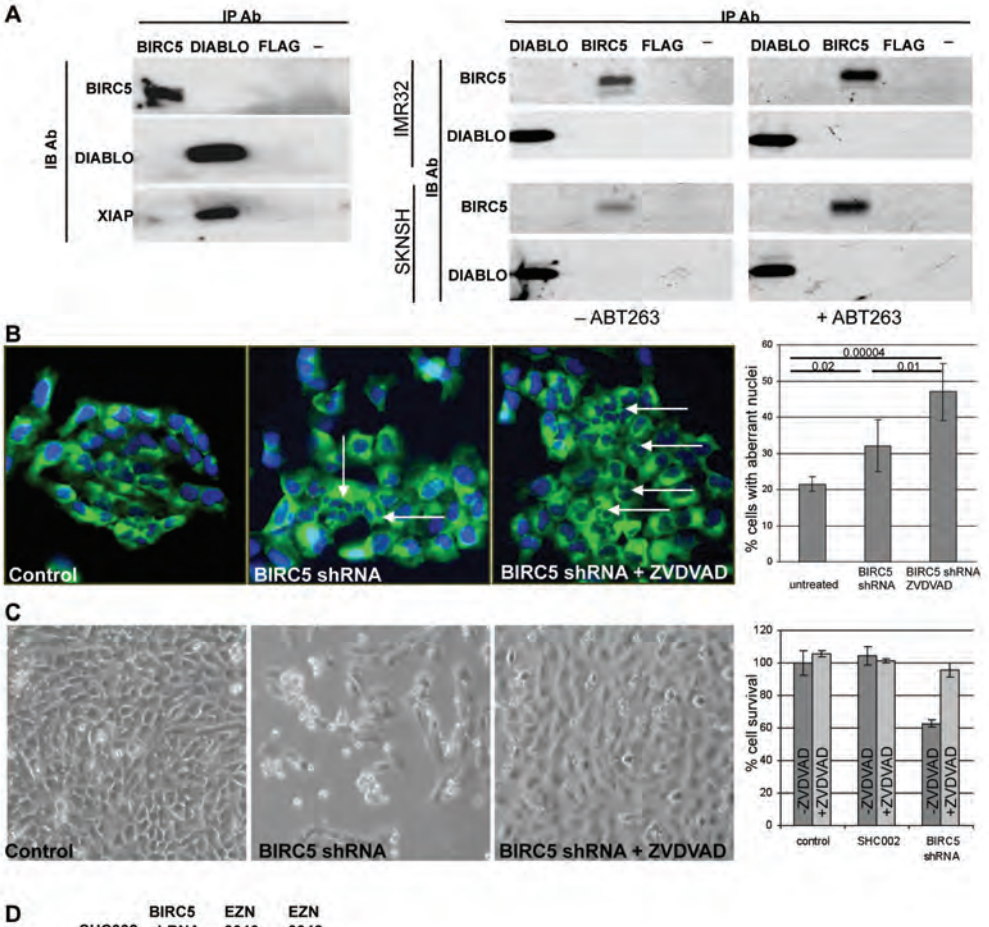

Figure 3: Anti-apoptotic effect of BIRC5 is mediated by its role in the chromosomal passenger complex

(A) Co-immunoprecipitation of untreated IMR32 cells (left) and IMR32 and SKNSH cells with or without ABT263 treatment (right). Co-immunoprecipitation was performed with BIRC5 and DIABLO antibodies. Western blot has been incubated with BIRC5, DIABLO, and XIAP antibodies. (B) IMR32 cells were transduced with BIRC5 shRNA and treated with ZVDVAD at the same time. 48 hours after treatment immunofluorescence was performed. The cells were stained with α-tubulin antibody (green) and DAPI (blue). Of each sample one picture is shown. Examples of cells with aberrant nuclei are indicated with an arrow. In the graph the percentage of cells with aberrant nuclei is represented and the P-values are indicated. (C) IMR32 cells were transduced with BIRC5 shRNA and treated with ZVDVAD at the same time. The phenotype is shown by the pictures. 48 hours after treatment, cell proliferation was determined by an MTT-assay. (D) Western blot after transduction of IMR32 with BIRC5 shRNA and after transfection with EZN-3042. The Western blot was incubated with BIRC5, P53, PARP and Actin.

but not from apoptosis resulting from inhibiting BIRC5 in the intrinsic apoptotic pathway. We therefore treated IMR32 cells with ZVDVAD, a widely used CASP2 inhibitor.[27-30] Silencing of BIRC5 expression with addition of ZVDVAD indeed rescued the cells from BIRC5 shRNA-induced apoptosis (fig 3c). Moreover, blocking of apoptosis by ZVDVAD increased the number of large cells with multiple micronuclei compared to cells treated with BIRC5 shRNA alone (fig 3b, panel 3 and 4; P = 0.01). Finally, we analyzed whether BIRC5 silencing results in P53 activation. Western blot analysis indeed showed a strong increase of the P53 levels after BIRC5 silencing with EZN-3042 as well as with lentiviral shRNA (fig 3d). We conclude that the apoptosis mediated by BIRC5 silencing is associated with mitotic catastrophe and P53 activation and can be rescued by CASP2 inhibition. These data strongly suggest that the anti-apoptotic function of BIRC5 in neuroblastoma cells is exerted by its role in the chromosomal passenger complex.

Combination of BIRC5 LNA-ASO with an AURKB inhibitor

The insight that mitotic catastrophe is involved in the apoptotic response after BIRC5 knockdown can guide compound combination strategies. Simultaneous inhibition of other genes in the same signal transduction pathway, such as AURKB could lead to additional or synergistic effects.

Therefore we performed MTT synergy assays of BIRC5 LNA-ASO combined with ZM447439 (AURKB inhibitor) in SKNBE and IMR32. In both cell lines BIRC5 LNA-ASO showed an additive effect with a combination index between 0.9 and 1.1 for all concentration combinations as calculated with the Chou Talalay method.[20] The dose-effect curves of BIRC5 LNA-ASO with ZM447439 in SKNBE are shown in Fig. 4.

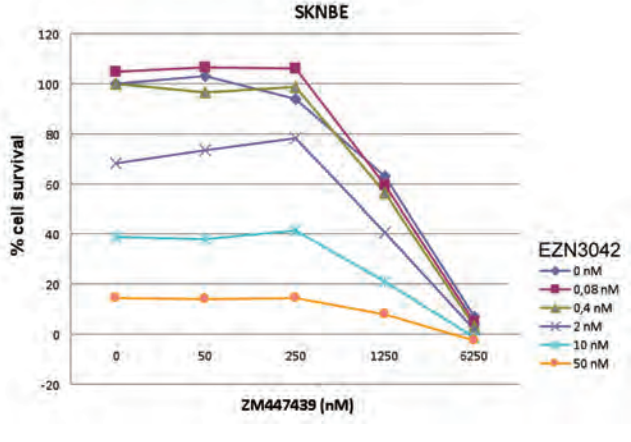

Figure 4: Combined dose dependency curves in SKNBE
The curves of cell viability determined by an MTT-assay after treatment with ZM447439 combined with fixed concentrations of EZN-3042. Cell viability is represented on the Y-axis and the ZM447439 concentration in nM is represented on the X-axis. The legend shows which line represents which BIRC5 LNA-ASO concentration.

Discussion

In this paper we show that *BIRC5* is strongly over-expressed in human neuroblastoma tumors compared to all other tissues and that over-expression correlates with a poor prognosis. BIRC5 inhibition with several antisense techniques causes a clear apoptotic response. We were not able to detect protein interactions between BIRC5 and DIABLO or XIAP. However, we could show mitotic catastrophe and P53 activation after BIRC5 inhibition and we could rescue apoptosis by a CASP2 inhibitor. We conclude that the microtubule stabilization and kinetochore functions of BIRC5 play a major role in neuroblastoma maintenance and that BIRC5 inhibition results in mitotic catastrophe and apoptosis.

The *BIRC5* over-expression and its correlation to poor prognostic factors in neuroblastoma patients that we found have been described before.[4,5] The high expression could partly depend on 17q gain but the significant correlation of *BIRC5* with prognosis independent of 17q gain suggests regulation of *BIRC5* by other mechanisms as well. One possibility is that the high expression is caused by its cell cycle dependent expression pattern[11] and because neuroblastoma are fast dividing tumors. This is supported by the fact that *BIRC5* expression is correlated to the expression of several important cell cycle genes (unpublished data). Also, *BIRC5* is established as an E2F target.[31] In neuroblastoma a high E2F activity is related to a bad prognosis (Molenaar et al., submitted).

An important role for BIRC5 in mitosis has extensively been shown in other tumors.[7,10,32-34] This role has also been described before in a neuroblastoma cell line, however unlike our data, BIRC5 knockdown induced Caspase independent cell death.[35] In addition, apoptosis after BIRC5 inhibition has been shown in neuroblastoma cell lines by others using compounds which are less specific and therefore less suitable for functional analysis of BIRC5 in neuroblastoma compared to BIRC5 antisense techniques.[36,37] The interactions between BIRC5, XIAP and DIABLO have never been shown in neuroblastoma cell lines, but data on these interactions are available from experiments in other tumor types using over-expression constructs of one of the interacting genes.[6-8] In this paper we investigated the endogenous interactions between BIRC5 and DIABLO or XIAP and found DIABLO and XIAP to only interact with each other but we did not find an interaction with BIRC5, neither after apoptosis induction. Our results do not rule out that BIRC5 in addition has a role in the intrinsic apoptotic pathway. However, such a

function does not seem to be essential in the apoptotic response triggered by BIRC5 silencing.

BIRC5 knockdown has often resulted in an 8N-peak on FACS analysis in cell lines of several tumor types.[11,32] Cells with 4N DNA cannot divide due to destabilized microtubules after which they start to re-duplicate the DNA. In our FACS analyses of neuroblastoma cell lines after BIRC5 silencing, we never observed an 8N peak (fig 2d). A possible explanation is that the apoptotic pathway is activated before the cells starts to re-duplicate their DNA, resulting in a tetraploid G1 phase arrests. This is in accordance with our finding with immunofluorescence (fig 3b). The cells become large with multiple micronuclei, indicating that they are not able to divide properly, while the amount of DNA does not increase. This phenotype is known as mitotic catastrophe.[13]

We validated BIRC5 as a drug target in neuroblastoma by showing an apoptotic response after BIRC5 knockdown using two independent antisense techniques. RNA interference functions via the RNA-Induced Silencing Complex (RISC), which can bind and cleave the target mRNA[26] while LNA-ASO such as EZN-3042 bind mRNA, and activate RNAse H dependent mRNA cleavage.[24,25,38] Since these antisense techniques have a different mechanism and since we chose different target sequences, it is unlikely that the apoptotic response after BIRC5 inhibition is caused by off-target effects. All cell lines tested appeared to undergo apoptosis after BIRC5 inhibition although some cell lines were less sensitive. This could be caused by a difference in transfection efficiency of EZN-3042.

The validation of BIRC5 as viable drug target in neuroblastoma warrants further development of targeted inhibition of BIRC5 in this pediatric malignancy. EZN-3042 is developed as a human treatment modality.[24,25,38] In general, due to insufficient delivery to solid tumors and low potency of traditional antisense oligonucleotides, pharmacological activity has been difficult to obtain in these tissues. However, it has been shown that solid tumors can be targeted by Locked Nucleic Acids.[38,39] BIRC5 based vaccines are found to reduce primary tumor growth and spontaneous liver metastasis in a neuroblastoma xenograft model and are currently in Phase I/II clinical trial in adult tumors.[40,41] Alternatively, small molecules are available that inhibit the BIRC5 activation pathway. One option is to use CDK1 inhibitors to block phosphorylation and activation of BIRC5 by this kinase. Also 2,5-Dimethyl-celecoxib (DMC), was shown to have an antitumor activity, possibly by inhibiting BIRC5.[37]

Promising results have been reached with YM155, a small molecule triggering transcriptional repression of BIRC5.[42-46] Phase-I and II clinical studies in various tumor types showed an antitumor effect of YM155 at a dose that does not cause severe toxicities.[43,45,46]

BIRC5 LNA-ASO combined with an AURKB inhibitor showed an additive effect for both cell lines tested, which suggests rational for combining BIRC5 inhibitors with one of these compounds in clinical trial. However, BIRC5 inhibition should first be tested in combination with the currently used cytostatics and before a clinical trial can be designed BIRC5 inhibitors should be extensively tested in in vivo neuroblastoma models.

Acknowledgements

This research was supported by grants from Top Institute Pharma, KIKA foundation, SKK and Netherlands Cancer Foundation.

Reference List

1. Henry, M.C.W., Tashjian, D.B., and Breuer, C.K., Neuroblastoma update. Current Opinion in Oncology, 2005; 17**:** 19-23.
2. Maris, J.M., Hogarty, M.D., Bagatell, R., and Cohn, S.L., Neuroblastoma. Lancet, 2007; 369**:** 2106-2120.
3. van Noesel, M.M. and Versteeg, R., Pediatric neuroblastomas: genetic and epigenetic 'Danse Macabre'. Gene, 2004; 325**:** 1-15.
4. Adida, C., Berrebi, D., Peuchmaur, M., Reyes-Mugica, M., and Altieri, D.C., Anti-apoptosis gene, survivin, and prognosis of neuroblastoma. Lancet, 1998; 351**:** 882-883.
5. Islam, A., Kageyama, H., Takada, N., Kawamato, T., Takayasu, H., Isogai, E. et al, High expression of Survivin, mapped to 17q25, is significantly associated with poor prognostic factors and promotes cell survival in human neuroblastoma. Oncogene, 2000; 19**:** 617-623.
6. Dohi, T., Okada, K., Xia, F., Wilford, C.E., Samuel, T., Welsh, K. et al, An IAP-IAP complex inhibits apoptosis. Journal of Biological Chemistry, 2004; 279**:** 34087-34090.
7. Marusawa, H., Matsuzawa, S., Welsh, K., Zou, H., Armstrong, R., Tamm, I. et al, HBXIP functions as a cofactor of survivin in apoptosis suppression. Embo Journal, 2003; 22**:** 2729-2740.
8. Song, Z.Y., Yao, X.B., and Wu, M., Direct interaction between survivin and Smac/DIABLO is essential for the anti-apoptotic activity of survivin during taxol-induced apoptosis. Journal of Biological Chemistry, 2003; 278**:** 23130-23140.
9. Zangemeister-Wittke, U. and Simon, H.U., An IAP in action - The multiple roles of survivin in differentiation, immunity and malignancy. Cell Cycle, 2004; 3**:** 1121-1123.
10. Altieri, D.C., The case for survivin as a regulator of microtubule dynamics and cell-death decisions. Current Opinion in Cell Biology, 2006; 18**:** 609-615.
11. Lens, S.M.A., Rodriguez, J.A., Vader, G., Span, S.W., Giaccone, G., and Medema, R.H., Uncoupling the central spindle-associated function of the chromosomal passenger complex from its role at centromeres. Molecular Biology of the Cell, 2006; 17**:** 1897-1909.
12. Ruchaud, S., Carmena, M., and Earnshaw, W.C., The chromosomal passenger complex: One for all and all for one. Cell, 2007; 131**:** 230-231.
13. Castedo, M., Perfettini, J.L., Roumie, T., Andreau, K., Medema, R., and Kroemer, G., Cell death by mitotic catastrophe: a molecular definition. Oncogene, 2004; 23**:** 2825-2837.
14. Castedo, M., Perfettini, J.L., Roumier, T., Valent, A., Raslova, H., Yakushijin, K. et al, Mitotic catastrophe constitutes a special case of apoptosis whose suppression entails aneuploidy. Oncogene, 2004; 23**:** 4362-4370.
15. Caldas, H., Honsey, L.E., and Altura, R.A., Survivin 2 alpha: a novel survivin splice variant expressed in human malignancies. Molecular Cancer, 2005; 4.
16. Fangusaro, J.R., Caldas, H., Jiang, Y.Y., and Altura, R.A., Survivin: An inhibitor of apoptosis in pediatric cancer. Pediatric Blood & Cancer, 2006; 47**:** 4-13.
17. Fix, A., Lucchesi, C., Ribeiro, A., Lequin, D., Pierron, G., Schleiermacher, G. et al, Characterization of amplicons in neuroblastoma: High-resolution mapping using DNA microarrays, relationship with outcome, and identification of overexpressed genes. Genes Chromosomes & Cancer, 2008; 47**:** 819-834.
18. De Preter, K., Vandesompele, J., Heimann, P., Yigit, N., Beckman, S., Schramm, A. et al, Human fetal neuroblast and neuroblastoma transcriptome analysis confirms neuroblast origin and highlights neuroblastoma candidate genes. Genome Biology, 2006; 7.
19. Molenaar, J.J., Ebus, M.E., Koster, J., van Sluis, P., van Noesel, C.J.M., Versteeg, R. et al, Cyclin D1 and CDK4 activity contribute to the undifferentiated phenotype in neuroblastoma. Cancer Research, 2008; 68**:** 2599-2609.
20. Chou, T.C. and Talalay, P., Quantitative-Analysis of Dose-Effect Relationships - the Combined Effects of Multiple-Drugs Or Enzyme-Inhibitors. Advances in Enzyme Regulation, 1984; 22**:** 27-55.
21. Altieri, D.C., Validating survivin as a cancer therapeutic target. Nature Reviews Cancer, 2003; 3**:** 46-54.
22. Beane, R.L., Ram, R., Gabillet, S., Arar, K., Monia, B.P., and Corey, D.R., Inhibiting gene expression with locked nucleic acids (LNAs) that target chromosomal DNA. Biochemistry, 2007; 46**:** 7572-7580.
23. Mook, O.R., Baas, F., de Wissel, M.B., and Fluiter, K., Evaluation of locked nucleic acid-modified small interfering RNA in vitro and in vivo. Molecular Cancer Therapeutics, 2007; 6**:** 833-843.
24. Petersen, M. and Wengel, J., LNA: a versatile tool for therapeutics and genomics. Trends in

Biotechnology, 2003; 21: 74-81.
25. Vester, B. and Wengel, J., LNA (Locked nucleic acid): High-affinity targeting of complementary RNA and DNA. Biochemistry, 2004; 43: 13233-13241.
26. Rubinson, D.A., Dillon, C.P., Kwiatkowski, A.V., Sievers, C., Yang, L.L., Kopinja, J. et al, A lentivirus-based system to functionally silence genes in primary mammalian cells, stem cells and transgenic mice by RNA interference. Nature Genetics, 2003; 33: 401-406.
27. Basu, A., Adkins, B., and Basu, C., Down-regulation of caspase-2 by rottlerin via protein kinase c-delta-independent pathway. Cancer Research, 2008; 68: 2795-2802.
28. Nutt, L.K., Margolis, S.S., Jensen, M., Herman, C.E., Dunphy, W.G., Rathmell, J.C. et al, Metabolic regulation of oocyte cell death through the CaMKII-mediated phosphorylation of caspase-2. Cell, 2005; 123: 89-103.
29. Shen, J., Vakifahmetoglu, H., Stridh, H., Zhivotovsky, B., and Wiman, K.G., PRIMA-1(MET) induces mitochondrial apoptosis through activation of caspase-2. Oncogene, 2008; 27: 6571-6580.
30. Tinnikov, A.A., Yeung, K.T., Das, S., and Samuels, H.H., Identification of a Novel Pathway That Selectively Modulates Apoptosis of Breast Cancer Cells. Cancer Research, 2009; 69: 1375-1382.
31. Jiang, Y.Y., Saavedra, H.I., Holloway, M.P., Leone, G., and Altura, R.A., Aberrant regulation of survivin by the RB/E2F family of proteins. Journal of Biological Chemistry, 2004; 279: 40511-40520.
32. Lens, S.M.A., Wolthuis, R.M.F., Klompmaker, R., Kauw, J., Agami, R., Brummelkamp, T. et al, Survivin is required for a sustained spindle checkpoint arrest in response to lack of tension. Embo Journal, 2003; 22: 2934-2947.
33. Wheatley, S.P. and McNeish, A., Survivin: A protein with dual roles in mitosis and apoptosis. International Review of Cytology - A Survey of Cell Biology, Vol 247, 2005; 247: 35-+.
34. Zangemeister-Wittke, U. and Simon, H.U., An IAP in action - The multiple roles of survivin in differentiation, immunity and malignancy. Cell Cycle, 2004; 3: 1121-1123.
35. Shankar, S.L., Mani, S., O'Guin, K.N., Kandimalla, E.R., Agrawal, S., and Shafit-Zagardo, B., Survivin inhibition induces human neural tumor cell death through caspase-independent and -dependent pathways. Journal of Neurochemistry, 2001; 79: 426-436.
36. Muhlethaler-Mottet, A., Meier, R., Flahaut, M., Bourloud, K.B., Nardou, K., Joseph, J.M. et al, Complex molecular mechanisms cooperate to mediate histone deacetylase inhibitors anti-tumour activity in neuroblastoma cells. Molecular Cancer, 2008; 7.
37. Pyrko, P., Soriano, N., Kardosh, A., Liu, Y.T., Uddin, J., Petasis, N.A. et al, Downregulation of survivin expression and concomitant induction of apoptosis by celecoxib and its non-cyclooxygenase-2-inhibitory analog, dimethyl-celecoxib (DMC), in tumor cells in vitro and in vivo. Mol.Cancer, 2006; 5: 19.
38. Hansen, J.B., Fisker, N., Westergaard, M., Kjaerulff, L.S., Hansen, H.F., Thrue, C.A. et al, SPC3042: a proapoptotic survivin inhibitor. Molecular Cancer Therapeutics, 2008; 7: 2736-2745.
39. Sapra, P., Wang, M., Bandaru, R., Zhao, H., Greenberger, L.M., and Horak, I.D., Down-modulation of survivin expression and inhibition of tumor growth in vivo by EZN-3042, a locked nucleic acid antisense oligonucleotide. Nucleosides Nucleotides Nucleic Acids, 2010.
40. Fest, S., Huebener, N., Bleeke, M., Durmus, T., Stermann, A., Woehler, A. et al, Survivin minigene DNA vaccination is effective against neuroblastoma. Int.J.Cancer, 2009; 125: 104-114.
41. Ryan, B.M., O'Donovan, N., and Duffy, M.J., Survivin: A new target for anti-cancer therapy. Cancer Treatment Reviews, 2009; 35: 553-562.
42. Altieri, D.C., Opinion - Survivin, cancer networks and pathway-directed drug discovery. Nature Reviews Cancer, 2008; 8: 61-70.
43. Giaccone, G., Zatloukal, P., Roubec, J., Floor, K., Musil, J., Kuta, M. et al, Multicenter Phase II Trial of YM155, a Small-Molecule Suppressor of Survivin, in Patients With Advanced, Refractory, Non-Small-Cell Lung Cancer. Journal of Clinical Oncology, 2009; 27: 4481-4486.
44. Nakahara, T., Takeuchi, M., Kinoyama, I., Minematsu, T., Shirasuna, K., Matsuhisa, A. et al, YM155, a novel small-molecule survivin suppressant, induces regression of established human hormone-refractory prostate tumor xenografts. Cancer Research, 2007; 67: 8014-8021.
45. Satoh, T., Okamoto, I., Miyazaki, M., Morinaga, R., Tsuya, A., Hasegawa, Y. et al, Phase I Study of YM155, a Novel Survivin Suppressant, in Patients with Advanced Solid Tumors. Clinical Cancer Research, 2009; 15: 3872-3880.
46. Tolcher, A.W., Mita, A., Lewis, L.D., Garrett, C.R., Till, E., Daud, A.I. et al, Phase I and Pharmacokinetic Study of YM155, a Small-Molecule Inhibitor of Survivin. Journal of Clinical Oncology, 2008; 26: 5198-5203.

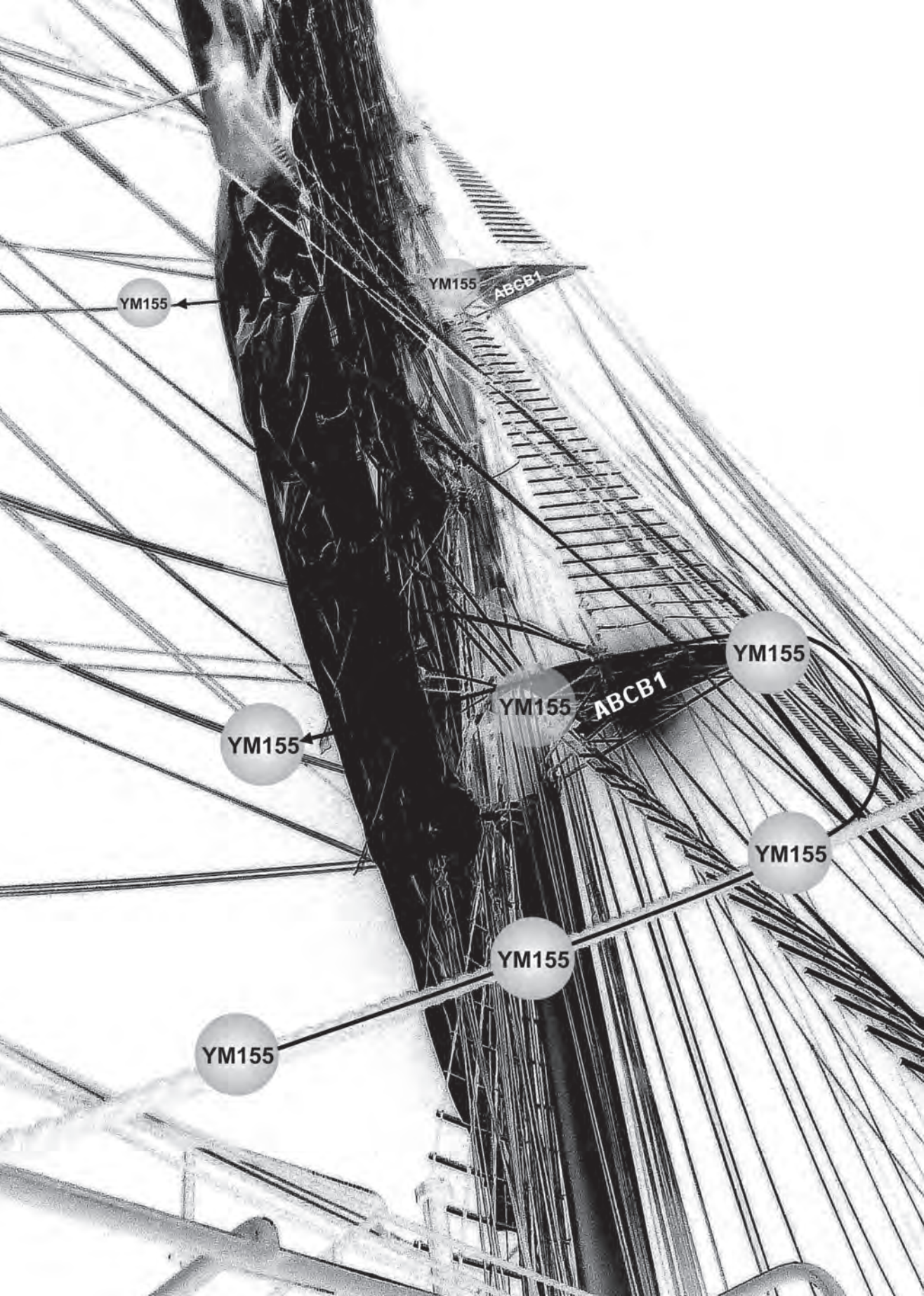
YM155
YM155
ABCB1
YM155
YM155
ABCB1
YM155
YM155
YM155
YM155

3

Targeted BIRC5 Silencing Using YM155 Causes Cell Death in Neuroblastoma Cells with Low ABCB1 Expression

Targeted BIRC5 Silencing Using YM155 Causes Cell Death in Neuroblastoma Cells with Low ABCB1 Expression

Fieke Lamers[1], Linda Schild[1], Jan Koster[1], Rogier Versteeg[1], Huib N. Caron[2], Jan J. Molenaar[1]

[1] Department of Oncogenomics, Academic Medical Center, University of Amsterdam, Meibergdreef 15, PO box 22700, 1105 AZ Amsterdam, The Netherlands. [2] Department of Pediatric Oncology, Emma Kinderziekenhuis, Academic Medical Center, University of Amsterdam, the Netherlands

Abstract

The *BIRC5* (Survivin) gene is located at chromosome 17q in the region that is frequently gained in high risk neuroblastoma. *BIRC5* is strongly over expressed in neuroblastoma tumor samples, which correlates to a poor prognosis. We recently validated *BIRC5* as a potential therapeutic target by showing that targeted knock down with shRNA's triggers an apoptotic response through mitotic catastrophe. We now tested YM155, a novel small molecule selective *BIRC5* suppressant that is currently in phase I/II clinical trials. Drug response curves showed IC50 values in the low nM range (median: 35 nM, range: 0.5 nM->10,000 nM) in a panel of 23 neuroblastoma cell lines and four TIC-lines, which resulted from an apoptotic response. Nine out 23 cell lines were relatively resistant to YM155 with IC50 values >200nM, although in the same cells shRNA mediated knock down of BIRC5 caused massive apoptosis. Analysis of differentially expressed genes between 5 most sensitive and 5 most resistant cell lines using Affymetrix mRNA expression data revealed *ABCB1* (MDR1) as the most predictive gene for resistance to YM155. Inhibition of the multi-drug resistance pump ABCB1 with cyclosporine or knockdown with shRNA prior to treatment with YM155 demonstrated that cell lines with *ABCB1* expression became 27 to 695 times more sensitive to YM155 treatment.
We conclude that most neuroblastoma cell lines are sensitive to YM155 in the low nM range and that resistant cells can be sensitized by ABCB1 inhibitors. Therefore YM155 is a promising novel compound for treatment of neuroblastoma with low *ABCB1* expression.

Introduction

BIRC5 (Survivin) is an Inhibitor of Apoptosis Protein (IAP) with a crucial function in cell cycle and apoptotic signaling. In the intrinsic apoptotic pathway it can bind and inhibit the pro-apoptotic protein DIABLO and it can bind and stabilize XIAP, another IAP. Inhibition of this function of BIRC5 induces apoptosis by activating the intrinsic apoptotic pathway.[1-3] In addition, BIRC5 can stabilize microtubules in the chromosomal passenger complex during mitosis. Inactivation of BIRC5 can therefore also lead to mitotic catastrophe which activates the intrinsic apoptotic pathway via TP53 and Caspase 2.[3-7] Genomic aberrations of the *BIRC5* locus at 17q occur in several malignancies. *BIRC5* is gained in almost all high risk neuroblastoma which is a pediatric tumor that originates from the neural crest derived precursor cells of the sympathetic nervous system.[8-10] *BIRC5* over expression in these tumors strongly correlates to a poor prognosis. BIRC5 knockdown in neuroblastoma causes apoptosis via mitotic catastrophe, suggesting that in these tumor cells the crucial function of BIRC5 is microtubule stabilization.[11]

In addition to gain of the *BIRC5* locus at 17q, only few other aberrations in apoptotic signaling have been reported in neuroblastoma tumors and cell lines.[12,13] *TP53* mutations are rare and many cell line experiments showed that TP53 can be activated to induce apoptosis[14,15]. *Caspase 8* is hypermethylated and thereby inactive in some neuroblastoma resulting in an inactive extrinsic apoptotic pathway.[16] And finally *BCL2* is often over expressed in neuroblastoma tumors and has been found to be a target for therapy.[17,18]

Thus, BIRC5 is one of the few drugged targets in the intrinsic apoptotic pathway. This warrants further validation in neuroblastoma since current treatment regimens can only cure 25-35% of high stage neuroblastoma patients and there is a strong need for new targeted therapies.[8-10] BIRC5 has shown to be a viable therapeutic target and several new strategies for inhibiting BIRC5 have recently become available. The Locked Nucleic Acid (LNA)[19] based antisense molecule EZN3042 was effective in vitro in NB cells[11]. The anti BIRC5 antisense LNA oligonucleotide LY2181308 (gataparsen sodium) is currently being tested in Phase II clinical trials in solid tumors and BIRC5 based vaccines are currently in Phase I/II clinical trial.[20] Though targeted therapy by antisense based compounds can be effective in hematological malignancies, they have been disappointing in solid tumors. A promising new small molecule BIRC5 suppressant is YM155, developed by Astellas Pharma. This compound was

selected by high throughput screening with a BIRC5 Promoter Luciferase Assay and inhibits mRNA expression of BIRC5[21]. Phase I/II clinical 'single agent' trials showed acceptable toxicity in patients with advanced solid malignancies.[22,23] In a Phase II trial in melanoma the pre-specified criterion for success was not reached[24], but in Non-small-cell-lung-cancer 5% of the patients showed a partial response, and 38% showed stable disease[25]. YM155 has also induced responses in a phase I trial in patients with non-Hodgkin's Lymphoma or prostate cancer.[23]

In this paper we investigated the efficacy of YM155 in 23 neuroblastoma cell lines and 4 neuroblastoma 'Tumor Initiating Cell' (TIC) lines. First, we validated BIRC5 as a therapeutic target by lentiviral shRNA mediated silencing of BIRC5, which resulted in massive apoptosis in all 6 neuroblastoma cell lines tested. Subsequent assays using YM155 induced apoptosis in the majority of 23 tested neuroblastoma cell lines as well. Surprisingly, some cell lines that were sensitive for targeted silencing using BIRC5 shRNA were resistant to YM155. Analysis of mRNA profiles of sensitive and insensitive cell lines identified the multi drug resistance pump *ABCB1* (MDR1)[26-28], as the best predictor of resistance. Inhibition of ABCB1 with cyclosporine or lentiviral shRNA sensitized the resistant cell lines to YM155 induced apoptosis.

Methods

Cell lines

All cell lines were grown in Dulbecco Modified Eagle Medium (DMEM), supplemented with 10% fetal calf serum, 10 mM L-glutamine, 10 U/ml penicillin/streptomycin, Non Essential Amino Acids (1x) and 10 µg/ml streptomycin. Cells were maintained at 37 ˚C under 5% CO_2. For primary references of these cell lines, see Molenaar et al[29]. The Tumor Initiating Cell (TIC) lines were isolated directly from patient tumor or bone marrow cells and cultured in neural specific stem cell medium (400 ml DMEM glutamax, 133 ml F12 medium, 2% B27, 20ng/ml EGF, 40 ng/ml FGF, 10 U/ml penicillin/streptomycin) as described previously[30].

Lentiviral shRNA production and transduction

Lentiviral particles were produced in HEK293T cells by cotransfection of lentiviral vector containing the short hairpin RNA (shRNA) with lentiviral packaging plasmids pMD2G, pRRE and pRSV/REV using FuGene HD. Supernatant of the HET293T

cells was harvested at 48 and 72 hours after transfection, which was purified by filtration and ultracentrifuging. The concentration was determined by a p24 ELISA.
Cells were plated in a 10% confluence. After 24 hours cells were transduced with lentiviral BIRC5 shRNA (Sigma, TRCN0000073720; coordinates: chromosome 17; 76212781-76212801; hg19), or ABCB1 shRNA B5 and B7 (Sigma, TRCN0000059684; coordinates: chromosome 7; 87190611-87190631; hg19, and TRCN0000059686; coordinates: chromosome 7; 87175290-87175310; hg19) in various concentrations (Multiplicity of infection (MOI): 1 - 3). SHC-002 shRNA (non-targeting shRNA: CAACAAGATGAAGAGCACCAA) was used as a negative control. 24 hours after transduction medium was refreshed and puromycin was added to determine the efficacy of transduction. Protein was harvested 72 hours after transduction and analyzed by Western blot. Nuclei were harvested 48 and 72 hours after transfection for FACS analysis.

Lentiviral over expression clones
BIRC5 over expression constructs 7 and 10 were produced from a PCR product of BIRC5 (CCDS11755.1: isoform 1) that was obtained from IMR32 cDNA (primers: TATATAGGATCCATTAACCGCCAGATTTGA/ TATATAGAATTCGGTGGCACCAGGGAATAAAC) and cloned into pLenti4/TO/V5-Dest according to manufacturer's procedures (Invitrogen). The sequence has been checked using the manufacturer's primers (pL4-TO/V5 fwd and pL4-dest rev)

Compounds
YM155 (provided by Astellas Pharma) was dissolved in DMSO in a stock concentration of 10 mM. It was added to the cells in concentrations from 0.1 nM to 10 μM 24 hours after plating the cells in 10 to 30% confluence. Cyclosporine (Sigma, C3662) was added to the cells in a concentration of 5 μM, 24 hours after plating. The cells were incubated with cyclosporine for 1 hour before YM155 was added without removal of cyclosporine.

RNA extraction and Affymetrix profiling
For profiling total RNA of neuroblastoma cell lines was extracted using Trizol reagent (Invitrogen) according to the manufacturer's protocol. RNA concentration was determined using the NanoDrop ND-1000 and quality was determined using the RNA 6000 Nano assay on the Agilent 2100 Bioanalyzer (Agilent Technologies). For Affymetrix Microarray analysis, fragmentation of RNA, labeling, hybridization to HG-U133 Plus 2.0 microarrays and scanning was carried out according to the

manufacturer's protocol (Affymetrix Inc.). The expression data were normalized with the MAS5.0 algorithm within the GCOS program of Affymetrix. Target intensity was set to 100 (α1=0.04 and α2 0.06). If more than one probe set was available for one gene the probe set with the highest expression and most present calls was selected, considered that the probe set was correctly located on the gene of interest. Mostly this is a probe set at the 3' end. The data were analyzed with the R2 microarray analysis and visualization platform (http://r2.amc.nl).

MTT-assay

Forty-eight hours after treatment with YM155, 10 µl of Thyazolyl blue tetrazolium bromide (MTT, Sigma M2128) was added to the cells. After 4-6 hours of incubation 100 µl of 10% SDS, 0.01 M HCl was added to stop the reaction. The absorbance was measured at 570 nm and 720 nm using a platereader (biotek). The IC50 (concentration drug needed for 50% cell viability reduction) was calculated using concentration vector curves.

Western Blotting

Twenty-four to fourty-eight hours after treatment with YM155 or 48 – 72 hours after transduction with shRNA, attached and floating cells were harvested on ice. Cells were lysated with Laemmlibuffer (20% glycerol, 4% SDS, 100mM Tris HCl pH 6.8 in mQ). Protein was quantified with RC-DC protein assay (Bio-Rad). Lysates were separated on a 10 % SDS-Page gel and electroblotted on a transfer membrane (Millipore, IPFL00010). Blocking and incubation were performed in OBB according to manufacturer's protocol (LI-COR). Primary antibodies used were BIRC5 (rabbit monoclonal antibody, cell signaling: 2808), PARP (rabbit polyclonal antibody, cell signaling: 9542), ABCB1 mouse monoclonal (abcam, ab3364) and β-actin mouse monoclonal (abcam, ab6276). The secondary antibodies used were provided by LI-COR. Proteins were visualized with the Odyssey bioanalyzer (LI-COR) and protein expression was quantified with the Odyssey software.

FACS analysis

Seventy-two hours after treatment with YM155 both the attached and the floating cells were fixed with 100% ethanol at -20 ºC. After fixing, the cells were stained with 0.05 mg/ml propidium iodide and 0.05 mg/ml RNAse A in PBS. After 1 hour incubation, DNA content of the nuclei was analyzed using a fluorescence activated cell sorter (Accuri). A total of 10,000 nuclei per sample were counted. The cell cycle distribution and apoptotic sub G1 fraction was determined using Flowjo.

Crystal Violet
Forty-eight hours after treatment the cells were fixed with 100% ice cold methanol for 10 minutes and stained with Crystal Violet (0.5% Crystal Violet in 25% MeOH/ 75% ddH2O) for 10 minutes. Wells were rinsed with ddH2O.

Results

BIRC5 shRNA induces apoptosis in neuroblastoma cell lines
We first validated BIRC5 as a drug target by silencing the expression using shRNA targeting the coding sequence of BIRC5 in a series of neuroblastoma cell lines. This resulted in a massive phenotypic response 72 hours after transduction in all six tested neuroblastoma cell lines (fig 1a). Western blot analysis confirmed targeted knockdown of BIRC5 in all cell lines tested. BIRC5 silencing resulted in PARP cleavage which confirms that the cells die from an apoptotic response (fig 1b). These findings establish targeted silencing of BIRC5 as a potential therapeutic intervention in neuroblastoma tumor cells and we therefore decided to test the efficacy of the small molecule BIRC5 suppressant YM155 in neuroblastoma cell lines.

YM155 sensitivity in neuroblastoma cell lines
First we determined the IC50 (concentration drug needed for 50% cell survival) for a panel of 23 neuroblastoma cell lines using an MTT-assay. This showed that 14 out of 23 cell lines were sensitive to YM155, with an IC50 below 200 nM (table 1). Examples of sensitive cell lines are SKNAS, IMR32 and SMSKCNR of which the dose-effect curves show sensitivity to YM155 in the low nM range (fig 2a). Pictures of SKNAS and IMR32 illustrate the increasing phenotypic response after treatment with accruing concentrations of YM155 (suppl fig 1a) and Crystal Violet assays showed a clear decrease of attached cells in SMSKCNR and SKNAS (suppl fig 1b). In addition to classical cell lines, we tested the sensitivity of 4 newly isolated TIC-lines to YM155. These cells were isolated directly from patient tumor or bone marrow material and maintained in neural stem cell specific medium. These TIC lines also showed sensitivity to YM155 in the low nM range (table 1).

YM155 causes apoptosis by specific silencing of BIRC5
To evaluate the phenotype after treatment with YM155, we performed Western blot analysis. SKNAS and IMR32 showed dose-dependent BIRC5 silencing, PARP cleavage occurred at 50 nM for SKNAS and 10 nM for IMR32 (fig 2b). FACS analysis

of SKNAS, IMR32 and SMSKCNR showed a large increase of the sub-G1 fraction of 32, 20 and 10 fold respectively, 48 hours after treatment with 10 nM YM155 (fig 2c). These findings indicate that YM155 causes targeted silencing of BIRC5, which induces apoptosis.

To verify if the apoptotic effect of YM155 is caused specifically by BIRC5 inhibition, we induced ectopic BIRC5 over expression in IMR32 clones with a BIRC5 cDNA construct under control of a constitutively active CMV promoter. In two independent IMR32-BIRC5 clones this resulted in rescue of the YM155-induced loss of cell viability (fig 2d). If these cells were also rescued from apoptosis induction we verified BIRC5 expression and PARP cleavage by Western blot and found a clear partial rescue from apoptosis (suppl fig 1c). This confirms that the apoptotic response after YM155 exposure results from targeted inhibition of BIRC5.

cell lines	IC50 (nM)
IMR32	0,5
AMC691T[1]	1.5
SKNAS	2
CHP134	3
AMC700B[1]	3
SMSKCNR	4
AMC700T[1]	5
GIMEN	6
LAN5	6
AMC 691B[1]	7
LAN1	10
SHEP21N	12
NMB	23
N206	35
SHEP2	39
SJNB8	73
SJNB12	78
SJNB6	192
SJNB10	306
SKNBE	356
NGP	375
SJNB1	496
UHGNP	1027
SHSY5Y	1282
SKNSH	6188
SKNFI	10000
TR14	10000

ABCB1 is the most predictive gene for YM155 resistance

These findings establish YM155 as an effective targeted compound in a series of neuroblastoma cell lines. However, in the full panel of 23 neuroblastoma cell lines the IC50 varied from 0.5 nM up to 10,000 nM and 9 out of 23 cell lines were relatively resistant to YM155 with an IC50 >200nM (table 1). We used the R2 bioinformatic platform, which contains Affymetrix mRNA expression data of 23 neuroblastoma cell lines, to identify genes that might predict or even cause resistance to YM155. Differential expression analysis between the 5 most sensitive versus the 5 most resistant classical cell lines, based on IC50 values, showed that *ABCB1* (MDR1) was the most differentially expressed gene in the analysis ($p<0.02$ Student T-test after FDR correction). *ABCB1* is an outlier as revealed from the volcano-plot of all genes, indicating its significance (fig 3a). Cell lines with a high *ABCB1* expression were resistant to YM155, whereas

Table 1: Most neuroblastoma cell lines are sensitive to YM155. The IC50 values were calculated from the curves as presented in Fig 2a. The IC50 values for YM155 of all 23 neuroblastoma cell lines and 4 TIC lines are shown in the second column of this table. [1] TIC-lines

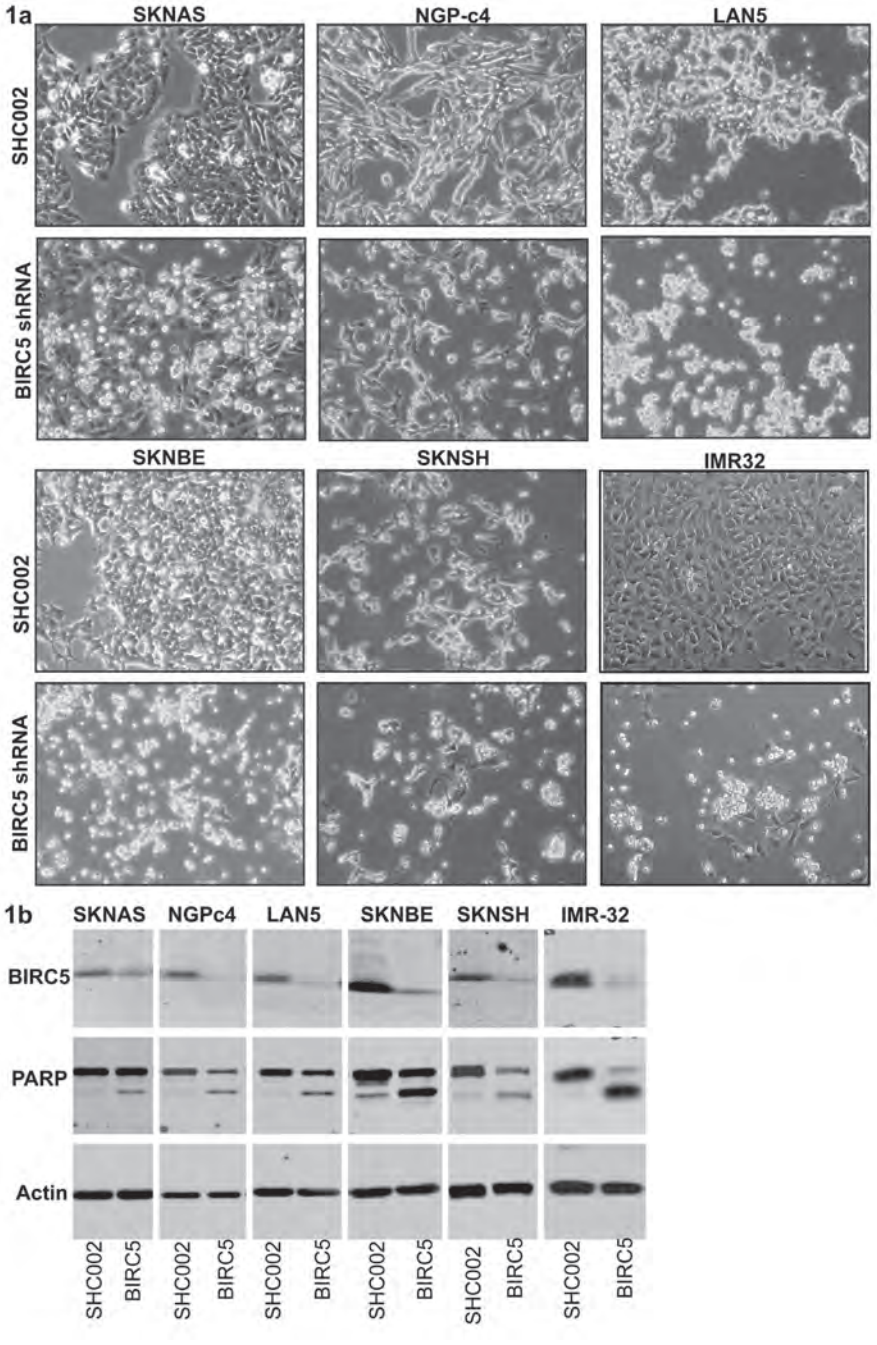

Figure 1: BIRC5 shRNA induces apoptosis in neuroblastoma cell lines

(A) 72 hours after transduction with BIRC5 shRNA or SHC002 pictures were made with a 100x magnitude. (B) Protein lysates were made of the cells of Fig 1a. Western blots were incubated with BIRC5, PARP, and Actin antibodies.

cell lines with a low ABCB1 expression were sensitive (fig 3b).

Targeted ABCB1 silencing can restore YM155 sensitivity in resistant cell lines

To confirm the functional importance of ABCB1, we combined targeted inhibition of the multidrug resistance pump with YM155 treatment. Cyclosporine can effectively and specifically inhibit ABCB1[27,31]. Eight YM155 resistant cell lines and one sensitive cell line as a control were treated with 5 μM of cyclosporine 1 hour prior to treatment with YM155. This resulted in a strong increase of sensitivity to YM155 of all cell lines with a high *ABCB1* expression (suppl fig 2a). Crystal Violet assays revealed that cyclosporine pretreated SKNSH cells survived much less efficient than YM155 only treated cells (suppl fig 2b). MTT-assays showed that cyclosporine reduced the IC50 values of all cell lines with *ABCB1* expression by 27 up to 695 fold (fig 4a, table 2). In SJNB12, which has a very low expression of *ABCB1*, co-incubation with cyclosporine did not result in a change of YM155 sensitivity (table 2). Western blot analysis of SKNSH, UHGNP and SHY5Y demonstrated that BIRC5 was inhibited when cells were pretreated with cyclosporine, but not when cells were treated with YM155 alone. In addition, cyclosporine pretreated cells showed sensitization to YM155 by an induction of PARP cleavage (fig 4b). Apoptosis was confirmed by FACS analysis, which showed that the apoptotic sub G1 fraction strongly increased in SKNSH (6 fold) and SHSY5Y (12 fold) when pretreated with cyclosporine before addition of YM155 (fig 4c).

We also knocked down ABCB1 in SKNSH with 2 lentiviral shRNAs targeting different parts of the coding sequence of ABCB1, which confirmed our findings with cyclosporine pretreated cells. The IC50 of SKNSH decreased from 370 nM in the untransduced control and 347 nM in the cells transduced with SHC002 to 35 and 29 nM in the cells transduced with either of the ABCB1 shRNAs (fig 4d). Knockdown

cell lines	IC50 (nM)	IC50 + cyclo (nM)	ratio	ABCB1 expression
SJNB10	306	9	36	155
SKNBE	356	7	51	604
SJNB1	496	2	248	747
UHGNP	1027	7	147	655
SHSY5Y	1282	8	169	522
SKNSH	6188	9	695	568
SKNFI	>10000	366	27	581
TR14	>10000	40	249	1100
SJNB12	*78*	*66*	*1*	*12*

Table 2: Resistant cell lines can be sensitized by Cyclosporine

The table represents the IC50 values for YM155 of all cell lines of the panel with *ABCB1* expression without and with pretreatment with cyclosporine (2nd and 3rd column), the ratio between these two values (4th column) and the ABCB1 RNA expression (5th column).

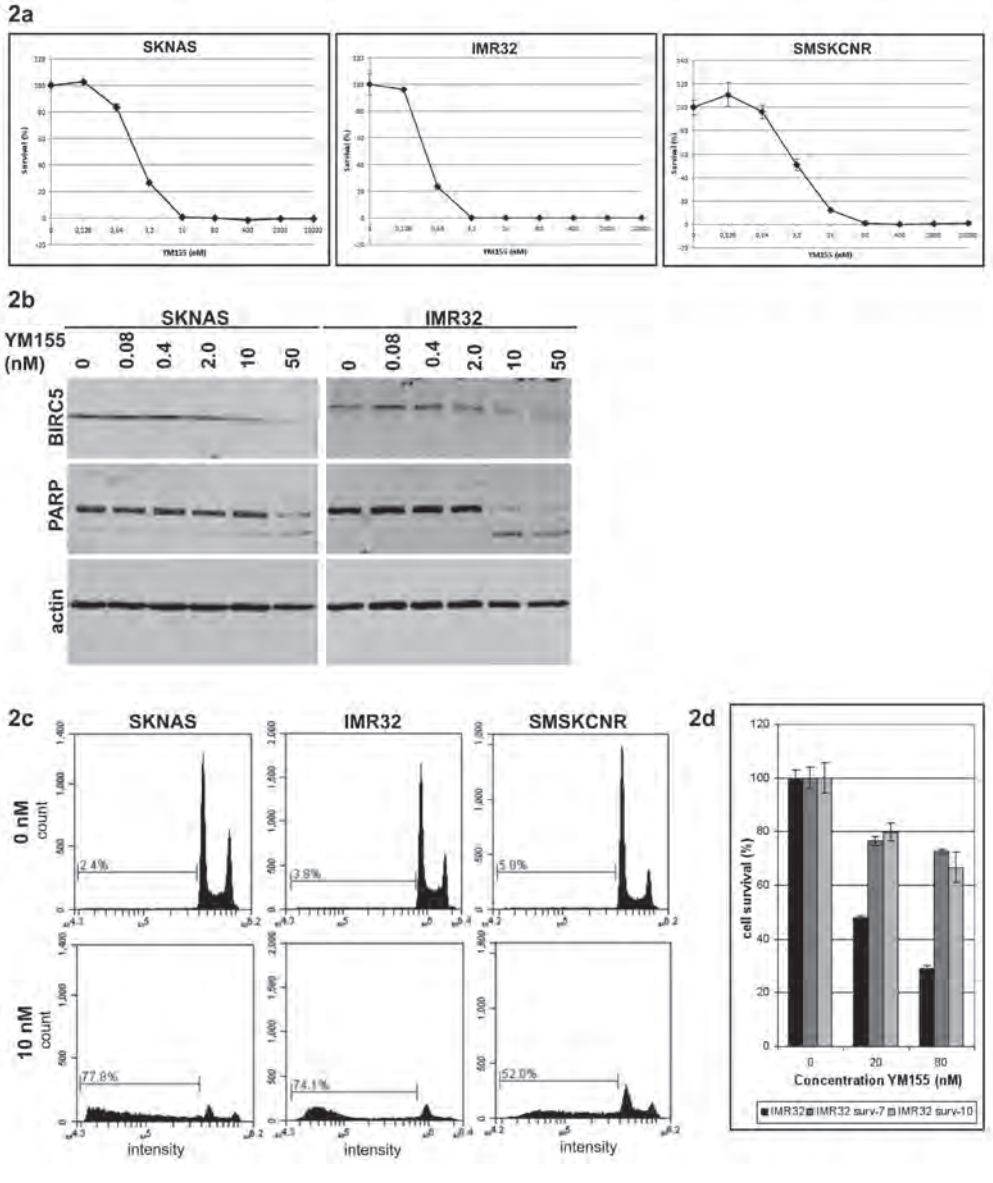

Figure 2: YM155 induces apoptosis in most neuroblastoma cell lines

(A) IC50 curves of SKNAS, IMR32 and SMSKCNR 48 hours after YM155 treatment are shown. The Y-axis represents the percentage of cell survival; the X-axis represents the concentration YM155 in nM. (B) Western blots of SKNAS and IMR32 were incubated with BIRC5, PARP and actin antibodies. The concentrations YM155 used are shown above the blots in nM. (C) FACS analysis of SKNAS, IMR32 and SMSKCNR 72 hours after treatment with YM155. The percentage of the sub G1 (apoptotic) fraction is presented in the graph. (D) MTT assay of IMR32 cells that were stably transduced with *BIRC5* over expression construct (IMR32-Surv-7 and IMR32-Surv-10) and treated with YM155 for 24 hours. The Y-axis represents the percentage of cell survival; the X-axis represents the concentration YM155.

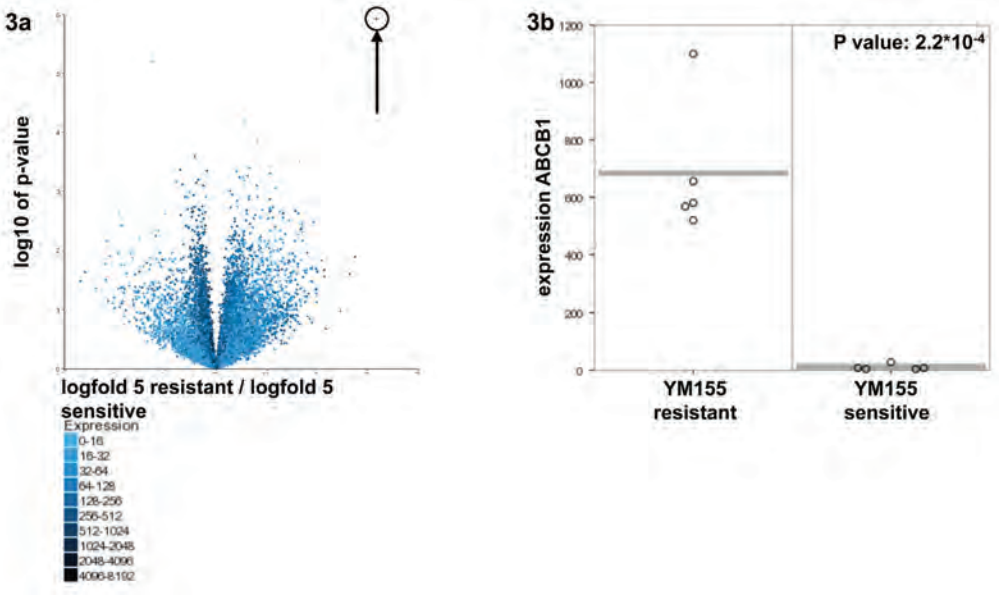

Figure 3: *ABCB1* **is the most differentially expressed gene between YM155 sensitive and resistant cell lines**

(A) Vulcano-plot of all genes based on Affymetrix Micro-array RNA expression data. The Y-axis represents the log10 of the P-value. The X-axis represents the logfold of the 5 most resistant cell lines (TR14, SKNFI, SKNSH, SHSY5Y, UHGNP) devided by the logfold of the 5 most sensitive cell lines (IMR32, SKNAS, CHP134, SMSKCNR, GIMEN). The arrow indicates *ABCB1*, which is the only significantly differentially expressed outlier. (B) Relative *ABCB1* RNA expression based on MAS5.0 corrected Affymetrix Micro-array data (Y-axis) of the 5 most sensitive versus the 5 most resistant cell lines (X-axis). The horizontal line represents the average expression.

of both ABCB1 shRNAs was validated as shown in fig 4e.

Clinical predictions with YM155 related biomarkers

ABCB1 is a multi drug resistance pump which is involved in chemoresistance in many types of cancer. Our results indicate that *ABCB1* is a potential biomarker for efficacy. The *ABCB1* mRNA expression pattern in neuroblastoma cell lines suggests dichotomy. This is to a lesser extend reflected in the neuroblastoma tumor series as shown in suppl fig 3a. We chose a cut-off value of 200 nM (as indicated in the figure) because at this value the slope of the samples ordered by *ABCB1* expression was the highest. Most interestingly, the subset of tumors with low *ABCB1* expression levels tends to correlate with prognostic factors such as age, stage, survival and *MYCN* amplification (suppl fig 3a). Also, children with a tumor with low *ABCB1* expression have a poor prognosis according to the Kaplan Meier curve ($p < 0.02$ after Bonferroni correction) (suppl fig 3b). This suggests that patients with a poor

prognosis are likely to be sensitive to YM155. In addition, we investigated if *BIRC5* could be a predictor for sensitivity. However, we did not find a correlation between the IC50 to YM155 and *BIRC5* expression in our cell line panel (suppl fig 3c) and *BIRC5* can therefore not be used as a predictor for sensitivity in neuroblastoma patients. This also holds true if we exclude the cell lines with high *ABCB1* expression (data not shown).

Discussion

We conclude that 14 out of 23 neuroblastoma cell lines are sensitive to YM155 in the low nM range. Most small molecule compounds used in anticancer treatment are known to inhibit a variety of genes. The lack of specificity is an important cause of the severe side effects of these compounds and it is well established that blocking a single target with high potency minimizes the side effects.[32] YM155 was picked up by a screen that was designed to select compounds in a chemical compound library efficiently inhibiting the *BIRC5* promoter.[21] This resulted in a highly effective BIRC5 suppressant as was validated in our experiments. We were able to rescue YM155 induced apoptosis by *BIRC5* over-expression, which suggests that YM155 is a highly specific BIRC5 suppressant. These findings establish YM155 as an interesting compound for treatment of neuroblastoma patients.

Most interestingly, also the 4 TIC lines we tested were shown to be very sensitive to YM155. These TIC lines are cultured in neural stem cell medium, grow in spheroids and have been cultured only for a limited number of passages. Therefore these cells are thought to be a better representation of in vivo neuroblastoma tumors.[33] In addition these cells have been shown to have increased tumorigenecity in in vivo models.

Analysis of the differential expression between the 5 most sensitive and the 5 most resistant classical cell lines revealed that increased expression of *ABCB1* is a good predictor for insensitivity to YM155. The other ABC transporters that are known as a multi drug resistant pump (*ABCC1* and *ABCG2*) did not reveal any significant correlation between these two groups (data not shown). Inhibition of ABCB1 with cyclosporine resulted in sensitization of all resistant cell lines with *ABCB1* expression, which was confirmed by shRNA mediated silencing of ABCB1. Cyclosporine is originally used as an immunosuppressant drug in patients after

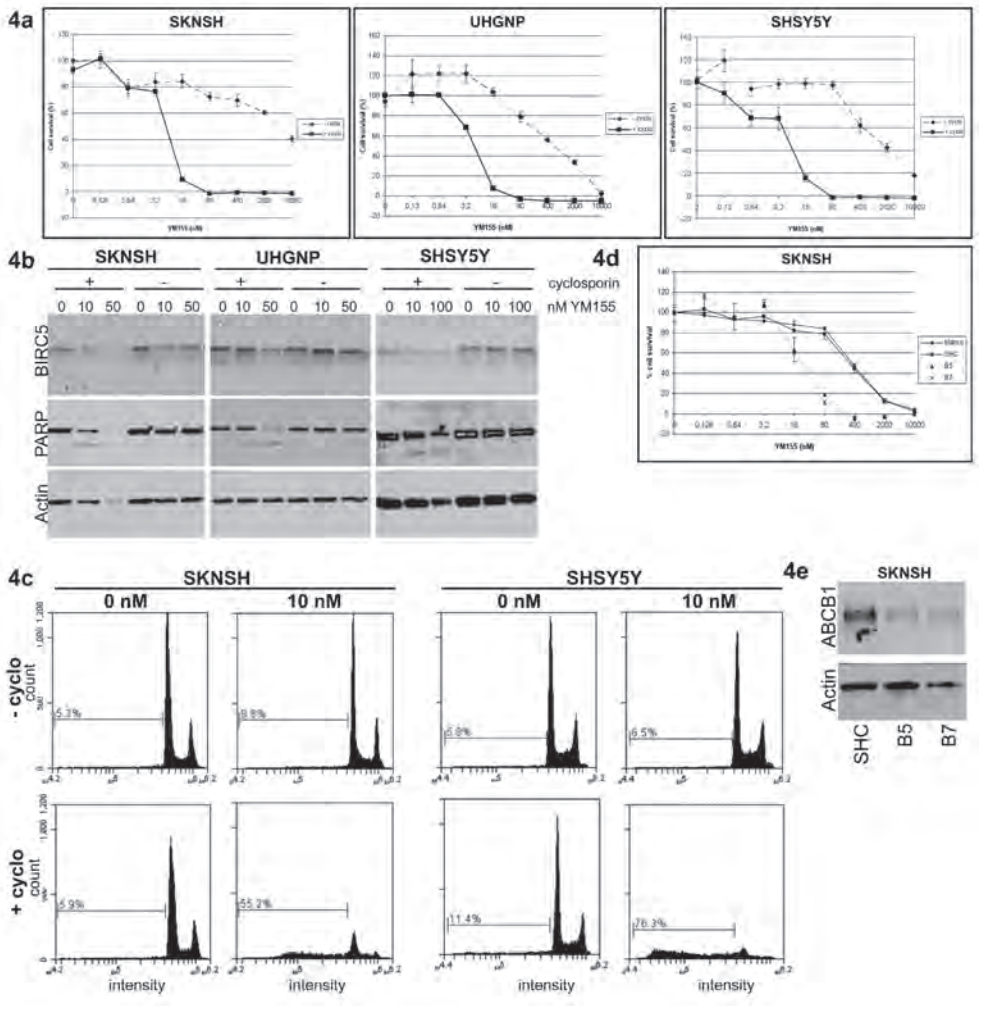

Figure 4: Resistant cell lines can be sensitized by Cyclosporine or ABCB1 shRNA

(A) MTT-assay was performed 72 hours after treatment with YM155. 3 cell lines that were treated with YM155 with or without cyclosporine are shown. The Y-axis represents the percentage cell survival; the X-axis represents the concentration YM155 in nM. The dotted line is the curve for YM155 without cyclosporine; the continuous line is the curve for the combination of YM155 and cyclosporine. (B) Western blots were incubated with BIRC5, PARP and actin antibodies. 3 Cell lines are shown, the concentration YM155 is depicted in nM. (C) FACS analysis of SKNSH and SHSY5Y treated with YM155 with or without cyclosporin. The percentage of the sub G1 (apoptotic) fraction is presented in the graph. (D) SKNSH cells were transduced with 2 different ABCB1 shRNAs (B5 and B7) or with SHC002 (control virus). 72 hours after transduction cells were treated with a concentration series of YM155. 72 hours after treatment an MTT-assay was performed as described previously. The Y-axis represents the percentage of cell survival; the X-axis represents the concentration YM155 in µM. (E) Knockdown of ABCB1 protein in SKNSH 72 hours after transduction with both ABCB1 shRNAs was checked by Western blot. Blots were incubated with ABCB1 and Actin antibodies.

organ transplantation. It is also an active inhibitor of ABCB1; however for this use high concentrations were needed and found to be toxic in combination treatment presumably because cyclosporine induced sensitization of the bone marrow to chemo therapy.[27,34] Currently, new inhibitors of ABC transporters are in clinical development, such as PSC833, V-104, tarquidar and ONT-093.[26-28] After clinical implementation these compounds could be combined with YM155.

Still, targeted ABCB1 inhibition is currently not possible in a clinical setting. The over-expression of ABCB1 in neuroblastoma however can be used as a selection biomarker. *BIRC5* is over-expressed in almost all high risk neuroblastoma and in principle serves as drug target in these patients. As high *ABCB1* expression prevents effective targeting, we propose to select ABCB1 negative patients for clinical testing of YM155. Most interestingly, this group of patients tends to have a very poor prognosis and new therapeutic options are urgently needed in this specific subgroup.

Before YM155 can be used in a Phase I/II clinical trial in neuroblastoma patients, the compound needs to be validated in a neuroblastoma mouse model. New compounds will only be used in neuroblastoma patients in combination with the currently used cytostatics. Therefore these interactions need to be evaluated. The knowledge that mitotic catastrophe is involved in the apoptotic response after BIRC5 knockdown can also guide compound combination strategies.[11] Simultaneous inhibition of other genes in the same signal transduction pathway could lead to additional or synergistic effects. For example AURKB inhibitors could potentially enhance the effect of BIRC5 inhibition as they both are part of the chromosomal passenger complex. Mitotic catastrophe results in an apoptotic response via mitochondrial release of pro-apoptotic proteins. Sensitization of this downstream signal transduction pathway by BCL2 inhibitors or SMAC mimetics might lead to synergism with a BIRC5 inhibitor. Based on in vivo experiments and on knowledge about the efficacy of YM155 combined with other drugs, a Phase I/II clinical trial can be designed.

Acknowledgements

This research was supported by grants from KIKA foundation, SKK and Netherlands Cancer Foundation.

23. Tolcher, A.W., Mita, A., Lewis, L.D., Garrett, C.R., Till, E., Daud, A.I. et al, Phase I and Pharmacokinetic Study of YM155, a Small-Molecule Inhibitor of Survivin. Journal of Clinical Oncology, 2008; 26**:** 5198-5203.
24. Lewis, K.D., Samlowski, W., Ward, J., Catlett, J., Cranmer, L., Kirkwood, J. et al, A multi-center phase II evaluation of the small molecule survivin suppressor YM155 in patients with unresectable stage III or IV melanoma. Invest New Drugs, 2009.
25. Giaccone, G., Zatloukal, P., Roubec, J., Floor, K., Musil, J., Kuta, M. et al, Multicenter Phase II Trial of YM155, a Small-Molecule Suppressor of Survivin, in Patients With Advanced, Refractory, Non-Small-Cell Lung Cancer. Journal of Clinical Oncology, 2009; 27**:** 4481-4486.
26. Evers, R., Kool, M., Smith, A.J., van Deemter, L., de Haas, M., and Borst, P., Inhibitory effect of the reversal agents V-104, GF120918 and pluronic L61 on MDR1 Pgp-, MRP1- and MRP2-mediated transport. British Journal of Cancer, 2000; 83**:** 366-374.
27. Shen, F., Chu, S., Bence, A.K., Bailey, B., Xue, X., Erickson, P.A. et al, Quantitation of doxorubicin uptake, efflux, and modulation of multidrug resistance (MDR) in MDR human cancer cells. Journal of Pharmacology and Experimental Therapeutics, 2008; 324**:** 95-102.
28. Smith, A.J., Mayer, U., Schinkel, A.H., and Borst, P., Availability of PSC833, a substrate and inhibitor of P-glycoproteins, in various concentrations of serum. Journal of the National Cancer Institute, 1998; 90**:** 1161-1166.
29. Molenaar, J.J., Ebus, M.E., Koster, J., van Sluis, P., van Noesel, C.J.M., Versteeg, R. et al, Cyclin D1 and CDK4 activity contribute to the undifferentiated phenotype in neuroblastoma. Cancer Research, 2008; 68**:** 2599-2609.
30. Morozova, O., Vojvodic, M., Grinshtein, N., Hansford, L.M., Blakely, K.M., Maslova, A. et al, System-Level Analysis of Neuroblastoma Tumor-Initiating Cells Implicates AURKB as a Novel Drug Target for Neuroblastoma. Clinical Cancer Research, 2010; 16**:** 4572-4582.
31. Glavinas, H., Krajcsi, P., Cserepes, J., and Sarkadi, B., The role of ABC transporters in drug resistance, metabolism and toxicity. Curr.Drug Deliv., 2004; 1**:** 27-42.
32. Imming, P., Sinning, C., and Meyer, A., Drugs, their targets and the nature and number of drug targets (vol 5, pg 821, 2006). Nature Reviews Drug Discovery, 2007; 6**:** 126.
33. Zhang, L., Smith, K.M., Chong, A.L., Stempak, D., Yeger, H., Marrano, P. et al, In vivo antitumor and antimetastatic activity of sunitinib in preclinical neuroblastoma mouse model. Neoplasia., 2009; 11**:** 426-435.
34. Nobili, S., Landini, I., Giglioni, B., and Mini, E., Pharmacological strategies for overcoming multidrug resistance. Current Drug Targets, 2006; 7**:** 861-879.

Reference List

1. Fangusaro, J.R., Caldas, H., Jiang, Y.Y., and Altura, R.A., Survivin: An inhibitor of apoptosis in pediatric cancer. Pediatric Blood & Cancer, 2006; 47**:** 4-13.
2. Song, Z.Y., Yao, X.B., and Wu, M., Direct interaction between survivin and Smac/DIABLO is essential for the anti-apoptotic activity of survivin during taxol-induced apoptosis. Journal of Biological Chemistry, 2003; 278**:** 23130-23140.
3. Wheatley, S.P. and McNeish, A., Survivin: A protein with dual roles in mitosis and apoptosis. International Review of Cytology - A Survey of Cell Biology, Vol 247, 2005; 247**:** 35-+.
4. Castedo, M., Perfettini, J.L., Roumie, T., Andreau, K., Medema, R., and Kroemer, G., Cell death by mitotic catastrophe: a molecular definition. Oncogene, 2004; 23**:** 2825-2837.
5. Castedo, M., Perfettini, J.L., Roumier, T., Valent, A., Raslova, H., Yakushijin, K. et al, Mitotic catastrophe constitutes a special case of apoptosis whose suppression entails aneuploidy. Oncogene, 2004; 23**:** 4362-4370.
6. Altieri, D.C., The case for survivin as a regulator of microtubule dynamics and cell-death decisions. Current Opinion in Cell Biology, 2006; 18**:** 609-615.
7. Lens, S.M.A., Wolthuis, R.M.F., Klompmaker, R., Kauw, J., Agami, R., Brummelkamp, T. et al, Survivin is required for a sustained spindle checkpoint arrest in response to lack of tension. Embo Journal, 2003; 22**:** 2934-2947.
8. Brodeur, G.M., Neuroblastoma: Biological insights into a clinical enigma. Nature Reviews Cancer, 2003; 3**:** 203-216.
9. Maris, J.M., Hogarty, M.D., Bagatell, R., and Cohn, S.L., Neuroblastoma. Lancet, 2007; 369**:** 2106-2120.
10. Maris, J.M., Medical Progress: Recent Advances in Neuroblastoma. New England Journal of Medicine, 2010; 362**:** 2202-2211.
11. Lamers, F., van der Ploeg, I., Schild, L., Ebus, M.E., Koster, J., Hansen, B.R. et al, Knockdown of Survivin (BIRC5) causes Apoptosis in Neuroblastoma via Mitotic Catastrophe. Endocrine Related Cancer, 2011;18(6):657-68.
12. Fesik, S.W., Promoting apoptosis as a strategy for cancer drug discovery. Nature Reviews Cancer, 2005; 5**:** 876-885.
13. Reed, J.C. and Pellecchia, M., Apoptosis-based therapies for hematologic malignancies. Blood, 2005; 106**:** 408-418.
14. Molenaar, J.J., Ebus, M.E., Geerts, D., Koster, J., Lamers, F., Valentijn, L.J. et al, Inactivation of CDK2 is synthetically lethal to MYCN over-expressing cancer cells. Proceedings of the National Academy of Sciences of the United States of America, 2009; 106**:** 12968-12973.
15. Van Maerken, T., Ferdinande, L., Taildeman, J., Lambertz, I., Yigit, N., Vercruysse, L. et al, Antitumor Activity of the Selective MDM2 Antagonist Nutlin-3 Against Chemoresistant Neuroblastoma With Wild-Type p53. Journal of the National Cancer Institute, 2009; 101**:** 1562-1574.
16. van Noesel, M.M. and Versteeg, R., Pediatric neuroblastomas: genetic and epigenetic 'Danse Macabre'. Gene, 2004; 325**:** 1-15.
17. Goldsmith, K.C., Lestini, B.J., Gross, M., Ip, L., Bhumbla, A., Zhang, X. et al, BH3 response profiles from neuroblastoma mitochondria predict activity of small molecule Bcl-2 family antagonists. Cell Death and Differentiation, 2010; 17**:** 872-882.
18. Lestini, B.J., Goldsmith, K.C., Fluchel, M.N., Liu, X.Y., Chen, N.L., Goyal, B. et al, Mcl1 downregulation sensitizes neuroblastoma to cytotoxic chemotherapy and small molecule Bcl2-family antagonists. Cancer Biology & Therapy, 2009; 8**:** 1587-1595.
19. Sapra, P., Wang, M., Bandaru, R., Zhao, H., Greenberger, L.M., and Horak, I.D., Down-modulation of survivin expression and inhibition of tumor growth in vivo by EZN-3042, a locked nucleic acid antisense oligonucleotide. Nucleosides Nucleotides Nucleic Acids, 2010.
20. Ryan, B.M., O'Donovan, N., and Duffy, M.J., Survivin: A new target for anti-cancer therapy. Cancer Treatment Reviews, 2009; 35**:** 553-562.
21. Nakahara, T., Takeuchi, M., Kinoyama, I., Minematsu, T., Shirasuna, K., Matsuhisa, A. et al, YM155, a novel small-molecule survivin suppressant, induces regression of established human hormone-refractory prostate tumor xenografts. Cancer Research, 2007; 67**:** 8014-8021.
22. Satoh, T., Okamoto, I., Miyazaki, M., Morinaga, R., Tsuya, A., Hasegawa, Y. et al, Phase I Study of YM155, a Novel Survivin Suppressant, in Patients with Advanced Solid Tumors. Clinical Cancer Research, 2009; 15**:** 3872-3880.

Supplementary Figures

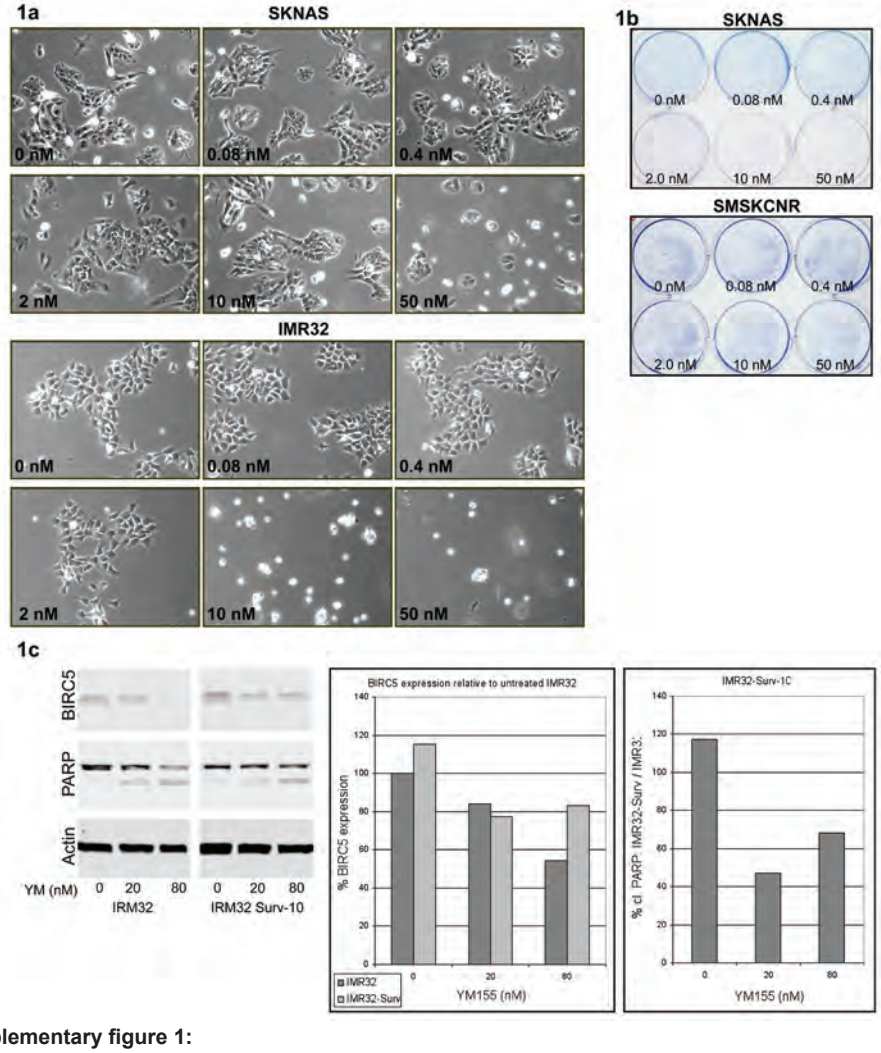

Supplementary figure 1:

(A) SKNAS and IMR32 cells were treated with a concentration series of YM155 24 hours after plating. Pictures were made 48 hours after treatment with a 100x magnitude. (B) 48 hours after treatment with YM155, SKNAS and SMSKCNR cells were fixed with methanol and stained with crystal violet (concentrations depicted in each well). (C) Left: Western blot of IMR32 and IMR32 with *BIRC5* over-expression treated with YM155. Concentrations YM155 are depicted below in nM. Blots were stained with BIRC5, PARP and Actin antibodies. These lanes were on the same blot. BIRC5 expression was quantified and corrected for actin which is represented in the middle panel. The Y-axis represents the percentage BIRC5 expression relative to IMR32 without YM155. On the X-axis the concentration YM155 is shown in nM. The dark bars represent IMR32 and the light bars represent IMR32-Surv-10. Right: PARP cleavage was quantified and corrected for actin. On the Y-axis the percentage of cleaved PARP in IMR32-Surv-10 relative to IMR32 treated with the same concentration YM155 is shown. The X-axis represents the concentration YM155 in nM.

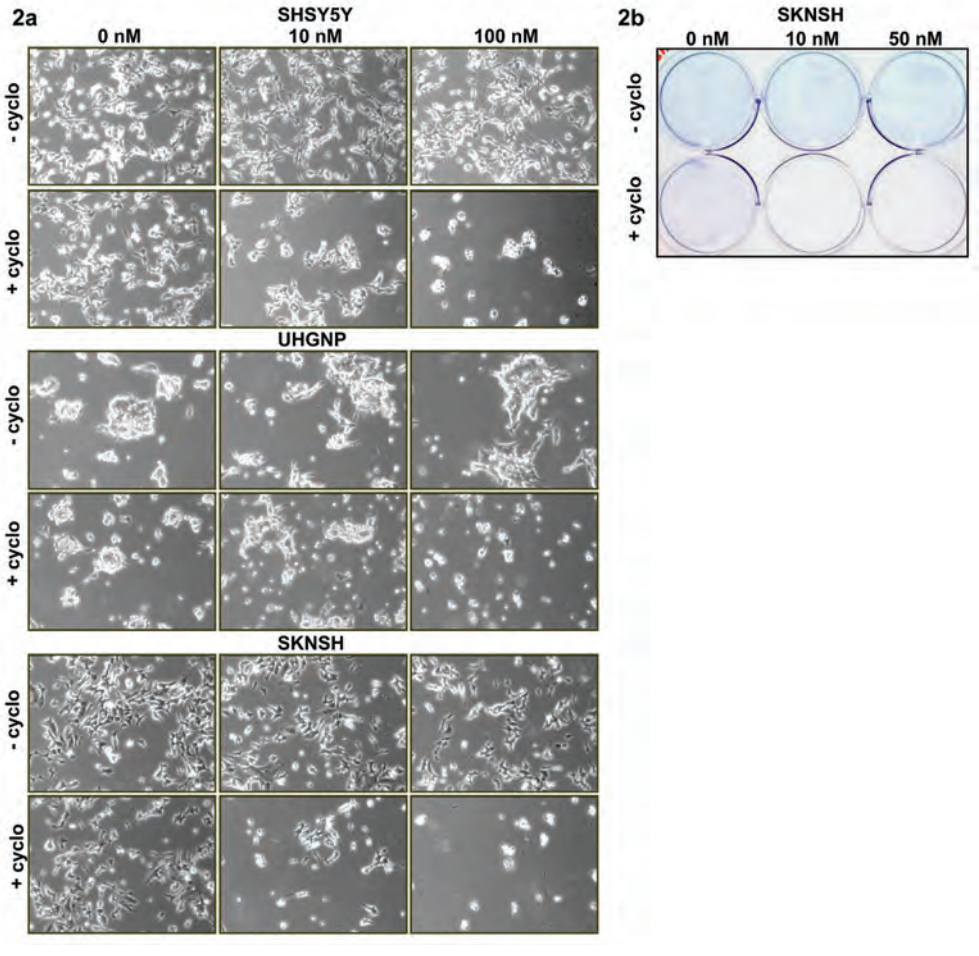

Supplementary figure 2:

(A) Cells were treated with cyclosporine 24 hours after plating. After 1 hour of incubation YM155 was added. Pictures were made 48 hours after treatment with a 100x magnitude. (B) SKNSH cells were treated with cyclosporine prior to treatment with YM155 (concentrations depicted above the wells) and fixed with methanol and stained with crystal violet.

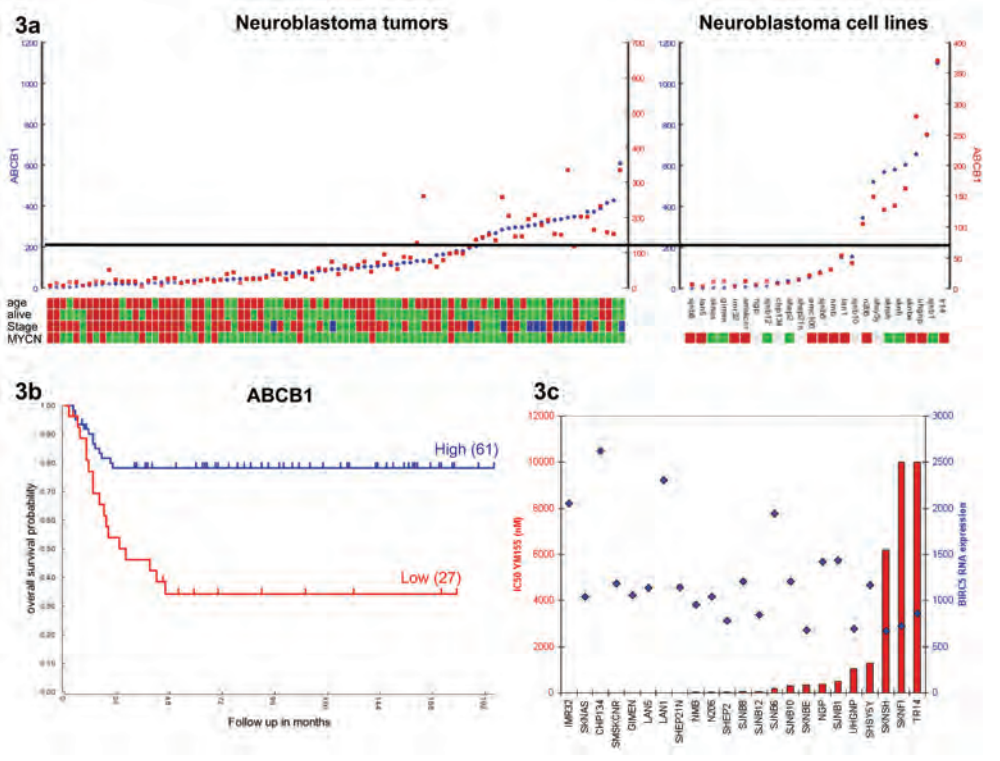

Supplementary figure 3:

(A) The left panel indicates the Relative ABCB1 RNA expression based on MAS5.0 corrected Affymetrix Micro-array data (Y-axis) of 88 neuroblastoma tumors (X-axis) ordered by *ABCB1* expression. *ABCB1* expression was determined by two different probe sets. Every dot represents one sample; below every dot clinical information is given. Age: red is >= 1 year; green is < 1 year. Alive: red = deceased, green = alive. Stage: red = stage 3 or 4, green = stage 1 or 2, blue = stage 4S. MYCN: red = amplified, green = not amplified. The right panel shows the ABCB1 RNA expression levels in the neuroblastoma cell lines of our panel ordered by *ABCB1*. Both Y-axes represent different probe sets for ABCB1; cell lines are depicted below together with the NMYC status: red = amplified, green = not amplified, grey = not determined. The black line indicates the proposed cut-off for YM155 sensitivity prediction. (B) Kaplan Meier curve of 88 neuroblastoma tumors based on Affymetrix Micro-array RNA expression data. On the Y-axis the overall survival probability is presented and on the X-axis the time in months after diagnosis. The blue line represents the patients with a tumor with high *ABCB1* expression; the red line represents the patients with a tumor with low *ABCB1* expression. The P-value is under 0.02 after Bonferroni correction with an RNA expression cutoff of 39.1. The cutoff was chosen that gives the lowest P-value with at least 10 samples in one group. (C) The red bars represent IC50 levels for all neuroblastoma cell lines tested; the blue dots represent BIRC5 RNA expression levels as determined by Affymetrix microarray. The cell lines are depicted below.


Apoptosis
C
CASP3
C
BAX
BAX
BAX
BCL2

4

Targeted BCL2 Inhibition Effectively Inhibits Neuroblastoma Tumor Growth

Targeted BCL2 Inhibition Effectively Inhibits Neuroblastoma Tumor Growth

Fieke Lamers[1], Linda Schild[1], Ilona J.M. den Hartog[1] Marli E. Ebus[1], Ellen M. Westerhout[1], Ingrid Øra[2], Jan Koster[1], Rogier Versteeg[1], Huib N. Caron[3], Jan J. Molenaar[1]

[1] Department of Oncogenomics, Academic Medical Center, University of Amsterdam, Meibergdreef 15, PO box 22700, 1105 AZ Amsterdam, The Netherlands.
[2] Department of Pediatric Oncology, Skåne University Hospital, Lund University, Lund, Sweden.
[3] Department of Pediatric Oncology, Emma Kinderziekenhuis, Academic Medical Center, University of Amsterdam, Meibergdreef 15, PO box 22700, 1105 AZ Amsterdam, the Netherlands

Abstract

Genomic aberrations of key regulators of the apoptotic pathway have hardly been identified in neuroblastoma. We detected high *BCL2* mRNA and protein levels in the majority of neuroblastoma tumors by Affymetrix expression profiling and Tissue Micro Array analysis. This *BCL2* mRNA expression is strongly elevated compared to normal tissues and other malignancies. Most neuroblastoma cell lines lack this high *BCL2* expression. Only two neuroblastoma cell lines (KCNR and SJNB12) show *BCL2* expression levels representative for neuroblastoma tumors. To validate *BCL2* as a therapeutic target in neuroblastoma we employed lentivirally mediated shRNA. Silencing of *BCL2* in KCNR and SJNB12 resulted in massive apoptosis, while cell lines with low *BCL2* expression were insensitive. Identical results were obtained by treatment of the neuroblastoma cell lines with the small molecule BCL2 inhibitor ABT263, which is currently being clinically evaluated. Combination assays of ABT263 with most classical cytostatics showed strong synergistic responses. Subcutaneous xenografts of a neuroblastoma cell line with high *BCL2* expression in NMRI nu/nu mice showed a strong response to ABT263. These findings establish BCL2 as a promising drug target in neuroblastoma and warrant further evaluation of ABT263 and other BCL2 inhibiting drugs.

Introduction

BCL2 is an anti-apoptotic member of the BCL2 family proteins.[1] When localized at the outer mitochondrial membrane it binds BAX and BAK resulting in inhibition of pore formation and prevention of cytosolic release of caspase-activating proteins.[1,2] *BCL2* was originally identified as a partner of t(14;18) translocations that occur in nearly all cases of follicular lymphoma and in some diffuse large B-cell lymphoma. Also amplification of *BCL2* is found in these malignancies.[3] *BCL2* transgenic mice are known to develop follicular lymphoma, indicating its oncogenic function.[4] Deregulation of other *BCL2* family members is found in several other tumor types and is correlated with therapy resistance.[1,2]. BCL2 inhibitors are in phase 1/2 clinical trials for several malignancies such as chronic lymphocytic leukemia, glioblastoma, small cell lung cancer and malignant melanoma, showing promising results.[1,5-7]

Neuroblastoma are pediatric tumors that originate from the embryonal precursor cells of the sympathetic nervous system. Despite extensive treatment, children with high stage neuroblastoma have a poor prognosis with 20 to 40% overall survival.[8-11] Genomic aberrations in genes directly involved in apoptotic signaling are rare in neuroblastoma. Deregulation seems to be caused by epigenetic events.[12,13] P53 is mostly intact in primary neuroblastoma although signaling has shown to be disturbed.[10] *CASP8 (Caspase 8)* is hypermethylated and thereby inactive in some neuroblastoma resulting in an inactive extrinsic apoptotic pathway.[10] And finally the inhibitor of apoptosis gene *BIRC5 (Survivin)* is highly expressed in neuroblastoma, which correlates to a poor prognosis.[14-16] None of these signaling proteins is currently a prime candidate for targeted inhibition. P53 inhibition by Nutlin has shown to be effective in neuroblastoma but clinical application awaits new generations of this type of compound.[17] Direct inhibitors of BIRC5 signaling are not available, but YM155, a transcriptional inhibitor of *BIRC5* has shown promising results in vitro and in vivo.[18-23] However, additional targets in the apoptotic pathway for which clinically applicable compounds are available are urgently needed.

The role of BCL2 family members in neuroblastoma has been subject of several studies. *BCL2* expression was reported to be strongly increased in developing sympathetic nervous system and was suggested to regulate survival during maturation.[24-26] Another member of the BCL2 family, *MCL1*, has been reported to mimic the BCL2 function and to circumvent the effects of BCL2 inhibition in neuroblastoma. Compounds that modulate both MCL1 and BCL2 were found to be

most effective in neuroblastoma cell lines and a profile of the pro-apoptotic members of the BCL2 family proteins can predict sensitivity of neuroblastoma cell lines to BCL2 inhibitors.[27,28]

Several inhibitors of BCL2 are currently in clinical trials.[5,12,13] G3139 is an antisense oligodeoxynucleotide targeting *BCL2* mRNA resulting in RNAse H activation. ABT263 is a small molecule mimetic of the BH3 domain of the pro-apoptotic BAD protein that is currently in clinical trial in chronic lymphatic leukemia.[29] ABT263 binds with high affinity to BCL2, BCLXL and BCLW resulting in inhibition of these proteins, but binds with a much lower affinity to MCL1 and BCL2A1[30] This BCL2 small molecule inhibitor has been studied in the Pediatric Preclinical drug Testing Program (PPTP) and was not found to be effective in five neuroblastoma in vivo tumor models.[31]

In this study we showed that most neuroblastoma tumors have high BCL2 expression, but most neuroblastoma cell lines lack BCL2. Targeted inhibition of *BCL2* by lentiviral shRNA resulted in massive apoptosis in two neuroblastoma cell lines with high BCL2 expression, but not in neuroblastoma cell lines with low or absent expression of *BCL2*. The small molecule BCL2 inhibitor ABT263 achieved the same results. Combination assays of ABT263 with most classical cytostatics showed strong synergistic responses. ABT263 showed anti-tumor efficacy in a neuroblastoma xenograft model. Our pre-clinical data package provides a strong rational for clinical development of ABT263 in neuroblastoma patients.

Methods

Patient Material

The neuroblastic tumor panel used for Affymetrix microarray analysis contains 88 neuroblastoma samples. All samples were derived from primary tumors obtained at diagnosis from patients treated at the Emma Childen's Hospital in Amsterdam from 1991. Material was obtained during surgery and immediately frozen in liquid nitrogen.

RNA extraction and Affymetrix profiling

For profiling total RNA of neuroblastoma cell lines and tumors was extracted using Trizol reagent (Invitrogen) according to the manufacturer's protocol. RNA concentration was determined using the NanoDrop ND-1000 and quality was

determined using the RNA 6000 Nano assay on the Agilent 2100 Bioanalyzer (Agilent Technologies). For Affymetrix Microarray analysis, fragmentation of RNA, labeling, hybridization to HG-U133 Plus 2.0 microarrays and scanning was carried out according to the manufacturer's protocol (Affymetrix Inc.). The expression data were normalized with the MAS5.0 algorithm within the GCOS program of Affymetrix. Target intensity was set to 100 (α1=0.04 and α2 0.06). If more than one probe set was available for one gene the probe set with the highest expression was selected, considered that the probe set was correctly located on the gene of interest. Mostly this is a probe set at the 3' end. Public available neuroblastoma datasets we used were of Delattre[32], Lastowska (geo ID: gse13136) and Speleman[33]. Public available datasets were used for comparing neuroblastoma with normal tissues (Roth dataset, geo ID: gse3526) and adult tumors (EXPO dataset, geo ID: gse2109). The data were analyzed with the R2 microarray analysis and visualization platform (http://r2.amc.nl).

Tissue array

Paraffin-embedded tumors were cut into 4-µm sections, mounted on aminoalkylsaline-coated glass slides, and dried overnight at 37°C. Sections were dewaxed in xylene and graded ethanol, and endogenous peroxidase was blocked in a 0.3% H2O2 solution in 100% methanol. Subsequently, the slides were rinsed thoroughly in distilled water and pretreated with a boiling procedure for 10 min in 10/1 mM Tris/EDTA pH 9 in an autoclave. After rinsing in distilled water and PBS, slides were incubated with primary antibody against BCL2 (M0887, DAKO). Slides were incubated for 1 hour in room temperature in a 1:100 solution (diluted in an antibody diluent). Slides were then blocked with a postantibody blocking (Power Vision kit, ImmunoLogic) 1:1 diluted in PBS for 15 minutes, followed by a 30-minute incubation with poly–horseradish peroxidase (HRP)–goat α mouse/rabbit IgG (Power Vision kit, ImmunoLogic) 1:1 diluted in PBS. Chromogen and substrate were 3,3′-diaminobenzidine (DAB) and peroxide (1% DAB and 1% peroxide in distilled water). Nuclear counterstaining was done with hematoxylin. After dewatering in graded ethanol and xylene, slides were coated with glass and evaluated independently by two observers. As a negative control we used liver tissue.

Cell lines

All cell lines were grown in Dulbecco Modified Eagle Medium (DMEM), supplemented with 10% fetal calf serum, 10 mM L-glutamine, 10 U/ml penicillin, Non Essential Amino Acids (1x) and 10 µg/ml streptomycin. Cells were maintained at 37 ˚C under

5% CO_2. For primary references of these cell lines, see Molenaar et al[34].

Lentiviral shRNA production and transduction

Lentiviral particles were produced in HEK293T cells by cotransfection of lentiviral vector containing the short hairpin RNA (shRNA) with lentiviral packaging plasmids pMD2G, pRRE and pRSV/REV using FuGene HD. Supernatant of the HEK293T cells was harvested at 48 and 72 hours after transfection, which was purified by filtration and ultracentrifuging. The concentration was determined by a p24 ELISA.

Cells were plated in a 10% confluence. After 24 hours cells were transduced with lentiviral BCL2 shRNA (Sigma, TRCN0000040069 and TRCN0000040071) in various concentrations (Multiplicity of infection (MOI): 1 – 3). SHC-002 shRNA (non-targeting shRNA: CAACAAGATGAAGAGCACCAA) was used as a negative control. 24 hours after transduction medium was refreshed and puromycin was added to determine the efficacy of transduction. Protein of floating and attached cells was harvested 72 hours after transduction and analyzed by Western blot. Nuclei were harvested 48 and 72 hours after transfection for FACS analysis.

Lentiviral over-expression clones

BCL2 and *MCL1* cDNA was obtained from a plasmid provided by addgene (plasmid 21605 and 8768:3336)[35,36] and cloned into pLenti4/TO/V5-Dest according to manufacturer's procedures (Invitrogen). The sequence has been checked using the manufacturer's primers (pL4-TO/V5 fwd and pL4-dest rev)

Compounds

ABT263 (Toronto Research Chemicals) was dissolved in DMSO in a stock concentration of 20 mM from which concentration series were made in medium from 0.001 to 100 µM. Other compounds used were obtained from Sigma-Aldrich. Stock solutions were made for Vincristin (10 mM in dH_2O), Etoposide (50 mM in DMSO), Cisplatin (50 mM in DMF) and doxorubicin (50 mM in dH_2O). Compound was added to the cells 24 hours after plating.

MTT-assay

Cells were plated in a 10-30% confluence in a 96-well plate and treated after 24 hours with ABT263 in a concentration range between 0.008 to 20 µM. 72 hours after treatment, 10 µl of Thyazolyl blue tetrazolium bromide (MTT, Sigma M2128) was added. After 4-6 hours of incubation 100 µl of 10% SDS, 0.01 M HCl was added to stop the reaction. The absorbance was measured at 570 nm and 720 nm using

a platereader (biotek). The IC50 (concentration drug needed for 50% cell viability reduction) was calculated using concentration vector curves. For synergy assays ABT263 was combined with doxorubicin, cisplatin, vincristin or etoposide in a 96-well plate format. 24 hours after plating the cells in a 10-30% confluence, both compounds were added at the same time. All experiments were performed multiple times in duplo. The Combination Index (CI) was calculated by the Chou Talalay method[37] using the CalcuSyn software.

Western Blotting

48 hours after treatment with ABT263, attached and floating cells were harvested on ice. Cells were lysated with Laemmlibuffer (20% glycerol, 4% SDS, 100mM Tris HCl pH 6.8 in mQ). Protein was quantified with RC-DC protein assay (Bio-Rad). Lysates were separated on a 10 % SDS-Page gel and electroblotted on a transfer membrane (Millipore, IPFL00010). Blocking and incubation were performed in OBB according to manufacturer's protocol (LI-COR). Primary antibodies used were BCL2 rabbit polyclonal (cell signaling, #2872), PARP rabbit polyclonal (cell signaling, #9542), Cytochrome C mouse monoclonal (BD Pharmingen, 556433) and β-actin mouse monoclonal (abcam, ab6276). The secondary antibodies used were provided by LI-COR. Proteins were visualized with the Odyssey bioanalyzer (LI-COR).

Cell fractionation

Protein of SJNB12 cells was harvested and fractionated using the Subcellular Proteome Extraction Kit according to manufacturer's protocol (Novagen, 539790). Fraction I (cytosol) and II (cell organelle) were used for Western blot

FACS analysis

72 hours after treatment with ABT263 both the attached and the floating cells were fixed with 100% ethanol at -20 ºC. After fixing, the cells were stained with 0.05 mg/ml propidium iodide and 0.05 mg/ml RNAse A in PBS. After 1 hour incubation, DNA content of the nuclei was analyzed using a fluorescence activated cell sorter. A total of 10,000 nuclei per sample were counted. The cell cycle distribution and apoptotic sub G1 fraction was determined using Flowjo.

Mouse model

The animal experiments were performed with permission and according to the standards of the Dutch committee for animal research ethics (DEC 101934). $2.5*10^6$ cells of KCNR were injected subcutaneously in both flanks of NMRI nu/nu mice.

Tumors were allowed to grow to 500 mm^3. One of these subcutaneous tumors was harvested and cut in pieces of 2 x 2 mm for subsequent subcutaneous transplantation in both flanks of the next generation mice. For the experiment we used 2 groups of 6 mice each and we started treatment 4 days after implantation of the tumors. One group was treated with ABT263 in a concentration of 100 mg/kg/day (in 100 µl 5% DMSO, 9.5% ethanol, 28.5% polyethylene glycol, 57% Phosal 50 PG) and the other group was treated with 100 µl of vehicle only for 21 days orally.

Results

BCL2 is over-expressed in most neuroblastoma tumors but only sporadic in cell lines

BCL2 family members are up-regulated in many kinds of cancer.[28] They include BCL2, MCL1, BCLXL, BCLW, BCLB and BFL1 and can be functionally redundant[1,38]. We therefore analyzed the expression of all family members in neuroblastoma tumors using Affymetrix expression data. *BCL2* is the only family member that shows a strong up-regulation in neuroblastoma tumors compared to other cancer types and compared to various normal tissues (fig 1a). The other anti-apoptotic BCL2 family members were equally or lower expressed in neuroblastoma compared to other tumors and normal tissues (suppl fig 1/2). To study the correlation between *BCL2* mRNA and protein expression in neuroblastoma, we performed tissue array analysis of 42 neuroblastoma tumors with 3 core biopsies per sample. All 42 tumors had cytoplasmic staining for BCL2 but a clear variation was visible (suppl fig 3). All tumors were scored and categorized into three groups. Low BCL2 protein expression was scored in 6 tumors whereas 14 tumors displayed intermediate and 22 tumors high BCL2 protein levels. Tumors with a high *BCL2* mRNA expression showed significantly higher BCL2 protein levels (fig 1b), indicating that *BCL2* mRNA levels are representative for BCL2 protein levels in neuroblastoma tumors.

Neuroblastoma cell lines have a much lower *BCL2* mRNA expression compared to neuroblastoma tumors (fig 1a). KCNR and SJNB12 were the only two cell lines with *BCL2* mRNA expression levels comparable to tumors. Western blot analysis of all cell lines in our panel revealed that, like in tumors, high *BCL2* mRNA levels correspond with high BCL2 protein levels (fig 1c). We conclude that only a few neuroblastoma cell lines are suited to study the effects of BCL2 inhibition in neuroblastoma.

To investigate whether high *BCL2* expression levels are related to genomic defects in

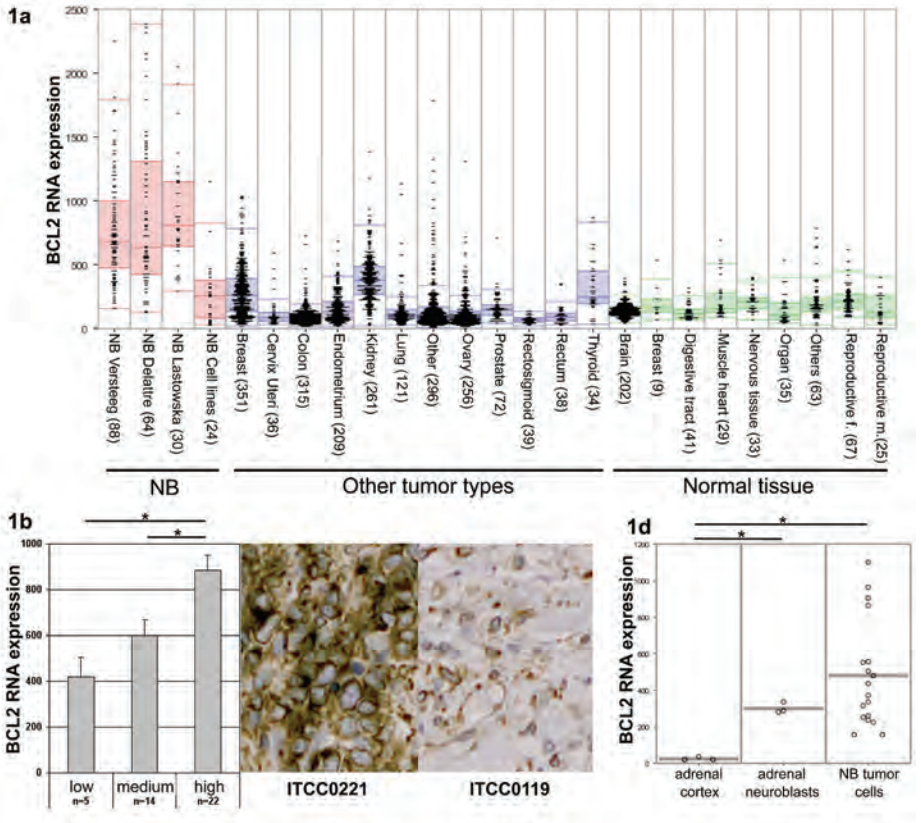

Figure 1: BCL2 expression in neuroblastoma tumors and cell lines (A) *BCL2* RNA expression data in Neuroblastoma tumors and cell lines (red), other tumors (blue) and normal tissue (green) based on Affymetrix profiling. In a combined boxdot-plot every dot represents one sample; the number of tumor samples is given between brackets. The colored boxes represent the area between the 25th and the 75th percentile with a line in between indicating the median. (B) Left: Correlation between Affymetrix *BCL2* RNA expression data (Y-axis) and BCL2 protein expression (3 expression groups are shown on the X-axis) based on a tissue array of the same tumors. Significance is indicated by *. Right: example of immunohistochemistry of a tumor with high BCL2 expression (ITCC0221) and low BCL2 expression (ITCC0119) (C) For all cell lines of the panel the *BCL2* RNA expression level based on Affymetrix profiling is represented. Red: >4x average (A), Orange: >2A <4A, Yellow: >0.5A <2A, Green: <0.5 A. Western blots of BCL2 expression in cell line panel were incubated with BCL2 and Actin antibodies. (D) *BCL2* RNA expression data in neuroblastoma tumor cells, adrenal neuroblasts and adrenal cortex. Every dot represents one sample. The line represents the average expression. Significance is indicated by *.

neuroblastoma, we analysed the *BCL2* locus on chromosome 18 in array CGH data of our neuroblastoma series. Whole chromosome 18 gain was detected in 15 out of 88 neuroblastoma tumors, but *BCL2* mRNA levels did not correlate to chr.18 gain (data not shown), suggesting that *BCL2* expression is transcriptionally regulated. To analyse whether high BCL2 expression is a property of the sympatho-adrenal lineage from which neuroblastoma are derived, we compared the *BCL2* mRNA expression of normal adrenal neuroblasts and tumors in a published series of de Preter et al.[33] and found no significant differences (fig 1d). This is in agreement with earlier immunohistochemical analyses[26], and suggests that high *BCL2* expression is a characteristic of the sympathetic adrenal lineage.

BCL2 silencing results in apoptosis in a subset of neuroblastoma cell lines

We selected five neuroblastoma cell lines with various *BCL2* expression levels, of which KCNR and SJNB12 have high expression, LAN5 and SKNBE have intermediate expression and SKNAS has low *BCL2* expression. In all cell lines *BCL2* was silenced using two lentiviral shRNAs, targeting different parts of the coding sequence. Western blot analysis showed a >80% decrease of BCL2 protein expression 72 hours after transduction in all cell lines with *BCL2* expression (fig 2a). *BCL2* silencing resulted in cell death 72 hours after transduction in the cell lines with high or intermediate *BCL2* expression as shown by PARP cleavage. SKNAS has no *BCL2* expression and did not show induction of PARP cleavage after treatment with the BCL2-specific shRNA vectors (fig 2a). The differences in phenotypic effect after *BCL2* silencing were confirmed using light microscopy (fig 2b) and MTT assays (fig 2c). Both assays showed a strong decrease of cell viability after silencing *BCL2* in cell lines with high expression of *BCL2* while SKNAS was completely insensitive. These findings suggest that *BCL2* is a potential target for therapy in neuroblastoma tumors with moderate to high expression of *BCL2*.

ABT263 induces apoptosis in NB cell lines with high expression of BCL2

The strong phenotypes induced by shRNA-mediated BCL2 inhibition urged us to test whether these results can also be achieved by a clinically applicable compound. ABT263 is a small molecule BCL2 inhibitor currently in clinical testing. We treated the same five neuroblastoma cell lines with ABT263. The results were strikingly similar to the phenotypes after *BCL2* shRNA treatment. The four cell lines with high or intermediate *BCL2* expression showed apoptotic cell death as indicated by Parp cleavage (fig 3a) and an increase in sub G1 fraction on FACS analysis (fig 3b, table 1), whereas SKNAS was completely insensitive for the compound at μM

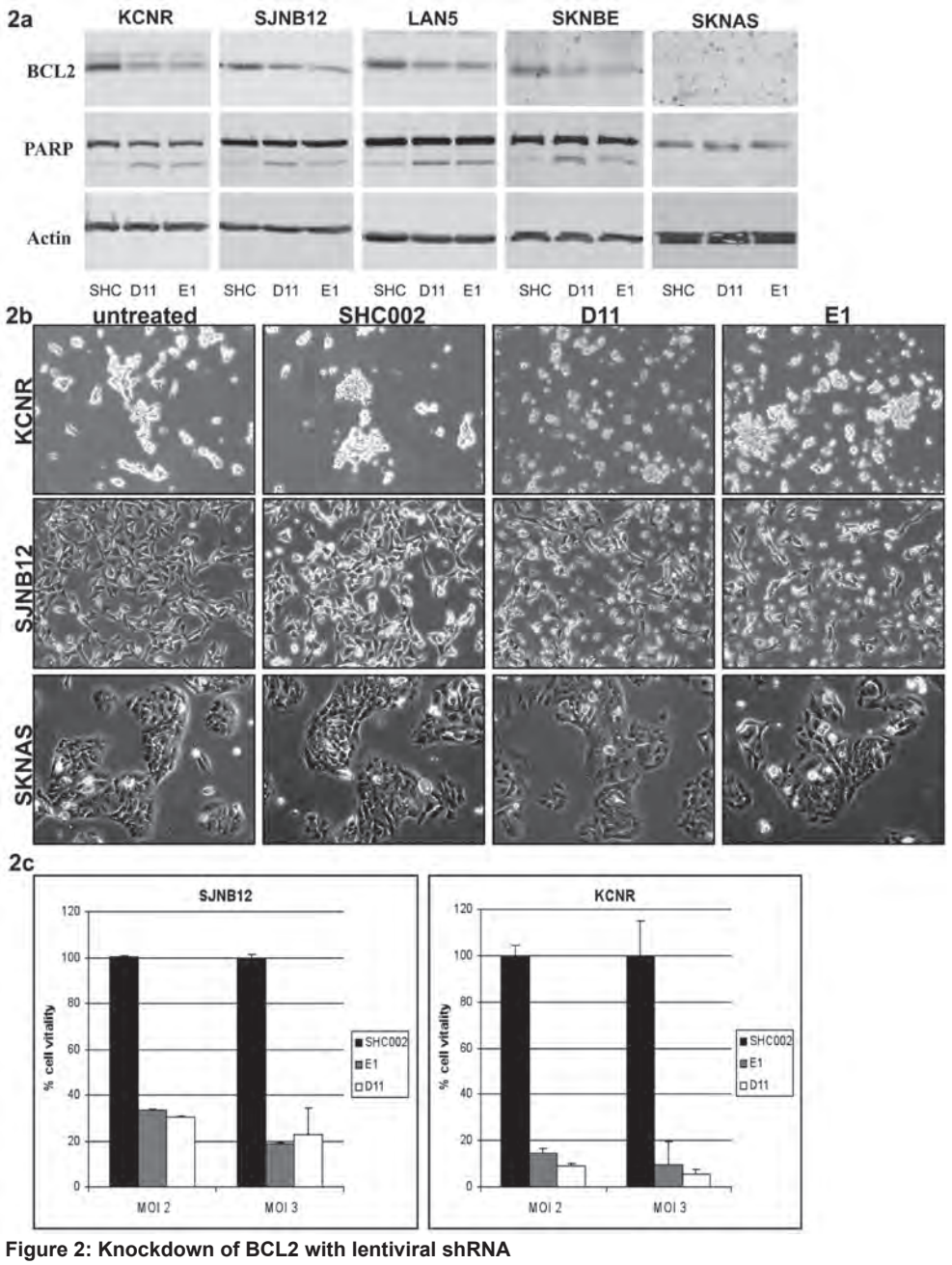

Figure 2: Knockdown of BCL2 with lentiviral shRNA

(A) Protein lysates were made of cells of Fig 2b. Western blot was performed and incubated with BCL2, PARP and Actin antibodies. (B) Pictures of the cells transduced with two different lentiviral BCL2 shRNAs were made 72 hours after transduction with a 100x magnitude. (C) MTT assay was performed 7 to 10 days after transduction with BCL2 shRNA. Cell viability is represented on the Y-axis and the multiplicity of infection (MOI) is represented on the X-axis.

ABT263 (uM)	sub G1 fraction(%)				
	KCNR	SJNB12	LAN5	SKNBE	SKNAS
0	14	16.1	4.3	10.2	2.2
0.008	19.7	14	*	*	*
0.04	19.1	18	*	*	*
0.2	31.7	28.6	30.5	*	*
1	41.2	32.1	40.7	14.5	2.6
5	55	37.6	42.5	19.7	3.7
10	*	*	36.2	22.5	3.3
15	*	*	40	22.5	4.1
20	*	*	*	28.9	5.5

Table 1. Apoptotic fraction after treatment with ABT263 in cell line panel
Percentage of the subG1 fraction as determined by FACS analysis.

concentrations and did not show induction of apoptosis (fig 3a-b). The concentration ABT263 required for 50% cell survival (IC50) was determined for all cell lines in our panel using MTT assays. The IC50 varied from 0.1 μM in KCNR to >100 μM in SKNAS (fig 3c) and showed an inverse correlation to the *BCL2* RNA expression (fig 3d).

These findings suggest that targeted inhibition of BCL2 by ABT263 leads to a similar response as targeted knock down of the *BCL2* mRNA. To further test the BCL2-inhibitory effect of ABT263, we performed a cell fractionation assay of neuroblastoma cells treated with ABT263. Western blot analysis showed at 24 h after treatment a strong transient increase of cytoplasmatic levels of Cytochrome C, which confirms mitochondrial release of Cytochrome C as a result of BCL2 inhibition (fig 3e).

ABT263 inhibits tumor growth in a neuroblastoma mouse model

The in vitro results of ABT263 urged us to test the compound in a neuroblastoma mouse model. We used serial transplants in NMRI Nu/Nu mice of xenografts of the human neuroblastoma cell line KCNR. Mice were treated orally with 100 mg/kg/day ABT263 for three weeks. After treatment, the mice were followed until they had to be terminated due to tumor volume. The ABT263-treated mice showed a strong delay in tumor growth and had a reduced tumor take. ABT263 induced a delay of 29 days on average compared to the DMSO-treated control mice (fig 4). In the ABT263 treated

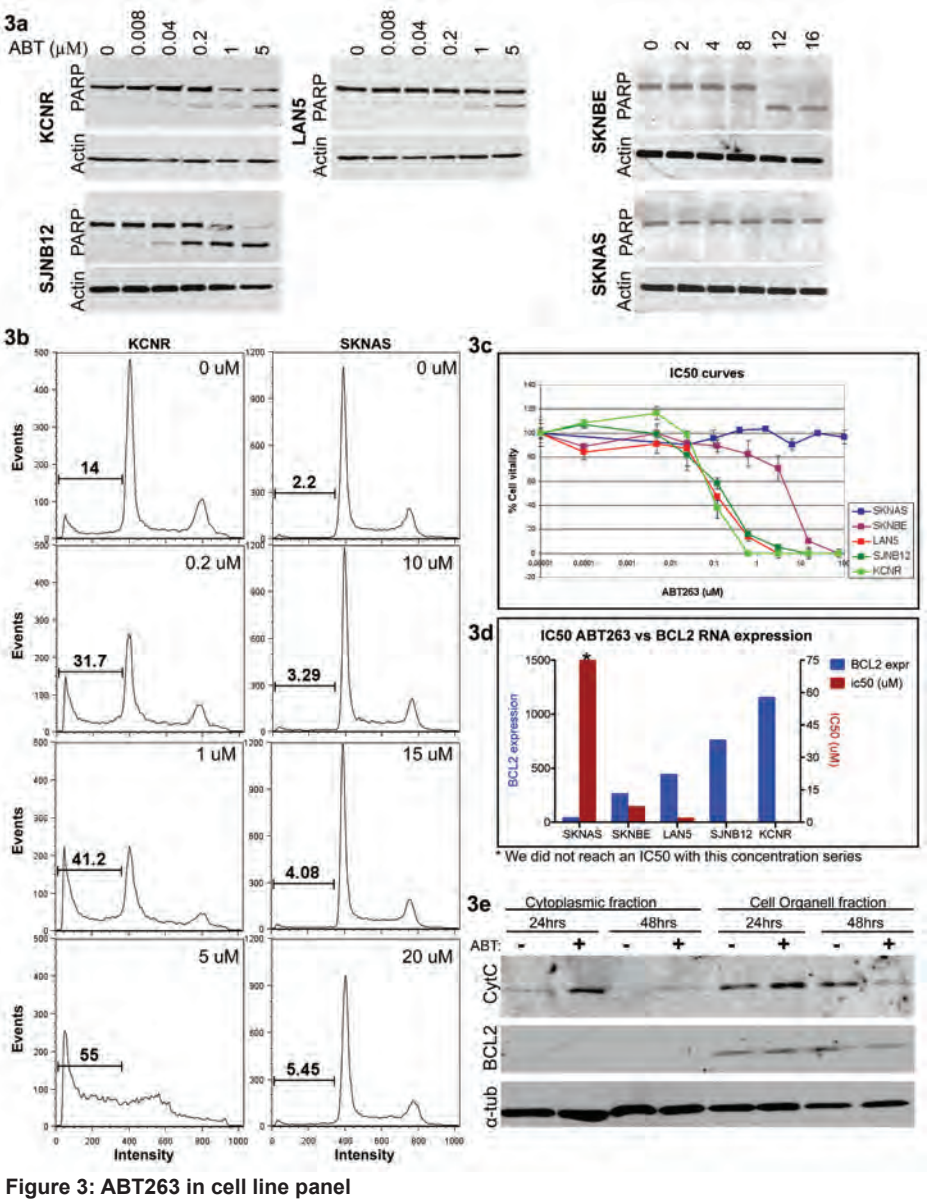

Figure 3: ABT263 in cell line panel

(A). Lysates were made of cells treated with ABT263. Western blots were incubated with PARP and Actin antibodies. (B) FACS analysis of cells treated with ABT263. The Y-axes of the graphs represent the number of events and the X-axes represent the size of the particles detected. Apoptosis is shown by the sub G1 fraction. (C) Cell viability curves of all cell lines of the panel after treatment with ABT263 as determined by an MTT-assay. Cell viability is represented on the Y-axis and the ABT263 concentration in μM is represented on the X-axis. (D) IC50 values of the cell lines tested for ABT263 that were calculated from the data in fig 3c are represented by the red bars. BCL2 RNA expression of these cell lines is shown by the blue bars. (E) Cell fractionation assay performed on SJNB12 cells treated with ABT263 for 24 hours. Blots were incubated with Cytochrome C, BCL2, and a-tubulin antibodies.

mice 5 tumors developed out of 12 tumors that were implanted, whereas in the DMSO treated group 9 out of 12 implants formed tumors. We conclude that ABT263 also in vivo shows a strong inhibitory effect on xenografts of a human neuroblastoma cell line with high *BCL2* expression.

Synergy between ABT263 and regular cytostatics

ABT263 potentiates an apoptotic response, suggesting that synergistic effects in combination with apoptosis inducing compounds might occur. In addition solid knowledge of combination treatment with classical cytostatics is a requisite for further clinical implementation of ABT263. We analyzed this in MTT synergy assays with the key compounds used in neuroblastoma treatment according to the DCOG NBL 2007 trial protocol. Doxorubicin, Vincristin and Etoposide showed strong synergistic responses with ABT263 in the two neuroblastoma cell lines SJNB12 and KCNR, which both have a high *BCL2* expression (table 2). ABT263 also showed synergy with cisplatin in SJNB12, but surprisingly an antagonistic effect with cisplatin in KCNR. As expected, no enhancement between ABT263 and the other compounds

	KCNR	SJNB12	SKNAS	F2112
doxorubicin	++++ (0.14)	++++ (0.19)	+ / -	+ / -
cisplatinum	- - - - - (>10)	+++ (0.58)	+ / -	+ / -
vincristine	+++ (0.51)	+++++ (<0.1)	+ / -	+ / -
etoposide	++++ (0.21)	+++++ (<0.1)	+ / -	+ / -

Table 2. Synergy assays

Combination Indexes for each cell line treated with ABT263 combined with each drug indicated are presented in this table. The degree of synergism is presented by + or -. +++++: very strong synergism; ++++: strong synergism; +++: synergism; - - - - -: very strong antagonism. +/-: no enhancement. Since SKNAS and F2112 were resistant to ABT263, an IC50 value for this compound was not reached. Therefore a combination index cannot be determined.

was observed in neuroblastoma cell line SKNAS, which lacks *BCL2* expression. Also exponentially growing human fibroblasts (F2112) did not show synergy (table 2), which indicates that the synergy is indeed *BCL2* dependent and tumor specific. The dose effect curve of SJNB12 treated with a concentration series of doxorubicin combined with a fixed concentration of ABT263 is represented in fig 5a. The isobologram of the combination of both compounds with various concentrations is shown in fig 5b. The Combination Index, which represents the degree of synergism of all drug combinations, is shown in table 2 for all cell lines tested. In this table the combination index at a fraction affected of 0.5 is shown (concentration combination

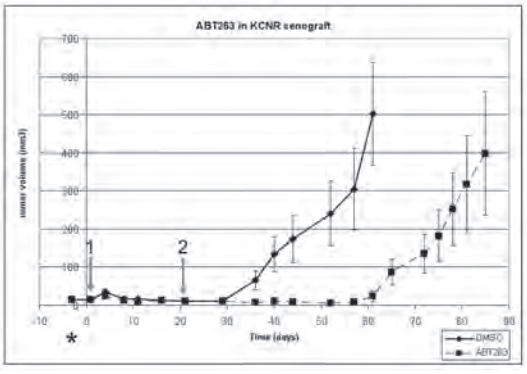

Figure 4: ABT263 in a KCNR xenograft model
The Y-axis represents tumor volume in mm3; the X-axis represents time in days after start of the treatment; * indicates the time point that tumor pieces were implanted; arrow 1 indicates the start of treatment and arrow 2 the end of the treatment. The solid line represents the average tumor volume of mice treated with DMSO; the dashed line represents the average tumor volume of mice treated with ABT263. From day 61 we had to terminate some mice in the control group because of large tumors.

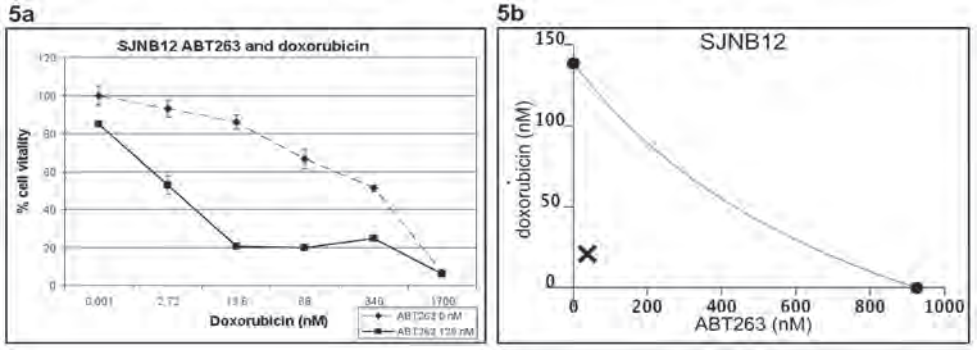

Figure 5: Synergy assays of ABT263 with doxorubicin in SJNB12
(A) the dose-effect curve of doxorubicin without ABT263 (dashed line) and with ABT263 (solid line). (B) Isobologram; The X-axis represents the concentration for ABT263 with a dot that represents its IC50 level. The Y-axis represents the concentration for doxorubicin, with a dot that represents its IC50 level. The line represents the expected curve for IC50 levels when both compounds are combined. X= actual concentrations of both drugs where an IC50 level was measured.

of compounds with 50% cell survival). However synergy was found at a large range of concentration combinations. These findings potentiate ABT263 for implementation in neuroblastoma treatment protocols and warrant further in vivo analysis.

Discussion

Neuroblastoma tumors have a very high *BCL2* RNA and protein expression, whereas the majority of neuroblastoma cell lines have not. Two cell lines (SJNB12 and KCNR)

show a *BCL2* expression that is comparable to the in vivo expression. Specific knockdown of *BCL2* with lentiviral shRNA resulted in the most abundant apoptotic response in these cell lines as shown by MTT assay and PARP cleavage. ABT263 synergistically sensitized neuroblastoma cell lines for most cytotoxic compounds. Treatment of neuroblastoma xenografts in a mouse model with ABT263 resulted in reduced and delayed tumor growth. We conclude that BCL2 is a potential new drug target in neuroblastoma and that further validation of the BCL2 inhibitor ABT263 in vivo and subsequently in patients is warranted.

Lestini et al[28] analyzed BCL2 and MCL1 protein expression on tissue arrays of neuroblastoma. Both proteins were expressed in the majority of neuroblastoma. Here we extend these observations by establishing that *BCL2* mRNA expression is much higher in neuroblastoma than in most other tumor types and normal tissues. In addition, we show that *BCL2* mRNA levels correlate very well with BCL2 protein levels as established by tissue arrays of tumors and western blot analysis of cell lines. Lestini et al. were successful in siRNA-mediated *BCL2* silencing in neuroblastoma cell lines, including SKNAS. In contrast to our SKNAS cells, their SKNAS cells showed BCL2 expression and knock-down, but just like our cells did not show an apoptotic response.

In other cancer models was also validated that sensitivity to BCL2 inhibition is dependent on levels of both pro- and anti-apoptotic members of the BCL2 family.[43,44] However, in neuroblastoma BCL2 is the only aberrantly expressed member of the BCL2 family, including the pro-apoptotic genes (data not shown). This indicates that BCL2 causes the unbalance in apoptosis and we think that the threshold of the BCL2 family members may be of importance. After inhibition of BCL2 the drop in BCL2 levels is big enough to induce apoptosis even though MCL1 is present.

ABT263 has previously been tested in a cell line panel by the Pediatric Preclinical Testing Program and relatively high IC50 values were found for the neuroblastoma cell lines tested.[31] *BCL2* expression has not been analyzed in these lines, but here we show that most neuroblastoma cell lines lack BCL2 expression, which might explain the weak responses to ABT263. The same holds for the neuroblastoma xenografts tested for ABT263 sensitivity as reported in the same paper. Also they were found to be relatively poor responders.

Essentially, our analyses showed that while neuroblastoma tumors have very high

BCL2 expression, most neuroblastoma cell lines have weak *BCL2* expression. Selection of high *BCL2* expressing cell lines for in vitro and in vivo testing of BCL2 inhibitory small molecules is therefore essential. The good responses in vitro and in vivo to ABT263 of neuroblastoma cell lines with high *BCL2* expression suggest that BCL2 might be a good target for therapy in neuroblastoma. Moreover, since the BCL2 expression in the selected cell lines is comparable to the BCL2 levels in most tumors, we expect that most tumors will be sensitive for ABT263.

Synergy of BCL2 inhibitors with etoposide or vincristine has previously been shown in other tumor types[39, 40]. We also found ABT263 to work synergistically with all of the currently used cytostatics in neuroblastoma treatment with the exception of cisplatin in SJNB12. The reason for this exception is unclear. For all other combinations, synergy could be explained by the working mechanisms of these compounds, which are all known to mediate DNA damage or microtubule destabilization. Cisplatin crosslinks DNA resulting in activation of DNA repair mechanisms and if that proves impossible it activates apoptosis. Doxorubicin is an inhibitor of reverse transcriptase and RNA polymerase, vincristin disrupts microtubules and etoposide blocks the cell cycle by inhibiting topoisomerase II.[41] All these mechanisms activate the mitochondrial apoptotic pathway.[42] This apoptotic route requires the release of Cytochrome C from the mitochondria, which is inhibited by BCL2.[2] Over-expression of *BCL2* therefore suppresses apoptosis and cells can be re-sensitized to these compounds by ABT263.

Combination treatment of ABT263 and currently used cytostatics might in addition increase the specificity of the anti-tumor treatment, as we show that *BCL2* is highly expressed in neuroblastoma but not in normal tissues. ABT263 is therefore a promising candidate for further in vitro testing and implementation in current treatment protocols of neuroblastoma patients.

Acknowledgements

This research was supported by grants from KIKA foundation, SKK and Netherlands Cancer Foundation. We would like to thank Thomas Klei and Lynne Rumping for their contribution.

Reference List

1. Yip, K.W. and Reed, J.C., Bcl-2 family proteins and cancer. Oncogene, 2008; 27**:** 6398-6406.
2. Frenzel, A., Grespi, F., Chmelewskij, W., and Villunger, A., Bcl2 family proteins in carcinogenesis and the treatment of cancer. Apoptosis, 2009; 14**:** 584-596.
3. Yecies, D., Carlson, N.E., Deng, J., and Letai, A., Acquired resistance to ABT-737 in lymphoma cells that up-regulate MCL-1 and BFL-1. Blood, 2010; 115**:** 3304-3313.
4. Egle, A., Harris, A.W., Bath, M.L., O'Reilly, L., and Cory, S., VavP-Bcl2 transgenic mice develop follicular lymphoma preceded by germinal center hyperplasia. Blood, 2004; 103**:** 2276-2283.
5. Vogler, M., Dinsdale, D., Dyer, M.J.S., and Cohen, G.M., Bcl-2 inhibitors: small molecules with a big impact on cancer therapy. Cell Death and Differentiation, 2009; 16**:** 360-367.
6. Zhang, L., Ming, L., and Yu, H., BH3 mimetics to improve cancer therapy; mechanisms and examples. Drug Resistance Updates, 2007; 10**:** 207-217.
7. Shoemaker, A.R., Mitten, M.J., Adickes, J., Ackler, S., Refici, M., Ferguson, D. et al, Activity of the Bcl-2 family inhibitor ABT-263 in a panel of small cell lung cancer xenograft models. Clinical Cancer Research, 2008; 14**:** 3268-3277.
8. Henry, M.C.W., Tashjian, D.B., and Breuer, C.K., Neuroblastoma update. Current Opinion in Oncology, 2005; 17**:** 19-23.
9. Maris, J.M., Hogarty, M.D., Bagatell, R., and Cohn, S.L., Neuroblastoma. Lancet, 2007; 369**:** 2106-2120.
10. van Noesel, M.M. and Versteeg, R., Pediatric neuroblastomas: genetic and epigenetic 'Danse Macabre'. Gene, 2004; 325**:** 1-15.
11. Maris, J.M., Medical Progress: Recent Advances in Neuroblastoma. New England Journal of Medicine, 2010; 362**:** 2202-2211.
12. Fesik, S.W., Promoting apoptosis as a strategy for cancer drug discovery. Nature Reviews Cancer, 2005; 5**:** 876-885.
13. Reed, J.C. and Pellecchia, M., Apoptosis-based therapies for hematologic malignancies. Blood, 2005; 106**:** 408-418.
14. Adida, C., Berrebi, D., Peuchmaur, M., Reyes-Mugica, M., and Altieri, D.C., Anti-apoptosis gene, survivin, and prognosis of neuroblastoma. Lancet, 1998; 351**:** 882-883.
15. Islam, A., Kageyama, H., Takada, N., Kawamato, T., Takayasu, H., Isogai, E. et al, High expression of Survivin, mapped to 17q25, is significantly associated with poor prognostic factors and promotes cell survival in human neuroblastoma. Oncogene, 2000; 19**:** 617-623.
16. Lamers, F., van der Ploeg, I., Schild, L., Ebus, M.E., Koster, J., Hansen, B.R. et al, Knockdown of Survivin (BIRC5) causes Apoptosis in Neuroblastoma via Mitotic Catastrophe. Endocrine Related Cancer, 2011;18(6):657-68.
17. Van Maerken, T., Ferdinande, L., Taildeman, J., Lambertz, I., Yigit, N., Vercruysse, L. et al, Antitumor Activity of the Selective MDM2 Antagonist Nutlin-3 Against Chemoresistant Neuroblastoma With Wild-Type p53. Journal of the National Cancer Institute, 2009; 101**:** 1562-1574.
18. Giaccone, G., Zatloukal, P., Roubec, J., Floor, K., Musil, J., Kuta, M. et al, Multicenter Phase II Trial of YM155, a Small-Molecule Suppressor of Survivin, in Patients With Advanced, Refractory, Non-Small-Cell Lung Cancer. Journal of Clinical Oncology, 2009; 27**:** 4481-4486.
19. Lewis, K.D., Samlowski, W., Ward, J., Catlett, J., Cranmer, L., Kirkwood, J. et al, A multi-center phase II evaluation of the small molecule survivin suppressor YM155 in patients with unresectable stage III or IV melanoma. Invest New Drugs, 2009.
20. Nakahara, T., Takeuchi, M., Kinoyama, I., Minematsu, T., Shirasuna, K., Matsuhisa, A. et al, YM155, a novel small-molecule survivin suppressant, induces regression of established human hormone-refractory prostate tumor xenografts. Cancer Research, 2007; 67**:** 8014-8021.
21. Satoh, T., Okamoto, I., Miyazaki, M., Morinaga, R., Tsuya, A., Hasegawa, Y. et al, Phase I Study of YM155, a Novel Survivin Suppressant, in Patients with Advanced Solid Tumors. Clinical Cancer Research, 2009; 15**:** 3872-3880.
22. Tolcher, A.W., Mita, A., Lewis, L.D., Garrett, C.R., Till, E., Daud, A.I. et al, Phase I and Pharmacokinetic Study of YM155, a Small-Molecule Inhibitor of Survivin. Journal of Clinical Oncology, 2008; 26**:** 5198-5203.
23. Lamers, F., Schild, L., Koster, J., Versteeg, R., Caron, H., and Molenaar, J. Targeted BIRC5 silencing using YM155 causes cell death in neuroblastoma cells with low ABCB1 expression. European Journal of Cancer, 2011; In Press.
24. Hoehner, J.C., Hedborg, F., Wiklund, H.J., Olsen, L., and Pahlman, S., Cellular Death in Neuroblastoma - In-Situ Correlation of Apoptosis and Bcl-2 Expression. International Journal of

Cancer, 1995; 62**:** 19-24.
25. Hoehner, J.C., Gestblom, C., Hedborg, F., Sandstedt, B., Olsen, L., and Pahlman, S., A developmental model of neuroblastoma: Differentiating stroma-poor tumors' progress along an extra-adrenal chromaffin lineage. Laboratory Investigation, 1996; 75**:** 659-675.
26. Hoehner, J.C., Hedborg, F., Eriksson, L., Sandstedt, B., Grimelius, L., Olsen, L. et al, Developmental gene expression of sympathetic nervous system tumors reflects their histogenesis. Laboratory Investigation, 1998; 78**:** 29-45.
27. Goldsmith, K.C., Lestini, B.J., Gross, M., Ip, L., Bhumbla, A., Zhang, X. et al, BH3 response profiles from neuroblastoma mitochondria predict activity of small molecule Bcl-2 family antagonists. Cell Death and Differentiation, 2010; 17**:** 872-882.
28. Lestini, B.J., Goldsmith, K.C., Fluchel, M.N., Liu, X.Y., Chen, N.L., Goyal, B. et al, Mcl1 downregulation sensitizes neuroblastoma to cytotoxic chemotherapy and small molecule Bcl2-family antagonists. Cancer Biology & Therapy, 2009; 8**:** 1587-1595.
29. Lin, T.S., New agents in chronic lymphocytic leukemia. Curr.Hematol.Malig.Rep., 2010; 5**:** 29-34.
30. Ackler, S., Xiao, Y., Mitten, M.J., Foster, K., Oleksijew, A., Refici, M. et al, ABT-263 and rapamycin act cooperatively to kill lymphoma cells in vitro and in vivo. Molecular Cancer Therapeutics, 2008; 7**:** 3265-3274.
31. Lock, R., Carol, H., Houghton, P.J., Morton, C.L., Kolb, E.A., Gorlick, R. et al, Initial testing (stage 1) of the BH3 mimetic ABT-263 by the pediatric preclinical testing program. Pediatric Blood & Cancer, 2008; 50**:** 1181-1189.
32. Fix, A., Lucchesi, C., Ribeiro, A., Lequin, D., Pierron, G., Schleiermacher, G. et al, Characterization of amplicons in neuroblastoma: High-resolution mapping using DNA microarrays, relationship with outcome, and identification of overexpressed genes. Genes Chromosomes & Cancer, 2008; 47**:** 819-834.
33. De Preter, K., Vandesompele, J., Heimann, P., Yigit, N., Beckman, S., Schramm, A. et al, Human fetal neuroblast and neuroblastoma transcriptome analysis confirms neuroblast origin and highlights neuroblastoma candidate genes. Genome Biology, 2006; 7.
34. Molenaar, J.J., Ebus, M.E., Koster, J., van Sluis, P., van Noesel, C.J.M., Versteeg, R. et al, Cyclin D1 and CDK4 activity contribute to the undifferentiated phenotype in neuroblastoma. Cancer Research, 2008; 68**:** 2599-2609.
35. Maurer, U., Charvet, C., Wagman, A.S., Dejardin, E., and Green, D.R., Glycogen synthase kinase-3 regulates mitochondrial outer membrane permeabilization and apoptosis by destabilization of MCL-1. Molecular Cell, 2006; 21**:** 749-760.
36. Yamamoto, K., Ichijo, H., and Korsmeyer, S.J., BCL-2 is phosphorylated and inactivated by an ASK1/Jun N-terminal protein kinase pathway normally activated at G(2)/M. Molecular and Cellular Biology, 1999; 19**:** 8469-8478.
37. Chou, T.C. and Talalay, P., Quantitative-Analysis of Dose-Effect Relationships - the Combined Effects of Multiple-Drugs Or Enzyme-Inhibitors. Advances in Enzyme Regulation, 1984; 22**:** 27-55.
38. Hagenbuchner, J., Ausserlechner, M.J., Porto, V., David, R., Meister, B., Bodner, M. et al, The Anti-apoptotic Protein BCL2L1/Bcl-xL Is Neutralized by Pro-apoptotic PMAIP1/Noxa in Neuroblastoma, Thereby Determining Bortezomib Sensitivity Independent of Prosurvival MCL1 Expression. Journal of Biological Chemistry, 2010; 285**:** 6904-6912.
39. High, L.M., Szymanska, B., Wilczynska-Kalak, U., Barber, N., O'Brien, R., Khaw, S.L. et al, The Bcl-2 Homology Domain 3 Mimetic ABT-737 Targets the Apoptotic Machinery in Acute Lymphoblastic Leukemia Resulting in Synergistic in Vitro and in Vivo Interactions with Established Drugs. Molecular Pharmacology, 2010; 77**:** 483-494.
40. Ackler, S., Mitten, M.J., Foster, K., Oleksijew, A., Refici, M., Tahir, S.K. et al, The Bcl-2 inhibitor ABT-263 enhances the response of multiple chemotherapeutic regimens in hematologic tumors in vivo. Cancer Chemotherapy and Pharmacology, 2010; 66**:** 869-880.
41. Imming, P., Sinning, C., and Meyer, A., Drugs, their targets and the nature and number of drug targets (vol 5, pg 821, 2006). Nature Reviews Drug Discovery, 2007; 6**:** 126.
42. Castedo, M., Perfettini, J.L., Roumie, T., Andreau, K., Medema, R., and Kroemer, G., Cell death by mitotic catastrophe: a molecular definition. Oncogene, 2004; 23**:** 2825-2837.
43. Moore, V.D., Brown, J.R., Certo, M., Love, T.M., Novina, C.D., and Letai, A., Chronic lymphocytic leukemia requires BCL2 to sequester prodeath BIM, explaining sensitivity to BCL2 antagonist ABT-737. Journal of Clinical Investigation, 2007; 117: 112-121.
44. Van Delft, M.F., Wei, A.H., Mason, K.D. et al, The BH3 mimetic ABT-737 targets selective Bcl-2 proteins and efficiently induces apoptosis via Bak/Bax if Mcl-1 is neutralized. Cancer Cell, 2006; 10: 389-399.

Supplementary Figures

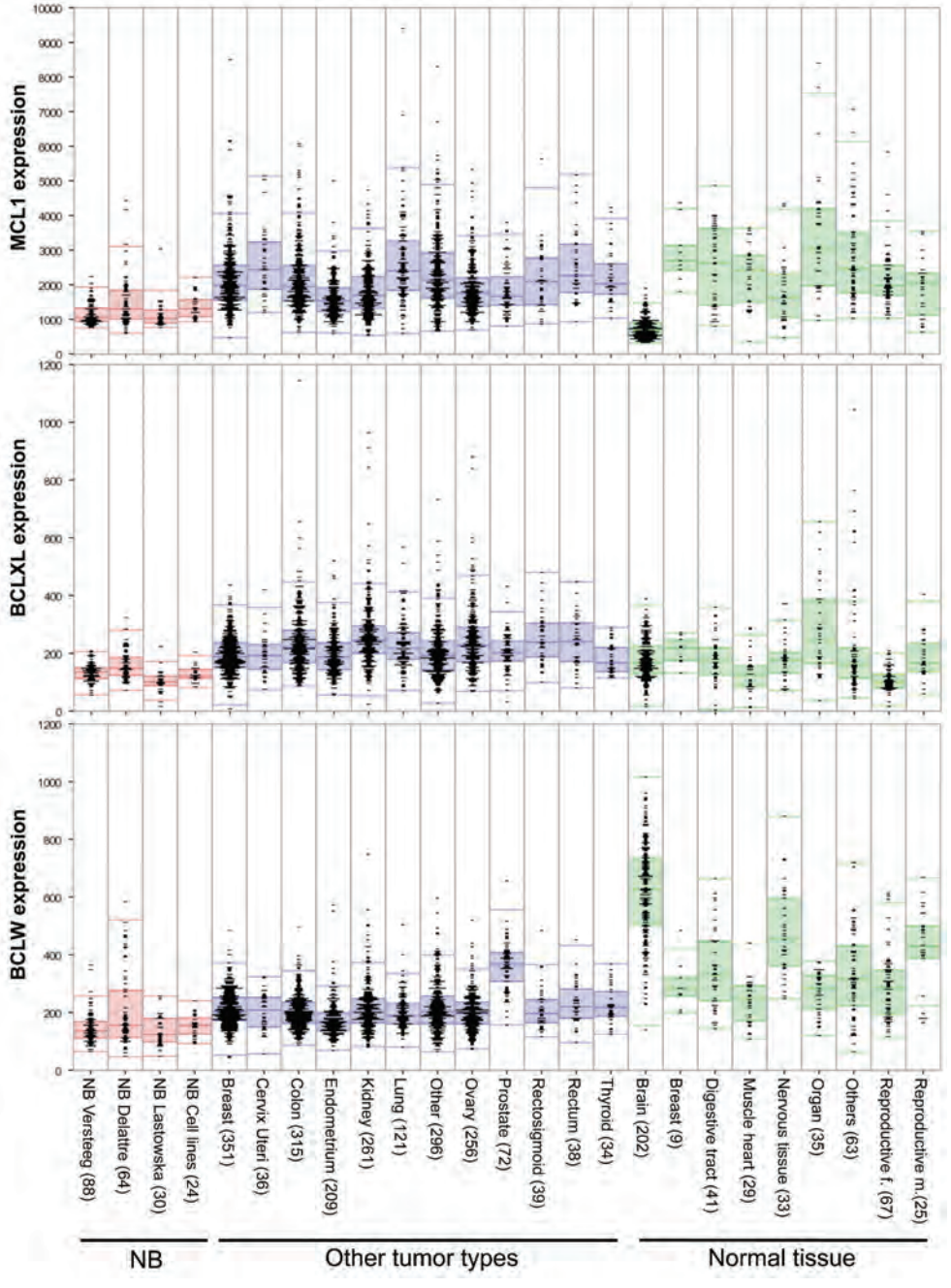

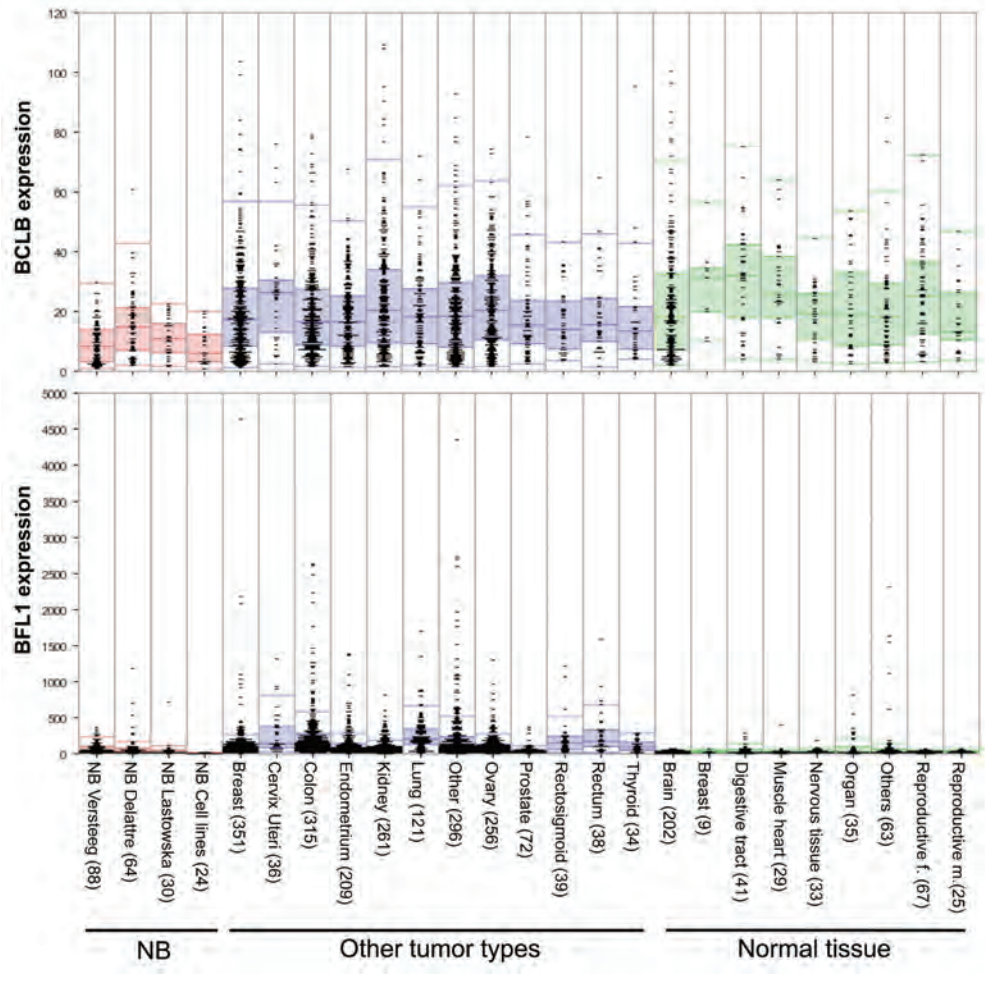

Supplementary figure 1/2. Expression of anti-apoptotic BCL2 family members in neuroblastoma tumors and cell lines

MCL1, BCLXL, BCLW, BCLB and BFL1 expression data in Neuroblastoma tumors and cell lines (red), other tumors (blue) and normal tissue (green) based on Affymetrix profiling. Every dot represents one sample; the number of tumor samples is given between brackets. The colored boxes represent the area between the 25th and the 75 percentile with a line in between indicating the median.

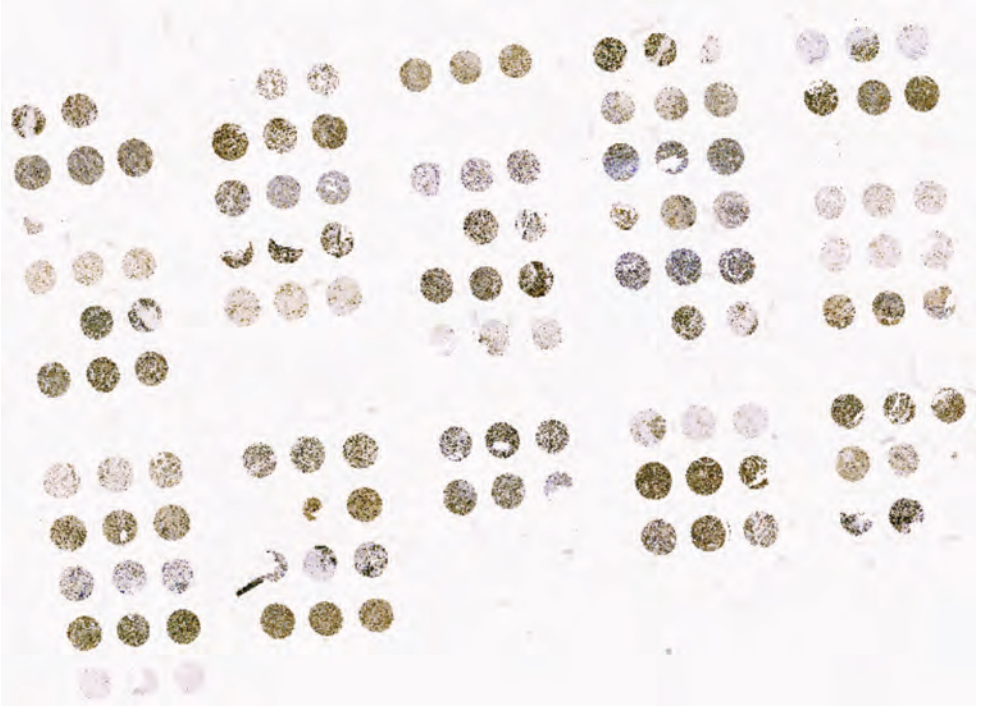

Supplementary figure 3. Tissue array of neuroblastoma tumors

Fig 1b is based on this tissue array. For each tumor 3 slides (shown next to each other) were stained.

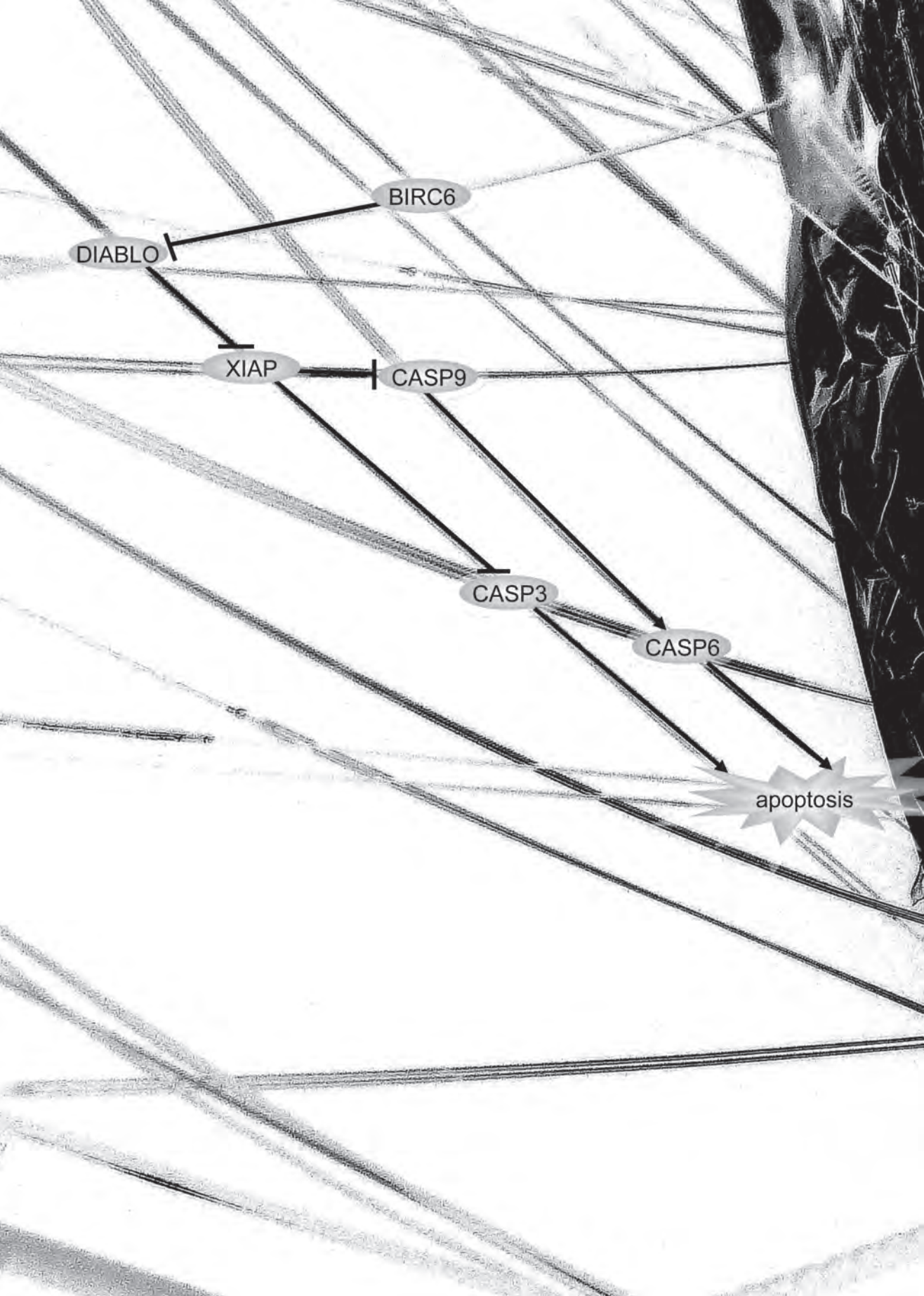
BIRC6
DIABLO
XIAP
CASP9
CASP3
CASP6
apoptosis

5

Identification and Validation of BIRC6 as a Novel Drug Target for Neuroblastoma Therapy

Identification and Validation of BIRC6 as a Novel Drug Target for Neuroblastoma Therapy

Fieke Lamers[1], Linda Schild[1], Jan Koster[1], Frank Speleman[2], Ingrid Øra[3], Peter van Sluis[1], Rogier Versteeg[1], Huib N. Caron[4], Jan J. Molenaar[1]

[1] Department of Oncogenomics, Academic Medical Center, University of Amsterdam, Meibergdreef 15, PO box 22700, 1105 AZ Amsterdam, The Netherlands.
[2] Center for Medical Genetics, Ghent University Hospital, Ghent, Belgium
[3] Department of Pediatric Oncology, Skåne University Hospital, Lund University, Lund, Sweden.
[4] Department of Pediatric Oncology, Emma Kinderziekenhuis, Academic Medical Center, University of Amsterdam, the Netherlands

5

Abstract

Neuroblastoma are pediatric tumors of the sympathetic nervous system with a poor prognosis. Apoptosis is often deregulated in cancer cells, but only few defects in apoptotic routes have been identified in neuroblastoma. Here we investigated genomic aberrations affecting genes of the intrinsic apoptotic pathway in neuroblastoma. We analyzed DNA profiling data (CGH and SNP arrays) and mRNA expression data of 31 genes of the intrinsic apoptotic pathway in a dataset of 88 neuroblastoma tumors using the R2 bioinformatic platform (http://r2.amc.nl). We observed frequent gain of the *BIRC6* gene on chromosome 2, which resulted in increased mRNA expression. BIRC6 is an inhibitor of apoptosis protein (IAP), that can bind and degrade the cytoplasmic fraction of the pro-apoptotic protein DIABLO. *DIABLO* expression was exceptionally high in neuroblastoma but the protein was only detected in the mitochondria. Upon silencing of BIRC6 by shRNA, DIABLO protein levels increased and cells went into apoptosis. Co-immunoprecipitation confirmed interaction between DIABLO and BIRC6 in neuroblastoma cell lines. Our findings indicate that BIRC6 may have an essential role in neuroblastoma by inactivating cytoplasmic DIABLO. BIRC6 inhibition may therefore provide a means for therapeutic intervention in neuroblastoma.

Introduction

BIRC6 (also known as BRUCE or APOLLON) is a cytoplasmic protein with a dual role. Firstly, BIRC6 has an anti-apoptotic function in the intrinsic apoptotic pathway. BIRC6 antagonizes the pro-apoptotic DIABLO protein. BIRC6 can bind the cytoplasmic DIABLO fraction and induce ubiquitination and proteasomal degradation of this protein.[1,2] BIRC6 thereby protects against the pro-apoptotic function of DIABLO. DIABLO is a mitochondrial protein which is released into the cytoplasm upon an apoptotic stimulus. This release is regulated by the levels of the BH3 family proteins, which induce pore formation in the mitochondrial membrane.[3-5] Cytoplasmic DIABLO can bind to the BIR domains of BIRC2 (cIAP1), BIRC3 (cIAP2) and BIRC4 (XIAP), thereby inhibiting the anti-apoptotic function of these proteins.[6] A second function of BIRC6 has been shown in recent studies where BIRC6 was required for abscission and membrane delivery during the midbody ring formation during cell division.[7,8]

BIRC6 is highly expressed in several types of cancer. *BIRC6* over-expression in acute myeloid leukemia correlated to a poor outcome.[9] A genome wide screening of chromosomal aberrations in Burkitt's lymphoma showed that a region of 2p including the *BIRC6* gene was gained in a few samples.[10] Also, high *BIRC6* expression in colon cancer stem cells was related to drug resistance.[11]

Neuroblastoma are pediatric tumors that originate from the embryonal precursor cells of the sympathetic nervous system. High stage tumors have a poor prognosis with 20 to 40% overall survival.[12-14] *BIRC6* is located on chromosome 2p in the region, which shows frequent gain in neuroblastoma.[12] This region includes *MYCN* and *ALK*, the two best known oncogenes in neuroblastoma. *MYCN* is amplified in 20-30% of neuroblastoma, which strongly correlates to a poor prognosis.[12-15] The other oncogene on 2p is *ALK*, which was recently found to be mutated in 6-10% of primary neuroblastoma.[16-20] *MYCN* amplification and *ALK* mutation seem to occur independent of the gain of chromosome 2p.[21] Therefore other additional tumor driving genes could be located on this frequently gained region.

The apoptotic pathway has been widely investigated in neuroblastoma and only few tumor driving events have been described. *TP53* is mostly intact in primary neuroblastoma although functional defects in the TP53 pathway have been described.[22] *Caspase 8 (CASP8)* is hypermethylated and thereby inactivated in some neuroblastoma resulting in an inactive extrinsic apoptotic pathway.[23] The IAP

BIRC5 (Survivin) is located on the chromosome 17q region frequently gained in neuroblastoma and high BIRC5 expression correlates to a poor prognosis.[24-26] Finally, the anti-apoptotic mitochondrial *BCL2* protein is highly expressed in neuroblastoma. Targeted inhibitors against BIRC5[27-32] and BCL2[33] are currently tested for further clinical implementation. The poor prognosis of high grade neuroblastoma urges to identify additional targets for therapeutic intervention.

To identify patterns in the aberrations of genes involved in intrinsic apoptotic signaling we combined high throughput analysis of DNA copy number and mRNA expression of these genes in a dataset of 88 neuroblastoma tumors. *BIRC5* and *BIRC6* were frequently gained and *CASP9* was often lost. *BIRC6* was not previously evaluated in a neuroblastoma model. Therefore we studied the potency of BIRC6 as a new drug target for neuroblastoma therapy. Silencing of BIRC6 induced apoptosis and BIRC6 physically interacted with DIABLO. Also BIRC6 knockdown induced DIABLO up-regulation, indicating that BIRC6 can degrade DIABLO very effectively. BIRC6 might therefore be a suitable target for therapeutic intervention in neuroblastoma.

Methods

Patient samples

We used a neuroblastoma tumor panel for Affymetrix Microarray analysis containing 88 primary neuroblastoma tumor samples of untreated patients, which were all included for mRNA analyses and of which 87 neuroblastoma tumor samples were used for CGH analysis and SNP array.[34] Material was obtained during surgery and immediately frozen in liquid nitrogen. Some samples were excluded because DNA quality was too low for high throughput analysis. Public available neuroblastoma datasets we used were of Delattre[35] and Lastowska (geo ID: gse13136). Public available datasets were used for comparing neuroblastoma with normal tissues (Roth dataset, geo ID: gse3526) and adult tumors (EXPO dataset, geo ID: gse2109).

Affymetrix expression analysis

Total RNA of neuroblastoma tumors was extracted using Trizol reagent (Invitrogen) according to the manufacturer's protocol. RNA concentration and quality were determined using the RNA 6000 nano assay on the Agilent 2100 Bioanalyzer (Agilent Technologies). Fragmentation of cRNA, hybridization to hg-u133 plus 2.0

microarrays and scanning were performed according to the manufacturer's protocol (Affymetrix inc).

CGH analysis

High-molecular-weight DNA was isolated from tumor tissue by a standard salt-chloroform extraction method.[36] For reference DNA we obtained healthy tissue. We used a custom 44K Agilent aCGH chip, enriched for critical regions of loss/gain for neuroblastoma (10 kb resolution), miRNAs/T-UCRs (5 oligos/gene) and cancer gene census genes (5 oligos/gene) (Agilent Technologies). A total of 150 ng of tumor and reference DNA was labeled with Cy3 and Cy5, respectively (BioPrime ArrayCGH Genomic Labeling System, Invitrogen). Further processing was done according to the manufacturer's guidelines. Features were extracted using the feature extraction v10.1.0.0.0 software program. Data were further analyzed using the R2 web application (see below). Circular binary segmentation was used for scoring the regions of gain, amplification and deletion.

Whole-Genome Genotyping

Tumor DNA was extracted as previously described, quantified with NanoDrop and the quality was determined by the Abs 260/280 and 230/260 ratio. SNP arrays were processed for analysis of copy number variations according to the manufacturer's recommendations with the Infinium II assay on Human370/660-quad arrays containing > 370 000/ > 660 000 markers and run on the Illumina Beadstation (Swegene Centre for Integrative Biology, Lund University – SCIBLU, Sweden) according to the manufacturer's recommendations. Raw data were processed using Illumina's BeadStudio software suite (Genotyping module 3.0), producing report files containing normalized intensity data and SNP genotypes. Subsequently, log 2 Ratio and B-allele frequency data were imported into the R2 web application for detailed analysis and comparison with the CGH and expression data.

Bioinformatics

All data were analyzed using the R2 web application, which is publicly available at http://r2.amc.nl. The expression data were normalized with the MAS5.0 algorithm within the GCOS program of Affymetrix Inc. Target intensity was set to 100. For scoring genomic aberrations of the 31 included genes, we considered CGH aberrant if the logfold value was more than 0.45 for gain or less than -0.45 for loss and if a breaking point was clearly visible. We excluded whole chromosome gains or losses. Also the detected gains or losses had to be confirmed by SNP array.

Cell lines

All cell lines were grown in Dulbecco Modified Eagle Medium (DMEM), supplemented with 10% fetal calf serum, 10 mM L-glutamine, 10 U/ml penicillin/streptomycin, Non Essential Amino Acids (1x) and 10 µg/ml streptomycin. Cells were maintained at 37 ˚C under 5% CO_2. For primary references of these cell lines, see Molenaar et al.[37]

Lentiviral shRNA production and transduction

Lentiviral particles were produced in HEK293T cells by cotransfection of lentiviral vector containing the short hairpin RNA (shRNA) with lentiviral packaging plasmids pMD2G, pRRE and pRSV/REV using FuGene HD. Supernatant of the HEK293T cells was harvested at 48 and 72 hours after transfection, which was purified by filtration and ultracentrifuging. The concentration was determined by a p24 ELISA. Cells were plated in a 10% confluence. After 24 hours cells were transduced with lentiviral DIABLO shRNA (Sigma, 'E8': TRCN0000004511 and 'E9': TRCN0000004512) or BIRC6 shRNA (Sigma, 'C7': TRCN0000004157 and 'C11': TRCN0000004161) in various concentrations (Multiplicity of infection (MOI): 1 - 3). SHC-002 shRNA (non-targeting shRNA: CAACAAGATGAAGAGCACCAA) was used as a negative control. 24 hours after transduction medium was refreshed and puromycin was added to determine the efficacy of transduction. Protein was harvested 72 hours after transduction and analyzed by Western blot.

Compounds

ABT263, a small molecule BCL2 inhibitor, was dissolved in DMSO with a concentration of 20 mM for stock solution. A final concentration of 200 nM ABT263 was used. For the experiment using this compound we chose SJNB12 instead of IMR32 or SKNSH because this cell line highly expresses BCL2, which makes it very sensitive to this compound.[33] Z-Val-Asp(OMe)-Val-Ala-Asp(OMe)-FMK (ZVDVAD-FMK , a widely used CASP2 inhibitor; R&D systems) was added to the cells following manufacturer's protocol in a concentration of 20 µM.

Western Blotting

72 hours after transduction with shRNA, attached and floating cells were harvested on ice. Cells were lysated with Laemmlibuffer (20% glycerol, 4% SDS, 100mM Tris HCl pH 6.8 in mQ). Protein was quantified with RC-DC protein assay (Bio-Rad). Lysates were separated on a 10 % SDS-Page gel and electroblotted on a transfer membrane (Millipore, IPFL00010). Blocking and incubation were performed in OBB according to manufacturer's protocol (LI-COR). Primary antibodies used were

BIRC6 (Abcam, ab19609), DIABLO (Abcam, ab32023), PARP (Cell Signaling: 9542) and BCL2 (Cell Signalling; 2872). Protein loading was checked by β-actin (Abcam, ab6276) or α-tubulin (Sigma, T5168). The secondary antibodies used were provided by LI-COR. Proteins were visualized with the Odyssey bioanalyzer (LI-COR).

In cell western

48 hours after transduction with BIRC6 shRNA, cells were fixed with 4% paraformaldehyde for 20 minutes. Blocking and incubation were performed in OBB according to manufacturer's protocol (LI-COR). Primary antibodies used were BIRC6 (BD Biosciences, 611193) and β-actin mouse monoclonal (Abcam, ab6276). Proteins were visualized with the Odyssey bioanalyzer (LI-COR) and quantified and corrected for actin using the Odyssey software.

Immunofluorescence

Cells were grown on glass slides in 6-well plates. Cells were fixed with 4% paraformaldehyde in PBS 48 hours after transduction. We used DIABLO (Abcam, ab32023) as a primary antibodiy, and anti-rabbit (Alexa, 11012) as a secondary antibody. Mitochondria were stained using Mitotracker (Invitrogen, M22426). Antibodies were dissolved in 5% ELK in PBS/0.2% tween-20. Slides were stained with DAPI (1:1000) in vectashield (Vector Laboratories).

Cell fractionation

Protein was harvested and fractionated using the Subcellular Proteome Extraction Kit according to manufacturer's protocol (Novagen, 539790). Fraction I (cytosol) and II (cell organelle) were used for Western blot.

Co-immunoprecipitation

Cells were lysed in a buffer containing 150 mM NaCl, 50 mM Hepes, 5 mM EDTA, 0.3% NP-40, 10 mM β-glycerophosphate, 6% glycerol, protease inhibitors (Complete mini, Roche) and Phosphatase inhibitors (5 mM NaF, 1 mM Na2VO3). The antibody used for IP was BIRC6 (Abcam, ab19609); negative controls were flag (Cell Signaling, 2368) and protein without antibody. Other negative controls were for every antibody a sample without protein (data not shown). Protein-G agarose beads (Roche) and antibody have been incubated for pre-coupling overnight after which lysate was added and incubated overnight. Immunocomplexes were washed, heated at 95ºC for 10 minutes and put on a gel for Western blot. Primary antibodies used were anti-BIRC6 and anti-DIABLO (Abcam; ab32023). Blots were incubated overnight with

primary antibodies, after which a one hour incubation step with anti-rabbit IgG (Cell Signaling; 3678) was performed followed by incubation with the secondary antibody that was provided by LI-COR.

MTT-assay

Cells were plated in 30% confluence in a 48-well plate and transduced with BIRC6 shRNA and treated with ZVDVAD after 24 hours. 72 hours after treatment, 25 µl of Thiazolyl blue tetrazolium bromide (MTT, Sigma M2128) was added. After 4-6 hours of incubation 250 µl of 10% SDS, 0.01 M HCl was added to stop the reaction. The absorbance was measured at 570 nm and 720 nm using a platereader (Biotek).

Results

Gain of BIRC5 and BIRC6 and loss of CASP9 in neuroblastoma tumors

To identify patterns in the aberrations of genes involved in intrinsic apoptotic signaling we combined high throughput analysis of DNA copy number and mRNA expression of these genes. We included all 31 genes that are directly involved in the mitochondrial apoptotic pathway and their downstream target genes (table 1). Array CGH data of 87 primary neuroblastoma tumor samples were analyzed for DNA copy number variations of the 31 genes included in our intrinsic apoptotic gene panel. Binary segmentation data was used to score the DNA copy number variations and they were subsequently confirmed using log fold data from SNP array analyses of the same tumors. Only three genes showed DNA copy number aberrations at a frequency above 10% (fig 1a). The *BIRC5* gene, which is located in the smallest region of overlap (SRO) of gain of chromosomal band 17q25[12], was gained in 49% of the tumors. *CASP9* is located at the SRO of deletions of 1p36[12] and it was lost in 30% of the tumors. *BIRC6*, which is located on 2p22, was gained in 24% of the neuroblastoma tumors. Distal chromosome 2p is a known region of gain in neuroblastoma. *BIRC6* is not located in the SRO of this gained region, but is gained in 84% of the tumors with 2p gain (fig 1b). Of these three genes, *BIRC6* was not studied before in neuroblastoma. We therefore investigated whether the gain of BIRC6 resulted in aberrant expression. We compared *BIRC6* expression in tumors with and without *BIRC6* gain, which showed that tumors with BIRC6 gain have significantly higher *BIRC6* RNA levels (Student T-test: $P = 3.1*10^{-6}$) (fig 1c). Moreover, *BIRC6* is also highly expressed compared to several adult tumors and various normal tissues (fig 1d). These findings suggest that the aberrant expression

of *BIRC6* is at least partially caused by genomic aberrations that often occur in neuroblastoma tumors.

BIRC6 knockdown induces apoptosis in neuroblastoma cells

We investigated whether the high *BIRC6* levels indeed counteract apoptosis in neuroblastoma. We used 2 lentiviral shRNAs targeting different parts of the coding sequence of BIRC6. SKNSH, one of the neuroblastoma cell lines with the highest BIRC6 expression, was transduced with these vectors (fig 2a). BIRC6 is a 528 kD protein and difficult to assess on Western blot. Therefore we first analyzed BIRC6 protein levels by in cell western. For this method cells are fixed directly in the culture well and stained with a BIRC6 antibody. Analysis showed concentration dependent down-regulation of BIRC6 protein with both BIRC6 shRNAs at 48 hours after transduction (fig 2b). Although less optimal, we could confirm BIRC6 down-regulation using Western blot (fig 2c). We then investigated whether BIRC6 silencing induced apoptosis. Light microscopy showed a decreased cell number and cell death at 72 hours after BIRC6 silencing (fig 2d). This was confirmed by MTT assays, which showed strongly reduced cell viability after transduction with both BIRC6 shRNAs (fig 2e, dark grey bars). This phenotype was caused by an apoptotic response as western blot demonstrated PARP cleavage at 72 hours after transduction with both BIRC6 shRNAs (fig 2f). These findings confirm an anti-apoptotic role for BIRC6 in neuroblastoma cells.

High BIRC6 levels keep cytoplasmic DIABLO levels low

The BIRC6 protein functions both by silencing of DIABLO and in the formation of the midbody ring during cell division. Inhibition of each of these functions can result in cell death. We therefore investigated which process caused apoptosis after BIRC6 silencing in neuroblastoma. Apoptosis induced after inhibiting the midbody-related function of BIRC6 has been found to be mediated by CASP2.[7,8,38] We inhibited CASP2 by ZVDVAD, a widely used CASP2 inhibitor[39-41] that we have previously used to show that apoptosis induced by silencing of BIRC5 is mediated by CASP2.[26] ZVDVAD however did not inhibit apoptosis induced by BIRC6 knockdown in SKNSH and IMR32 cells (fig 2e). This indicates that this process is not CASP2-mediated, implying that the role of BIRC6 in neuroblastoma is not essential for completion of cell division during midbody ring formation.

Alternatively, BIRC6 functions as an IAP that binds DIABLO in the cytoplasm and thereby induces ubiquitination and degradation of DIABLO.[1,2] DIABLO mRNA expression levels in neuroblastoma tumors were surprisingly high compared to other

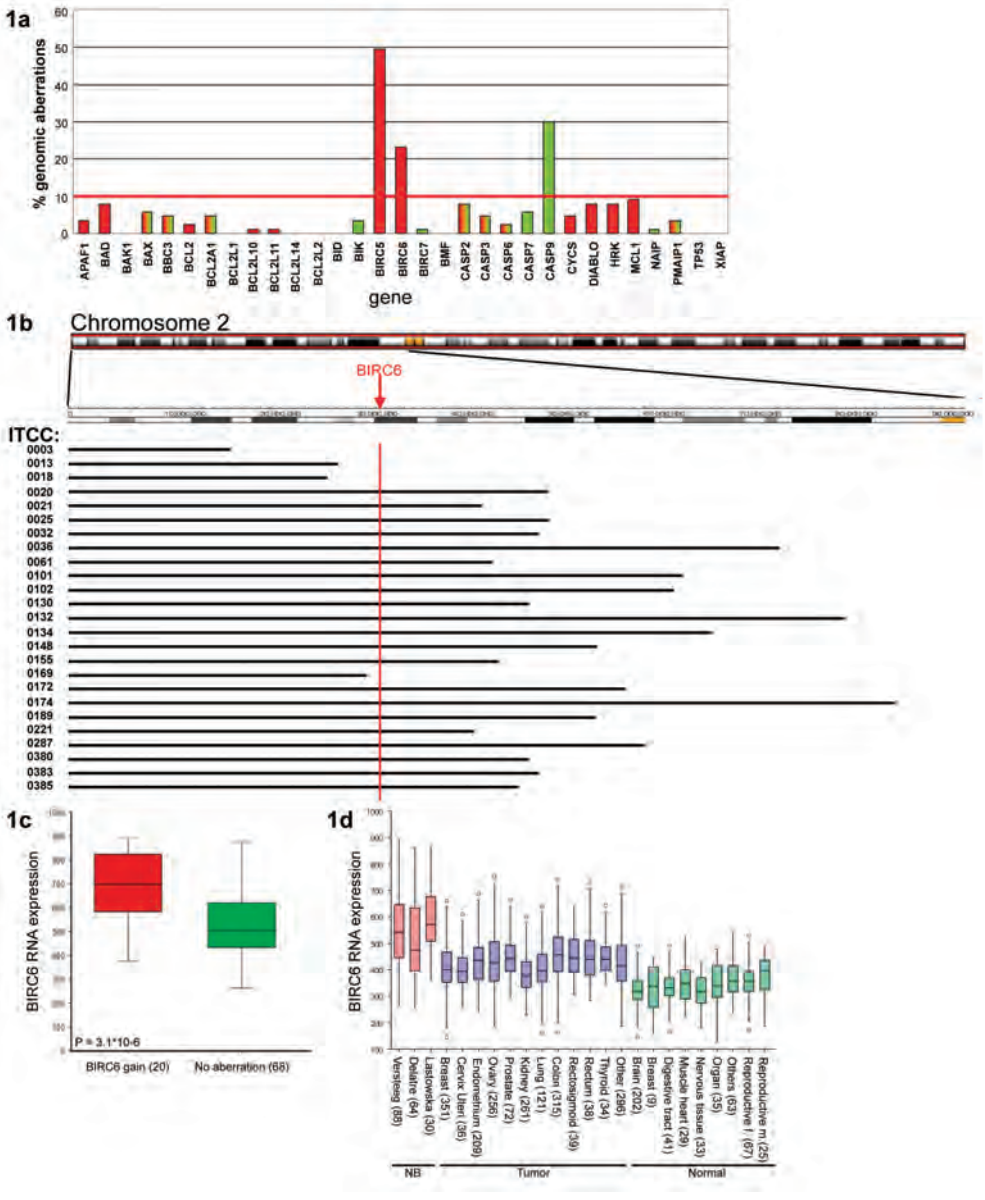

Fig 1: Gain of BIRC5 and BIRC6 and loss of CASP9 in neuroblastoma tumors

(A) The percentage of genomic aberrations is presented on the Y-axis and all selected genes in the intrinsic apoptotic pathway on the X-axis. Red bars indicate gained genes and green bars indicate lost genes. When a bar is green/red combined, it means that both gains and losses in that gene occurred. The red horizontal line represents the cut-off for further analysis. (B) Chromosome 2 is represented with the regions of 2p that are gained in our dataset of 88 neuroblastoma tumors. The BIRC6 locus is indicated with a red arrow. (C) Boxplots of BIRC6 mRNA expression in tumors with or without gain of BIRC6. (D) Boxplots of BIRC6 mRNA expression in 3 neuroblastoma datasets (red), adult tumors (blue) and various normal tissues (green). The boxes represent the 25th to 75th percentile with the median depicted as a horizontal line. Extremes are indicated by the whiskers, and the presence of outliers is indicated by (o).

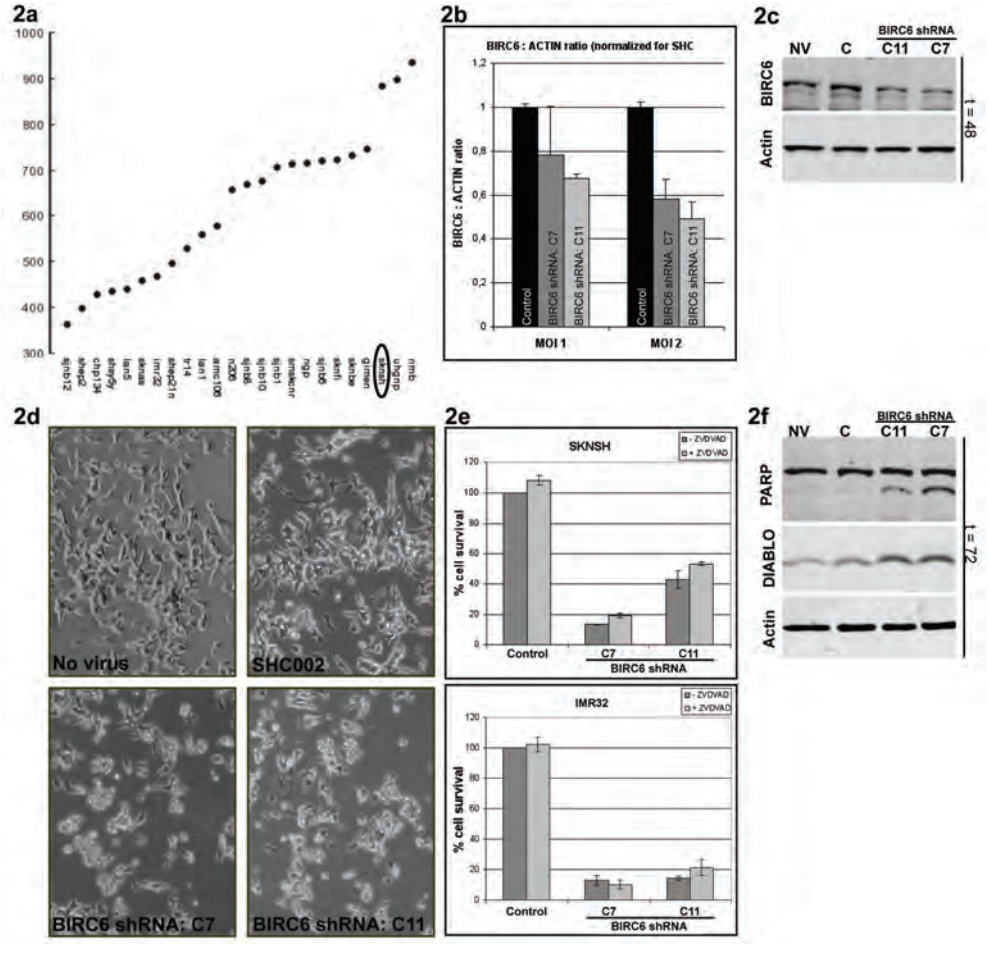

Fig 2: Knockdown of BIRC6 in SKNSH induces apoptosis

(A) BIRC6 mRNA expression in 24 neuroblastoma cell lines. (B) In cell western of SKNSH 48 hours after transduction. The Y-axis represents the ratio between BIRC6 and Actin protein expression as determined by the Odyssey bioanalyzer. The X-axis represents the concentration BIRC6 shRNA that was added. Black bars are cells transduced with control virus (SHC002), dark grey: C7 BIRC6 shRNA and light grey: C11 BIRC6 shRNA. MOI = Multiplicity of Infection. (C) Western blot of SKNSH 48 hours after transduction with no virus (NV), control virus SHC002 (C) or BIRC6 shRNA (C11 and C7). Blots were incubated with BIRC6 and actin antibodies. (D) Pictures were made 72 hours after transduction before protein harvest with a 100x magnitude. (E) MTT-assay of SKNSH and IMR32 transduced with control virus (SHC) or BIRC6 shRNA (C7 and C11). The dark grey bars represent cells transduced with virus alone; the light grey bars represent cells that are treated with BIRC6 shRNA combined with ZVDVAD, a CASP2 inhibitor. Fig 2f: Western blot of SKNSH 72 hours after transduction with no virus (NV), control virus SHC002 (C) or BIRC6 shRNA (C11 and C7). Blots were incubated with PARP, DIABLO and actin antibodies.

types of tumors and compared to normal tissue (fig 3a). Moreover, we confirmed an amplification of a region on the chromosome 12q arm in the neuroblastoma cell line NGP, which included the DIABLO locus (fig 3b).[42] We therefore investigated whether the high BIRC6 expression allows neuroblastoma cells to survive the high levels of the pro-apoptotic protein DIABLO. DIABLO is a mitochondrial protein, which translocates to the cytoplasm after apoptotic stimuli where it can be degraded by BIRC6. We therefore investigated the cellular localization of DIABLO. Immunofluorescence indeed showed a clear localization of DIABLO within the mitochondria (fig 3c), which was confirmed by cell fractionation showing that the majority of DIABLO is localized in the cell organelle fraction (fig 3d). To test whether DIABLO can be functionally activated upon an apoptotic stimulus, we treated neuroblastoma cells with the BCL2 inhibitor ABT263, which results in stimulation of pore formation in the mitochondria[43]. Cell fractionation indicated that the cytosolic DIABLO levels increased 24 hours after ABT263 treatment (fig 3d). This shows that DIABLO can be released from the mitochondria and stimulate apoptosis.

Untreated cells show low cytoplasmic DIABLO levels (fig. 3d). These levels are probably restricted by BIRC6 activity. To test this hypothesis, we first investigated whether BIRC6 and DIABLO physically interact in neuroblastoma cells by a co-immunoprecipitation analysis. Cell lysates of SKNSH and IMR32 cells were immunoprecipitated with a BIRC6 antibody. Western blot analysis of these precipitates with a DIABLO antibody showed a strong signal at the correct position for DIABLO. This confirms a physical interaction between both proteins (fig 3e). Finally, we investigated whether silencing of BIRC6 results in increased DIABLO protein levels. Western blot analysis of SKNSH cells treated with two different shRNAs for BIRC6 showed that the silencing of BIRC6 induced by both viruses resulted in a clear increase of DIABLO protein levels (fig 2f).

These experiments suggest that BIRC6 effectively inactivates cytoplasmic DIABLO in neuroblastoma cells and thereby prevents an apoptotic response. Since BIRC6 knockdown induced apoptosis, BIRC6 might represent an interesting new target for targeted inhibition in neuroblastoma.

Discussion

In this paper we analyzed aberrations in gene copy number and mRNA expression of genes directly involved in the intrinsic apoptotic pathway in neuroblastoma. BIRC6, known as an inhibitor of the pro-apoptotic protein DIABLO, showed gene

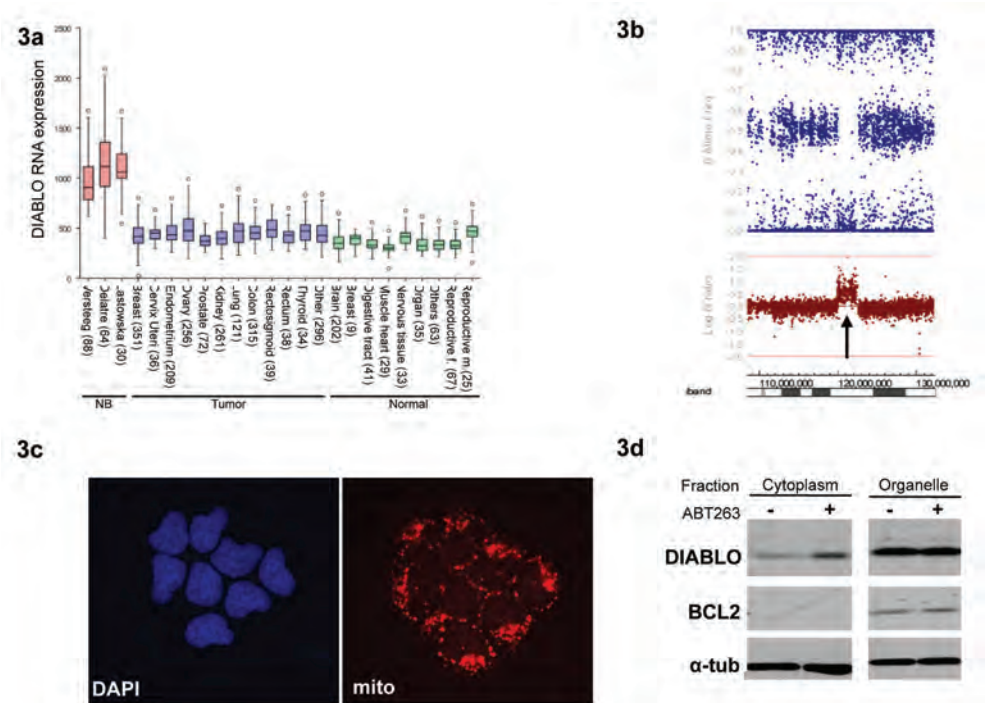

Fig 3: DIABLO mRNA and protein expression

(A) Boxplots of DIABLO mRNA expression in 3 neuroblastoma datasets (red), adult tumors (blue) and various normal tissues (green). The boxes represent the 25th to 75th percentile with the median depicted as a horizontal line. Extremes are indicated by the whiskers, and the presence of outliers is indicated by (o). (B) Array CGH of NGP of the region of chromosome 12q24.31 in which DIABLO is located (arrow). Both the B allele frequency (top) and the Log R ratio (bottom) are shown. The chromosome region is shown underneath the picture. (C) Immunofluorescence of untreated IMR32 cells. Blue is DAPI, red is mitotracker, green is DIABLO antibody. In the right lower corner the merged pictures are shown. (D) Cell fractionation of SJNB12 cells 24 hours after addition of ABT263. The cytoplasmic fraction (cyto) and organelle fraction (organelle) are shown. Blots were incubated with DIABLO, BCL2 and a-tubulin antibodies. (E) Co-immunoprecipitation of IMR32 (top) and SKNSH (bottom) with BIRC6 and DIABLO antibodies. Negative control was the immunoprecipitation antibody Flag. Also a protein sample without antibody and for every antibody a sample without protein was used as negative control. Both blots were incubated with DIABLO antibody. IP antibodies are indicated above the blots.

copy number gains and increased expression. Silencing of BIRC6 with two shRNAs targeting different parts of the coding sequence resulted in increased cytoplasmic DIABLO levels and triggered apoptosis. BIRC6 indeed interacted with DIABLO proteins. Targeted inhibition of BIRC6 therefore might offer new therapeutic openings in neuroblastoma treatment.

The apoptotic response in neuroblastoma cells upon BIRC6 silencing occurs in a background of surprisingly high DIABLO expression levels. High cytoplasmic levels of DIABLO can be tumor inhibitory through binding of IAPs in the cytoplasm. We suggest two mechanisms why high DIABLO expression does not induce apoptosis in neuroblastoma. Firstly, we show that the major fraction of DIABLO protein has a mitochondrial localization. This mitochondrial sequestration is probably mediated by the exceptionally high levels of BCL2 that we have recently described.[33] Targeted inhibition of BCL2 caused an increase in cytoplasmic DIABLO levels, suggesting that sequestration of DIABLO in the mitochondria occurs by inhibition of pore formation through BCL2. Secondly, we show that DIABLO is effectively bound by BIRC6 in neuroblastoma and that DIABLO levels increase upon silencing of BIRC6. This suggests effective degradation of cytoplasmic DIABLO by BIRC6. The function of high mitochondrial DIABLO levels in neuroblastoma remains elusive. Other pro-apoptotic proteins in the mitochondria, like cytochrome C, have shown to be involved in energy metabolism[44] but no such mechanism has been found for DIABLO yet.

Release of the strongly increased mitochondrial DIABLO levels would offer a therapeutic potential in neuroblastoma. This suggests that the proteins that impair the pro-apoptotic function of DIABLO could be effective drug targets. The previously shown efficacy of targeted BCL2 inhibitions could relate to high DIABLO levels.[33] Moreover, direct BIRC6 inhibition would also increase the cytoplasmic pro-apototic function of DIABLO. BIRC6 inhibitors are not available at this moment but targeted drug development might be worth to consider. BIRC6 is not located on the SRO of 2p, but it is frequently gained and functionally active and we therefore consider BIRC6 as an important player in the dysfunction of apoptosis in neuroblastoma. The BIRC6 gene is validated as a potential therapeutic target. If BIRC6 inhibitors are developed, a combined inhibition of BIRC6 and BCL2 could yield synergistic effects.

Acknowledgements

This research was supported by grants from KIKA foundation, SKK and Netherlands Cancer Foundation.

Reference List

1. Hao, Y.Y., Sekine, K., Kawabata, A., Nakamura, H., Ishioka, T., Ohata, H. et al, Apollon ubiquitinates SMAC and caspase-9, and has an essential cytoprotection function. Nature Cell Biology, 2004; 6**:** 849-860.
2. Qiu, X.B. and Goldberg, A.L., The membrane-associated inhibitor of apoptosis protein, BRUCE/Apollon, antagonizes both the precursor and mature forms of Smac and caspase-9. Journal of Biological Chemistry, 2005; 280**:** 174-182.
3. Buron, N., Porceddu, M., Brabant, M., Desgue, D., Racoeur, C., Lassalle, M. et al, Use of Human Cancer Cell Lines Mitochondria to Explore the Mechanisms of BH3 Peptides and ABT-737-Induced Mitochondrial Membrane Permeabilization. Plos One, 2010; 5.
4. Ceballos-Cancino, G., Espinosa, M., Maldonado, V., and Melendez-Zajgla, J., Regulation of mitochondrial Smac/DIABLO-selective release by survivin. Oncogene, 2007; 26**:** 7569-7575.
5. Yu, J., Wang, P., Ming, L., Wood, M.A., and Zhang, L., SMAC/Diablo mediates the proapoptotic function of PUMA by regulating PUMA-induced mitochondrial events. Oncogene, 2007; 26**:** 4189-4198.
6. Du, C.Y., Fang, M., Li, Y.C., Li, L., and Wang, X.D., Smac, a mitochondrial protein that promotes cytochrome c-dependent caspase activation by eliminating IAP inhibition. Cell, 2000; 102**:** 33-42.
7. Martin, S.J., An Apollon vista of death and destruction. Nature Cell Biology, 2004; 6**:** 804-806.
8. Pohl, C. and Jentsch, S., Final stages of cytokinesis and midbody ring formation are controlled by BRUCE. Cell, 2008; 132**:** 832-845.
9. Sung, K.W., Choi, J., Hwang, Y.K., Lee, S.J., Kim, H.J., Lee, S.H. et al, Overexpression of apollon, an antiapoptotic protein, is associated with poor prognosis in childhood De novo acute myeloid leukemia. Clinical Cancer Research, 2007; 13**:** 5109-5114.
10. Toujani, S., Dessen, P., Ithzar, N., Danglot, G., Richon, C., Vassetzky, Y. et al, High Resolution Genome-Wide Analysis of Chromosomal Alterations in Burkitt's Lymphoma. Plos One, 2009; 4.
11. Van Houdt, W.J., Emmink, B.L., Pham, T.V., Piersma, S.R., Verheem, A., Vries, R.G. et al, Comparative Proteomics of Colon Cancer Stem Cells and Differentiated Tumor Cells Identifies BIRC6 as a Potential Therapeutic Target. Molecular & Cellular Proteomics, 2011; 10.
12. Brodeur, G.M., Neuroblastoma: Biological insights into a clinical enigma. Nature Reviews Cancer, 2003; 3**:** 203-216.
13. Maris, J.M., Hogarty, M.D., Bagatell, R., and Cohn, S.L., Neuroblastoma. Lancet, 2007; 369**:** 2106-2120.
14. Maris, J.M., Medical Progress: Recent Advances in Neuroblastoma. New England Journal of Medicine, 2010; 362**:** 2202-2211.
15. Meyer, N. and Penn, L.Z., MYC - TIMELINE Reflecting on 25 years with MYC. Nature Reviews Cancer, 2008; 8**:** 976-990.
16. Chen, Y.Y., Takita, J., Choi, Y.L., Kato, M., Ohira, M., Sanada, M. et al, Oncogenic mutations of ALK kinase in neuroblastoma. Nature, 2008; 455**:** 971-U56.
17. George, R.E., Sanda, T., Hanna, M., Frohling, S., Luther, W., Zhang, J.M. et al, Activating mutations in ALK provide a therapeutic target in neuroblastoma. Nature, 2008; 455**:** 975-978.
18. Janoueix-Lerosey, I., Lequin, D., Brugieres, L., Ribeiro, A., de Pontual, L., Combaret, V. et al, Somatic and germline activating mutations of the ALK kinase receptor in neuroblastoma. Nature, 2008; 455**:** 967-U51.
19. Janoueix-Lerosey, I., Schleiermacher, G., and Delattre, O., Molecular pathogenesis of peripheral neuroblastic tumors. Oncogene, 2010; 29**:** 1566-1579.
20. Mosse, Y.P., Laudenslager, M., Longo, L., Cole, K.A., Wood, A., Attiyeh, E.F. et al, Identification of ALK as a major familial neuroblastoma predisposition gene. Nature, 2008; 455**:** 930-U22.
21. De Brouwer, S., De Preter, K., Kumps, C., Zabrocki, P., Porcu, M., Westerhout, E.M. et al, Meta-analysis of Neuroblastomas Reveals a Skewed ALK Mutation Spectrum in Tumors with MYCN Amplification. Clinical Cancer Research, 2010; 16**:** 4353-4362.
22. Van Maerken, T., Ferdinande, L., Taildeman, J., Lambertz, I., Yigit, N., Vercruysse, L. et al, Antitumor Activity of the Selective MDM2 Antagonist Nutlin-3 Against Chemoresistant Neuroblastoma With Wild-Type p53. Journal of the National Cancer Institute, 2009; 101**:** 1562-1574.
23. van Noesel, M.M. and Versteeg, R., Pediatric neuroblastomas: genetic and epigenetic 'Danse Macabre'. Gene, 2004; 325**:** 1-15.
24. Adida, C., Berrebi, D., Peuchmaur, M., Reyes-Mugica, M., and Altieri, D.C., Anti-apoptosis gene,

survivin, and prognosis of neuroblastoma. Lancet, 1998; 351**:** 882-883.
25. Islam, A., Kageyama, H., Takada, N., Kawamato, T., Takayasu, H., Isogai, E. et al, High expression of Survivin, mapped to 17q25, is significantly associated with poor prognostic factors and promotes cell survival in human neuroblastoma. Oncogene, 2000; 19**:** 617-623.
26. Lamers, F., van der Ploeg, I., Schild, L., Ebus, M.E., Koster, J., Hansen, B.R. et al, Knockdown of Survivin (BIRC5) causes Apoptosis in Neuroblastoma via Mitotic Catastrophe. Endocrine Related Cancer, 2011; 18**:** 657-668.
27. Giaccone, G., Zatloukal, P., Roubec, J., Floor, K., Musil, J., Kuta, M. et al, Multicenter Phase II Trial of YM155, a Small-Molecule Suppressor of Survivin, in Patients With Advanced, Refractory, Non-Small-Cell Lung Cancer. Journal of Clinical Oncology, 2009; 27**:** 4481-4486.
28. Lamers, F., Schild, L., Koster, J., Versteeg, R., Caron, H., and Molenaar, J., Targeted BIRC5 silencing using YM155 causes cell death in neuroblastoma cells with low ABCB1 expression. Eur J Cancer, 2011; In Press
29. Lewis, K.D., Samlowski, W., Ward, J., Catlett, J., Cranmer, L., Kirkwood, J. et al, A multi-center phase II evaluation of the small molecule survivin suppressor YM155 in patients with unresectable stage III or IV melanoma. Invest New Drugs, 2009.
30. Nakahara, T., Takeuchi, M., Kinoyama, I., Minematsu, T., Shirasuna, K., Matsuhisa, A. et al, YM155, a novel small-molecule survivin suppressant, induces regression of established human hormone-refractory prostate tumor xenografts. Cancer Research, 2007; 67**:** 8014-8021.
31. Satoh, T., Okamoto, I., Miyazaki, M., Morinaga, R., Tsuya, A., Hasegawa, Y. et al, Phase I Study of YM155, a Novel Survivin Suppressant, in Patients with Advanced Solid Tumors. Clinical Cancer Research, 2009; 15**:** 3872-3880.
32. Tolcher, A.W., Mita, A., Lewis, L.D., Garrett, C.R., Till, E., Daud, A.I. et al, Phase I and Pharmacokinetic Study of YM155, a Small-Molecule Inhibitor of Survivin. Journal of Clinical Oncology, 2008; 26**:** 5198-5203.
33. Lamers, F., Schild, L., den Hartog, I.J.M., Ebus, M.E., Westerhout, E.M., Ora I., Koster, J., Versteeg, R., Caron H.N., and Molenaar J.J. Targeted BCL2 inhibition effectively inhibits Neuroblastoma tumor growth. European Journal of Cancer, 2012; In Press
34. Santo E.E., Ebus M.E., Koster J., Schulte J.H., Lakeman A., van Sluis P. et al, Oncogenic activation of FOXR1 by 11q23 intrachromosomal deletion-fusions in neuroblastoma. Oncogene, 2012.
35. Fix, A., Lucchesi, C., Ribeiro, A., Lequin, D., Pierron, G., Schleiermacher, G. et al, Characterization of amplicons in neuroblastoma: High-resolution mapping using DNA microarrays, relationship with outcome, and identification of overexpressed genes. Genes Chromosomes & Cancer, 2008; 47**:** 819-834.
36. Mullenbach, R., Lagoda, P.J.L., and Welter, C., An Efficient Salt-Chloroform Extraction of Dna from Blood and Tissues. Trends in Genetics, 1989; 5**:** 391.
37. Molenaar, J.J., Ebus, M.E., Koster, J., van Sluis, P., van Noesel, C.J.M., Versteeg, R. et al, Cyclin D1 and CDK4 activity contribute to the undifferentiated phenotype in neuroblastoma. Cancer Research, 2008; 68**:** 2599-2609.
38. Ren, J.Y., Shi, M.G., Liu, R.S., Yang, Q.H., Johnson, T., Skarnes, W.C. et al, The Birc6 (Bruce) gene regulates p53 and the mitochondrial pathway of apoptosis and is essential for mouse embryonic development. Proceedings of the National Academy of Sciences of the United States of America, 2005; 102**:** 565-570.
39. Basu, A., Adkins, B., and Basu, C., Down-regulation of caspase-2 by rottlerin via protein kinase c-delta-independent pathway. Cancer Research, 2008; 68**:** 2795-2802.
40. Nutt, L.K., Margolis, S.S., Jensen, M., Herman, C.E., Dunphy, W.G., Rathmell, J.C. et al, Metabolic regulation of oocyte cell death through the CaMKII-mediated phosphorylation of caspase-2. Cell, 2005; 123**:** 89-103.
41. Shen, J., Vakifahmetoglu, H., Stridh, H., Zhivotovsky, B., and Wiman, K.G., PRIMA-1(MET) induces mitochondrial apoptosis through activation of caspase-2. Oncogene, 2008; 27**:** 6571-6580.
42. Wolf, M., Korja, M., Karhu, R., Edgren, H., Kilpinen, S., Ojala, K. et al, Array-based gene expression, CGH and tissue data defines a 12q24 gain in neuroblastic tumors with prognostic implication. BMC Cancer, 2010; 10.
43. Lestini, B.J., Goldsmith, K.C., Fluchel, M.N., Liu, X.Y., Chen, N.L., Goyal, B. et al, Mcl1 downregulation sensitizes neuroblastoma to cytotoxic chemotherapy and small molecule Bcl2-family antagonists. Cancer Biology & Therapy, 2009; 8**:** 1587-1595.
44. Kushnareva, Y. and Newmeyer, D.D., Bioenergetics and cell death. Mitochondrial Research in Translational Medicine, 2010; 1201**:** 50-57.

6

Summary and Discussion

Summary of research

In this thesis we have focused on the systematic validation of potential drug targets in the intrinsic apoptotic pathway in neuroblastoma. For targeted drug development we follow a stepwise procedure. First a potential drug target gene is identified based on genomic and expressional aberrations. Subsequently, the target is validated by silencing and over-expression experiments. Finally, a clinically applicable compound can be tested for in vitro efficacy and in vivo efficacy. Targets and targeted compounds that show consistent results and a favorable phenotype (e.g. apoptosis or growth inhibition) in all these steps can be used for further development towards a Phase I/II clinical trial.

In chapter 2 we showed that *Survivin* (BIRC5) was highly expressed in neuroblastoma, which correlated to a poor prognosis. We functionally validated BIRC5 by targeted silencing using lentiviral shRNA. BIRC5 knockdown induced apoptosis in neuroblastoma cells via mitotic catastrophe, indicating that BIRC5 may indeed be a viable target for therapy.

In chapter 3 we therefore tested the efficacy of YM155, a novel small molecule BIRC5 inhibitor[1-5], which induced apoptosis in a large subset of neuroblastoma cell lines as a result of specific BIRC5 inhibition. However, we also identified a subgroup of cell lines to be resistant to YM155, even though these cell lines were sensitive to lentiviral BIRC5 knockdown. Resistance to YM155 was strongly related to *ABCB1* over-expression. ABCB1 is a protein that functions as a multidrug resistance pump[6-8] and we were able to sensitize resistant cell lines to YM155 by pre-treatment with cyclosporine, a known ABCB1 inhibitor.[7,9]

In chapter 4 we identified a high expression of *BCL2* in neuroblastoma. BCL2 knockdown induced apoptosis in neuroblastoma cells with high *BCL2* expression, but not in neuroblastoma cells without *BCL2* expression or in normal fibroblasts. We validated ABT263, a small molecule BCL2 inhibitor[10-13], which showed the same BCL2-dependent efficacy in neuroblastoma cells compared to BCL2 shRNA. ABT263 was also very effective in our neuroblastoma xenograft model and worked synergistically with doxorubicin, etoposide and vincristin in vitro.

Finally, in chapter 5, we investigated the intrinsic apoptotic genes as a group and concluded that BIRC5, BIRC6 and BCL2 are the most promising drug targets in the

intrinsic apoptotic pathway in neuroblastoma. Since BIRC5 and BCL2 were already validated in the previous chapters, we investigated the potency of BIRC6 as a drug target. *BIRC6* is highly expressed in neuroblastoma and knockdown induced apoptosis. Functional analysis indicated that BIRC6 functions in neuroblastoma cells as an inhibitor of apoptosis protein in the cytoplasm where it can bind and degrade DIABLO. We hypothesized that BIRC6 is a viable target for neuroblastoma therapy especially in combination with ABT263. However, no clinically applicable BIRC6 inhibitor is currently available.

Discussion

Clinical implementation of YM155 in neuroblastoma treatment

Phase I/II clinical trials with YM155 show promising results.[1,2,4,5] Also in vitro and in vivo BIRC5 knock-down experiments and experiments with BIRC5 inhibitors have shown consistent apoptotic responses. The next step is in vivo testing of the efficacy and pharmacokinetics of YM155. Preliminary data showed that this compound is very effective in a neuroblastoma xenograft mouse model and therefore we aim at a Phase I/II clinical trial in pediatric neuroblastoma. A preclinical evaluation of patient selection biomarkers and biomarkers for efficacy is needed.

Almost all high risk neuroblastoma tumors present with gain of 17q and high *BIRC5* levels. Therefore, neither *BIRC5* DNA copy number nor mRNA expression are adequate biomarkers for neuroblastoma patient selection. However, we showed in chapter 3 that ABCB1 can induce resistance to YM155. *ABCB1* could be a biomarker for patient selection if expression can be detected in tumor material before starting YM155 treatment. *ABCB1* detection methods such as qPCR or immunohistochemistry have to be developed and optimized for diagnostics. Because *BIRC5* expression is inhibited by YM155, *BIRC5* mRNA and protein expression are potential biomarkers for efficacy. Therefore multiple tumor biopsies are required during treatment for detection of BIRC5 inhibition. BIRC5 levels could be measured using Western blot or immunohistochemistry on tumor biopsies. Alternatively, analysis in surrogate tissue (hair) could be used to prevent multiple biopsies.

New compounds can be implemented in therapy either as a single compound or in combination with currently used cytostatics if there is rationale for combined treatment. It is therefore necessary to perform in vitro and in vivo combination assays especially with compounds that are used in current treatment protocols. In addition

to the cytostatics that are currently used, new compounds could be tested for synergy. In chapter 2 we have provided evidence for BIRC5 as a microtubule stabilizing protein during cell division, which could guide combinatorial treatment of a BIRC5 inhibitor with other compounds. Most interestingly, preliminary data showed that ABT263 and YM155 combined are synergistic in neuroblastoma cell lines with high BCL2 expression (data not shown). Mitotic catastrophe induced apoptosis by YM155 activates apoptosis by Cytochrome C release from the mitochondria. This can be blocked by high BCL2 levels. It would be of major interest to test this combination in an in vivo assay as well.

We have shown that ABCB1 induced resistance to YM155 in neuroblastoma cells. We were able to resensitize cell lines with high *ABCB1* expression with cyclosporine. However, cyclosporine concentrations needed for this application in patients were toxic in combination treatment, presumably because cyclosporine induced sensitization of the bone marrow to chemo therapy.[7,14] Next-generation ABCB1 inhibitors are currently in clinical trial. PSC833 is a non-immunosuppressant derivative ABCB1 inhibitor with promising in vitro and in vivo results.[15] Clinical trials with PSC833 show mixed results. In patients with Acute Myeloid Leukemia (AML) PSC833 did not improve outcome, however some patients with pediatric acute leukemia showed complete remission or a partial response.[16,17] In vitro testing of this compound in neuroblastoma cells is currently ongoing.

Clinical implementation of ABT263 in neuroblastoma treatment

ABT263, a small molecule BCL2 inhibitor, was also validated as a potential target for intervention in neuroblastoma. Targeted BCL2 inhibition has been investigated in a neuroblastoma model earlier by Lestini et al.[18] They concluded that BCL2 knockdown in neuroblastoma cell lines did not induce apoptosis. Our BCL2 knockdown experiments are in line with their results, as SKNAS was resistant to knockdown or inhibition of BCL2. However, they concluded that this cell line is resistant to BCL2 knockdown, possibly because of a high *MCL1* expression, whereas we concluded that the resistance in SKNAS results from the absence of *BCL2* expression. Our studies show that only two neuroblastoma cell lines have *BCL2* and *MCL1* expression levels comparable to neuroblastoma tumors. Both cell lines were very sensitive to BCL2 shRNA. Therefore we concluded, unlike Lestini et al[18], that BCL2 alone can be a good target for neuroblastoma therapy.

We are currently further validating ABT263 in vivo. We have shown that this com-

pound delays tumor growth, but we also have to demonstrate growth inhibition in more established tumors. In addition, we will verify if the synergy that we detected in vitro between ABT263 and commonly used cytostatics can be confirmed in vivo. Since new compounds in Phase I/II clinical trial will be implemented in relapse patients first, in vivo synergy assays will include cytostatics that are currently used in these patients, such as etoposide, topotecan and temozolomide.

In parallel, we will start collaborations with Abbott to explore the possibilities for a combined Phase I/II clinical trial for ABT263 in neuroblastoma. Since neuroblastoma with low BCL2 expression will probably not respond to treatment with this compound, an assay to predict sensitivity based on BCL2 expression levels has to be optimized for diagnostics. In chapter 4 we showed that BCL2 RNA levels showed a very strong correlation with BCL2 protein expression. This suggests that BCL2 protein levels could be used as a biomarker for patient selection. Goldsmith et al[19] previously published an assay to predict sensitivity of cell lines to AT-101 and ABT-737. BCL2 and NOXA were elevated in ABT263 sensitive cell lines, whereas *MCL1* expression was higher in resistant cell lines.[20] However it is impossible to use this assay in a clinical setting since viable cells are needed. We conclude that BCL2 protein expression analysis has to be optimized as a patient selection biomarker. Patients with low *BCL2* expression levels should be excluded from the ABT263 trial.

BIRC6 as a potential drug target

In chapter 5 we validated BIRC6 as a potential new drug target for neuroblastoma treatment. We observed that knockdown of BIRC6 induced apoptosis and we showed that BIRC6 is functional as an IAP in the cytoplasm in neuroblastoma cells[21,22]. We have shown that neuroblastoma have extensively increased levels of DIABLO in the mitochondria. BIRC6 seems crucial in this specific setting where DIABLO in the cytoplasm has to be degraded very effectively by BIRC6 to prevent an apoptotic response. We hypothesize that cells with high levels of DIABLO are therefore extremely sensitive for BIRC6 inhibition. Targeted inhibition of BIRC6 using an inhibiting compound is therefore a potential new intervention that could specifically affect neuroblastoma cells and not other cells. However, a BIRC6 inhibitor is currently not available. Alternatively BIRC6 could be inhibited using bortezomib, a proteasome inhibitor that may inhibit the DIABLO degradation by BIRC6. This compound can indeed induce apoptosis in neuroblastoma cell lines.[23,24]

Lack of mutations in the intrinsic apoptotic pathway in neuroblastoma

Activating or inactivating mutations in the intrinsic apoptotic pathway are rare in primary neuroblastoma tumors. Recent analysis of 87 primary neuroblastoma in our lab using whole genome sequencing by Complete Genomics[25,26], also revealed an absence of somatic events in the coding sequence of these genes. Therefore we concluded that inhibition of the intrinsic apoptotic pathway results from upstream transcriptional deregulation, epigenetic events and/or copy number alterations as a result of gains or losses of larger chromosomal regions. The latter point is analyzed in chapter 5 using CGH analysis and SNP arrays. Apoptosis does occur in untreated neuroblastoma as is clearly visible on cleaved caspase 3 stainings of neuroblastoma tumors. This is however fully compensated by the extensive tumor growth. We conclude that apoptosis is not completely inactivated in neuroblastoma, but it is rather unbalanced by a combination of events that lead to a change in expression of genes.

The extrinsic apoptotic pathway

This thesis focuses on the intrinsic apoptotic pathway and we validated two clinically available inhibitors as potential drugs in neuroblastoma treatment. However, the extrinsic apoptotic pathway has also been studied in neuroblastoma. *CASP8* is hypermethylated and thereby inactive in some neuroblastoma resulting in an inactive extrinsic apoptotic pathway.[27,28] Also the NF-κB pathway, which has many target genes that are involved in cell death and survival, has been widely investigated.[29-32] Combinations of drugs targeting both the intrinsic and extrinsic apoptotic pathway should be explored, since this may lead to a synergistic effect.

References

1. Giaccone, G., Zatloukal, P., Roubec, J., Floor, K., Musil, J., Kuta, M. et al, Multicenter Phase II Trial of YM155, a Small-Molecule Suppressor of Survivin, in Patients With Advanced, Refractory, Non-Small-Cell Lung Cancer. Journal of Clinical Oncology, 2009; 27: 4481-4486.
2. Lewis, K.D., Samlowski, W., Ward, J., Catlett, J., Cranmer, L., Kirkwood, J. et al, A multi-center phase II evaluation of the small molecule survivin suppressor YM155 in patients with unresectable stage III or IV melanoma. Invest New Drugs, 2009.
3. Nakahara, T., Takeuchi, M., Kinoyama, I., Minematsu, T., Shirasuna, K., Matsuhisa, A. et al, YM155, a novel small-molecule survivin suppressant, induces regression of established human hormone-refractory prostate tumor xenografts. Cancer Research, 2007; 67: 8014-8021.
4. Satoh, T., Okamoto, I., Miyazaki, M., Morinaga, R., Tsuya, A., Hasegawa, Y. et al, Phase I Study of YM155, a Novel Survivin Suppressant, in Patients with Advanced Solid Tumors. Clinical Cancer Research, 2009; 15: 3872-3880.
5. Tolcher, A.W., Mita, A., Lewis, L.D., Garrett, C.R., Till, E., Daud, A.I. et al, Phase I and Pharmacokinetic Study of YM155, a Small-Molecule Inhibitor of Survivin. Journal of Clinical Oncology, 2008; 26: 5198-5203.
6. Evers, R., Kool, M., Smith, A.J., van Deemter, L., de Haas, M., and Borst, P., Inhibitory effect of the reversal agents V-104, GF120918 and pluronic L61 on MDR1 Pgp-, MRP1- and MRP2-mediated transport. British Journal of Cancer, 2000; 83: 366-374.
7. Shen, F., Chu, S., Bence, A.K., Bailey, B., Xue, X., Erickson, P.A. et al, Quantitation of doxorubicin uptake, efflux, and modulation of multidrug resistance (MDR) in MDR human cancer cells. Journal of Pharmacology and Experimental Therapeutics, 2008; 324: 95-102.
8. Smith, A.J., Mayer, U., Schinkel, A.H., and Borst, P., Availability of PSC833, a substrate and inhibitor of P-glycoproteins, in various concentrations of serum. Journal of the National Cancer Institute, 1998; 90: 1161-1166.
9. Glavinas, H., Krajcsi, P., Cserepes, J., and Sarkadi, B., The role of ABC transporters in drug resistance, metabolism and toxicity. Curr.Drug Deliv., 2004; 1: 27-42.
10. Ackler, S., Xiao, Y., Mitten, M.J., Foster, K., Oleksijew, A., Refici, M. et al, ABT-263 and rapamycin act cooperatively to kill lymphoma cells in vitro and in vivo. Molecular Cancer Therapeutics, 2008; 7: 3265-3274.
11. Ackler, S., Mitten, M.J., Foster, K., Oleksijew, A., Refici, M., Tahir, S.K. et al, The Bcl-2 inhibitor ABT-263 enhances the response of multiple chemotherapeutic regimens in hematologic tumors in vivo. Cancer Chemotherapy and Pharmacology, 2010; 66: 869-880.
12. Lin, T.S., New agents in chronic lymphocytic leukemia. Curr.Hematol.Malig.Rep., 2010; 5: 29-34.
13. Lock, R., Carol, H., Houghton, P.J., Morton, C.L., Kolb, E.A., Gorlick, R. et al, Initial testing (stage 1) of the BH3 mimetic ABT-263 by the pediatric preclinical testing program. Pediatric Blood & Cancer, 2008; 50: 1181-1189.
14. Nobili, S., Landini, I., Giglioni, B., and Mini, E., Pharmacological strategies for overcoming multidrug resistance. Current Drug Targets, 2006; 7: 861-879.
15. Emmink, B.L., Van Houdt, W.J., Vries, R.G., Hoogwater, F.J.H., Govaert, K.M., Verheem, A. et al, Differentiated Human Colorectal Cancer Cells Protect Tumor-Initiating Cells From Irinotecan. Gastroenterology, 2011; 141: 269-278.
16. Kolitz, J.E., George, S.L., Marcucci, G., Vij, R., Powell, B.L., Allen, S.L. et al, P-glycoprotein inhibition using valspodar (PSC-833) does not improve outcomes for patients younger than age 60 years with newly diagnosed acute myeloid leukemia: Cancer and Leukemia Group B study 19808. Blood, 2010; 116: 1413-1421.
17. O'Brien, M.M., Lacayo, N.J., Lum, B.L., Kshirsagar, S., Buck, S., Ravindranath, Y. et al, Phase I Study of Valspodar (PSC-833) With Mitoxantrone and Etoposide in Refractory and Relapsed Pediatric Acute Leukemia: A Report From the Children's Oncology Group. Pediatric Blood & Cancer, 2010; 54: 694-702.
18. Lestini, B.J., Goldsmith, K.C., Fluchel, M.N., Liu, X.Y., Chen, N.L., Goyal, B. et al, Mcl1 downregulation sensitizes neuroblastoma to cytotoxic chemotherapy and small molecule Bcl2-family antagonists. Cancer Biology & Therapy, 2009; 8: 1587-1595.
19. Goldsmith, K.C., Lestini, B.J., Gross, M., Ip, L., Bhumbla, A., Zhang, X. et al, BH3 response profiles from neuroblastoma mitochondria predict activity of small molecule Bcl-2 family antagonists. Cell Death and Differentiation, 2010; 17: 872-882.

20. Tahir, S.K., Wass, J., Joseph, M.K., Devanarayan, V., Hessler, P., Zhang, H.C. et al, Identification of Expression Signatures Predictive of Sensitivity to the Bcl-2 Family Member Inhibitor ABT-263 in Small Cell Lung Carcinoma and Leukemia/Lymphoma Cell Lines. Molecular Cancer Therapeutics, 2010; 9: 545-557.
21. Hao, Y.Y., Sekine, K., Kawabata, A., Nakamura, H., Ishioka, T., Ohata, H. et al, Apollon ubiquitinates SMAC and caspase-9, and has an essential cytoprotection function. Nature Cell Biology, 2004; 6: 849-860.
22. Qiu, X.B. and Goldberg, A.L., The membrane-associated inhibitor of apoptosis protein, BRUCE/Apollon, antagonizes both the precursor and mature forms of Smac and caspase-9. Journal of Biological Chemistry, 2005; 280: 174-182.
23. Naumann, I., Kappler, R., von Schweinitz, D., Debatin, K.M., and Fulda, S., Bortezomib Primes Neuroblastoma Cells for TRAIL-Induced Apoptosis by Linking the Death Receptor to the Mitochondrial Pathway. Clinical Cancer Research, 2011; 17: 3204-3218.
24. Pagnan, G., Di Paolo, D., Carosio, R., Pastorino, F., Marimpietri, D., Brignole, C. et al, The Combined Therapeutic Effects of Bortezomib and Fenretinide on Neuroblastoma Cells Involve Endoplasmic Reticulum Stress Response. Clinical Cancer Research, 2009; 15: 1199-1209.
25. Drmanac, R., Sparks, A.B., Callow, M.J., Halpern, A.L., Burns, N.L., Kermani, B.G. et al, Human Genome Sequencing Using Unchained Base Reads on Self-Assembling DNA Nanoarrays. Science, 2010; 327: 78-81.
26. Negrini, S., Gorgoulis, V.G., and Halazonetis, T.D., Genomic instability - an evolving hallmark of cancer. Nature Reviews Molecular Cell Biology, 2010; 11: 220-228.
27. Brodeur, G.M., Neuroblastoma: Biological insights into a clinical enigma. Nature Reviews Cancer, 2003; 3: 203-216.
28. van Noesel, M.M. and Versteeg, R., Pediatric neuroblastomas: genetic and epigenetic 'Danse Macabre'. Gene, 2004; 325: 1-15.
29. Baud, V. and Karin, M., OPINION Is NF-kappa B a good target for cancer therapy? Hopes and pitfalls. Nature Reviews Drug Discovery, 2009; 8: 33-40.
30. Varfolomeev, E., Blankenship, J.W., Wayson, S.M., Fedorova, A.V., Kayagaki, N., Garg, P. et al, IAP antagonists induce autoubiquitination of c-IAPs, NF-kappa B activation, and TNF alpha-dependent apoptosis. Cell, 2007; 131: 669-681.
31. Vince, J.E., Wong, W.W.L., Khan, N., Feltham, R., Chau, D., Ahmed, A.U. et al, IAP antagonists target cIAP1 to induce TNF alpha- dependent apoptosis. Cell, 2007; 131: 682-693.
32. Kasperczyk, H., La Ferla-Bruhl, K., Westhoff, M.A., Behrend, L., Zwacka, R.M., Debatin, K.M. et al, Betulinic acid as new activator of NF-kappa B: molecular mechanisms and implications for cancer therapy. Oncogene, 2005; 24: 6945-6956.

7

Nederlandse samenvatting en dankwoord

Nederlandse samenvatting

Het neuroblastoom

Het neuroblastoom is een zeldzame en zeer agressieve tumor die uitgaat van het sympathische zenuwstelsel bij kleine kinderen. Dat is het zenuwstelsel waar je zelf geen invloed op hebt en het regelt onder andere de hartslag en ademhaling. De tumor zit meestal in de bijnier, een orgaantje dat boven op de nier zit en verantwoordelijk is voor de adrenalineproductie. Ook kan de tumor uitgaan van zenuwbanen die langs de wervelkolom lopen. Vanuit deze plekken kan de tumor uitzaaien naar lymfeknopen, de lever, botten en naar het beenmerg. Per jaar zijn er in Nederland ongeveer 30 tot 40 kinderen waarbij een neuroblastoom wordt vastgesteld. Kinderen met een laag stadium neuroblastoom zijn nog redelijk goed te behandelen. Sommige kinderen genezen zelfs spontaan. Maar helaas blijkt bij veel kinderen dat het om een hoog stadium neuroblastoom gaat, wat betekent dat de kans op overleving slechts 30-40% is. De behandeling van het neuroblastoom bestaat uit een combinatie van radiotherapie, chemotherapie en chirurgie en is hierdoor heel zwaar. Veel mensen kennen de bijwerkingen van chemotherapie. Door al die medicijnen worden patiënten heel misselijk, vermageren en hebben haaruitval. Ook wordt het afweersysteem aangetast, waardoor patiënten ernstig ziek kunnen worden van een simpele infectie. Hierdoor moet de behandeling met chemotherapie soms zelfs gestaakt worden. Mensen die als kind behandeld zijn voor kanker krijgen ook vaak last van lange termijn-bijwerkingen. De medicijnen hebben niet alleen tumorcellen kapot gemaakt, maar ook gezonde cellen. Er kan bijvoorbeeld permanente schade ontstaan aan het hart, de nieren, de lever en de longen. Ook is de kans om weer opnieuw kanker te krijgen groter.
Omdat er nog veel kinderen aan het neuroblastoom overlijden en omdat de huidige medicijnen veel bijwerkingen hebben, is het belangrijk om nieuwe therapeutische mogelijkheden te ontwikkelen die specifieker zijn, en daardoor effectiever zijn met minder bijwerkingen. Dat is wat we met dit onderzoek hebben gedaan.

Apoptose

Apoptose is geprogrammeerde celdood. Alle cellen in je lichaam zijn in staat zichzelf of de naastliggende cellen dood te maken, zodra er bijvoorbeeld een fout in het DNA (het erfelijke materiaal) wordt gedetecteerd. Normaalgesproken is er een balans tussen cellen die zich vermenigvuldigen en cellen die doodgaan. Cellen vermenigvuldi-

gen zich door in tweeën te delen. Hierbij wordt al het DNA gekopieerd. Elke keer dat een cel deelt, is er een kans dat er een fout optreedt bij het kopiëren van het DNA. Normaalgesproken is dit geen probleem, omdat deze cellen met een 'foute' kopie weer worden opgeruimd. Maar als de fout in het DNA ervoor zorgt dat de cel niet meer dood kan gaan, is er wel een probleem. De cel groeit ongecontroleerd door en er ontstaat een tumor. Voor dit onderzoek hebben we gekeken naar alle genen (stukjes DNA) die apoptose kunnen remmen of activeren in neuroblastomen. Dit hebben we vergeleken met dezelfde genen in normale cellen. Het bleek dat sommige genen die de apoptose remmen versterkt aanwezig waren in de tumor. Dit zou kunnen verklaren dat de tumorcellen niet dood gaan. De volgende stap was te onderzoeken of de theorie klopt dat deze genen (genaamd: BIRC5 en BCL2) ervoor zorgen dat de tumorcellen niet in apoptose gaan.

BIRC5-remmer als nieuwe therapie

Op het lab kunnen we neuroblastoomcellen op plastic schaaltjes groeien. We hebben 24 verschillende cellijnen; elke cellijn is oorspronkelijk afkomstig van één tumor. Er zijn technieken beschikbaar waarbij je individuele genen specifiek kunt uitschakelen. Als je dat met BIRC5 zou doen verwacht je dat de apoptose wordt geactiveerd. In hoofdstuk 2 hebben we gevonden dat het uitschakelen van BIRC5 er inderdaad voor zorgt dat neuroblastoomcellen in apoptose gaan. BIRC5 heeft twee verschillende functies in de cel en we hebben onderzocht welke van de twee functies van groter belang is. Het bleek dat BIRC5 vooral een belangrijke rol heeft tijdens de celcyclus. Vlak voordat de cel bij het delen in tweeën splitst, moet het gekopieerde DNA eerst netjes verdeeld worden tussen de twee toekomstige 'dochter' cellen. BIRC5 zorgt voor deze verdeling en als je BIRC5 remt, wordt het DNA niet goed verdeeld, en zullen de twee dochtercellen om die reden in apoptose gaan.

De technieken die we op het lab gebruiken zijn echter niet bij patiënten te gebruiken. Een volgende stap is dus op zoek te gaan naar een bestaand medicijn dat deze genen (of de producten daarvan) kan remmen. We hebben dan de voorkeur voor medicijnen die al iets langer op de markt zijn, zodat er al wat meer bekend is over de bijwerkingen en omdat het dan zekerder is dat het medicijn beschikbaar zal blijven. BIRC5 kan geremd worden door YM155, een medicijn dat al veelbelovende resultaten heeft opgeleverd bij volwassenen met kanker. In hoofdstuk 3 hebben we YM155 getest op neuroblastoomcellen en het bleek dat de meeste cellijnen in apoptose gingen, maar sommige cellijnen niet. Het bleek dat sommige cellijnen

een soort pompje hadden dat YM155 uit de cel kan pompen, waardoor het zijn werk niet kan doen. Deze neuroblastoomcellen waren dus resistent tegen YM155. Als we het pompje eerst uitschakelden, waren de cellen wel weer gevoelig voor YM155. Dit is belangrijk om te weten, want als dit medicijn bij kinderen gebruikt gaat worden, moet in de tumor van die kinderen eerst getest worden of die pomp aanwezig is. Als dit het geval is, is YM155 geen geschikt medicijn voor behandeling. Bij kinderen met een neuroblastoom kan de pomp niet worden uitgeschakeld, omdat het middel dat de pomp uitschakelt bij de voor kinderen benodigde concentratie giftig is voor mensen. Inmiddels hebben we dit medicijn ook getest in muizen met een neuroblastoom 'zonder pomp', waaruit bleek dat het hiertegen heel effectief was.

BCL2-remmer als nieuwe therapie

Net zoals voor BIRC5, laten we in hoofdstuk 4 zien dat het uitschakelen van BCL2 ook apoptose veroorzaakt. Het bleek dat hoe meer BCL2 aanwezig was in de cellen, hoe makkelijker ze in apoptose gingen na het uitschakelen van BCL2. Cellen die helemaal geen BCL2 hadden, bleven gewoon doorgroeien. Omdat neuroblastomen extreem veel BCL2 hebben, terwijl normale cellen bijna geen BCL2 hebben, verwachten we dat een BCL2 remmer een hele specifieke therapie zal zijn.

ABT263 is een medicijn dat BCL2 kan remmen. Ook deze heeft al veelbelovende resultaten gegeven bij volwassenen met kanker. In neuroblastoomcellen bleek het ook zeer effectief te zijn, zoals in hoofdstuk 4 staat beschreven. Net zoals met de 'specifieke uitschakelmethode' die we al eerder hadden gebruikt, bleek ABT263 effectiever te zijn in cellen die meer BCL2 hadden dan in cellen met weinig BCL2. Gewone cellen hebben vrijwel geen BCL2 en hadden zelfs helemaal geen last van het medicijn. Ook in muizen met een neuroblastoom bleek ABT263 een antitumor-effect te hebben. Omdat kinderen met kanker nooit behandeld worden met één medicijn, maar altijd met een combinatie, is het belangrijk te weten hoe een nieuw medicijn werkt in combinatie met de huidige chemotherapeutica. Het bleek dat ABT263 het antitumor-effect van deze chemotherapeutica meer versterkte dan verwacht. Dit betekent dat je van beide medicijnen dan minder nodig hebt voor hetzelfde effect en dit maakt ABT263 een extra goede kandidaat om klinisch te testen.

Klinisch onderzoek

De volgende stap voor zowel YM155 als ABT263 is om het bij kinderen met een

neuroblastoom te gaan testen. In eerste instantie zal dit bij kinderen worden gedaan die voor de tweede keer een neuroblastoom krijgen en waarbij de huidige therapie blijkbaar niet werkt. Als hier goede resultaten uit komen, zullen ook kinderen die nieuw gediagnosticeerd zijn met een neuroblastoom hiermee behandeld worden. Voor YM155 is het dan van belang dat de tumor getest wordt op de aanwezigheid van de pomp. Alleen kinderen met een tumor waarvan de cellen geen pomp hebben kunnen behandeld worden met YM155. Voor ABT263 is het belangrijk dat de tumor getest wordt op de hoeveelheid BCL2. Alleen kinderen met een tumor met veel BCL2 komen in aanmerking voor behandeling met ABT263.

Dankwoord

Dit alles was hartstikke veel werk en het zou me nooit zijn gelukt als er niet zo veel geweldige mensen waren die me hierbij hebben geholpen. Sommigen door middel van advies en door alle onderzoekslijnen en experimenten te bediscussiëren, sommigen door praktische hulp op het lab. Sommigen gaven mentale steun of zorgden voor afleiding, zodat ik later weer kon focussen. Deze mensen zou ik graag willen bedanken.

Er was één persoon die me van al het bovengenoemde voorzag: **Linda**, ik heb er bewondering voor dat je 10 experimenten tegelijk kunt inzetten, ondertussen de volgende experimenten kunt bespreken of gewoon gezellig kunt kletsen, ook om 8 uur 's morgens nadat je al 2 uur reistijd achter de rug hebt. Je bent een schat en wat was het leuk om met je te werken. Bedankt voor de bergen werk die je verzet hebt, bedankt voor je steun, bedankt voor je vriendschap! En **Wilco** ook bedankt natuurlijk, zonder jou zou zelfs een duizendpoot als Linda zo'n druk leven niet trekken!

Jan, je had vanaf het begin het vertrouwen dat ik dit zou kunnen, ondanks mijn minimale (of afwezige) biologische achtergrond. Gelukkig kan je goed uitleggen en heb je geduld als het nodig is, waardoor ik deze achterstand kon inhalen. Maar je kunt ook spijkers met koppen slaan, zodat het onderzoek een beetje opschiet. En je kunt ook heel hard rennen: op het lab, als je praat, maar je bent pas echt niet bij te houden als je een marathon loopt! Gelukkig heb ik je toch nog heel even in gouden legging mogen bewonderen, werkelijk beeldig. Jan, bedankt voor de begeleiding, het vertrouwen en de gezelligheid.

In het rijtje 'snel' mag **Huib** natuurlijk niet ontbreken, want hij is de definitie van snel. Huib, die snelheid en kordaatheid spreekt me heel erg aan, en het was één van de vele redenen waarom ik het zo prettig vond met je samen te werken. Na een bespreking met jou, leek de wetenschap ineens niet meer zo vreselijk moeilijk. Huib je bent bijzonder, omdat je het belang van anderen zo hoog hebt staan. Ik hoop er snel getuige van te mogen zijn hoe je met het NKOC 95% van de kinderen met kanker gaat genezen.

Bij **Rogier** staan nauwkeurigheid en degelijkheid hoog in het vaandel en dat zie je terug in zijn onderzoek en begeleiding. Rogier, ik ben blij dat je mij dit ook (zoveel mogelijk) hebt bijgebracht en dat je me de kans hebt gegeven me te verdiepen in

de biologische wetenschap. Ik heb veel plezier beleefd aan onze discussies en had altijd het idee, een stukje wijzer uit je kamer weg te lopen dan dat ik binnen kwam.

Marli heeft me in het begin een spoedcursus pipetteren gegeven en zo de fijne kneepjes van het vak geleerd. Dat was behalve leerzaam ook heel leuk en gezellig! Marli, je bent altijd opgewekt, spraakzaam, lekker nuchter en je hebt een goed gevoel voor humor. Daardoor ben je een hele fijne collega. En omdat je m'n chocoladeverslaving begrijpt en omdat je lief bent voor Flip natuurlijk...

Ida, ik heb in het eerste jaar met heel veel plezier met je samen gewerkt. Het was leuk om met jou de trukendoos samen te stellen die we nodig hadden voor al het geplande onderzoek. Na een jaar verhuisde je naar Curacao. Hoewel dat officieel in Noord-Holland ligt, werd de reistijd toch wat lang, dus waren we je helaas even kwijt. Gelukkig ben je weer terug en is team-Jan met jouw aanwezigheid verrijkt. En het marathon team! Hartelijk bedankt ook, dat je paranimf wilt zijn!

Dan de nieuwe aanwinsten in team-Jan: Het nieuwe muis-model begon pas echt soepeltjes te lopen toen **Ilona** erbij kwam. Met jouw ervaring en sluitende administratie kwam er orde in de chaos. **Emmy**, je bent een hele leuke collega door je spontaniteit en enthousiasme. En omdat je energie nooit opraakt bij het dansen of tafelvoetballen. **Thomas**: eindelijk een man bij de groep! Het kippenhok van Jan, kan wel een nuchtere gebruiken zoals jij. Heel erg veel succes met je promotie, ik weet zeker dat je het goed zult doen, de start belooft veel goeds.

Jens, Ellen en **Mohamed**. Het duurde niet lang voordat kamergenoten vrienden werden. Samen barbecueën, sporten, feesten en slap (of heel zinnig) ouwehoeren. Jens, we missen je heel erg, nu je in het verre Australië woont. Des te leuker was het om jou en Antony te bezoeken tijdens onze vakantie. Mohamed, je bent enerzijds een oase van rust en geduld, en anderzijds verraste je me altijd met je grappen. Ellen, je hebt me naar de marathon toe gesleept tijdens de doordeweekse trainingen. En bedankt dat je als ware kloneerkoningin me uit m'n lijden hebt verlost met dat kloneergeklungel.

Ja, kloneren was niet m'n sterkste kant. **Arjan** en **Linda V**, jullie hebben me ook enorm geholpen, want zonder jullie hulp zat ik nog steeds op dat survivin construct te knutselen! **Johan**, jij weet altijd de vinger op de zere plek van m'n onderzoek te leggen. Ik ben blij dat je dat ook deed, want het heeft me ervoor behoed om af en

toe te kort door de bocht te gaan.

Gitta, Saskia, Janine en **Lieve** zorgen ervoor, dat op een biologisch lab het klinisch belang in beeld blijft. Hierdoor is er een evenwicht tussen fundamentele wetenschap en klinische toepassing, waar volgens mij iedereen baat bij heeft. Gitta en Sas, het was supergezellig met jullie op congres en inderdaad: de co-schappen zijn hartstikke leuk! Bedankt voor jullie hulp bij de (mentale) voorbereiding hierop. Janine: dat hebben we toch maar leuk bedacht dat speeddate spel! Lieve, het was leuk brainstormen over hoe we fundamenteel onderzoek zouden kunnen toepassen in de kliniek.

Waar zouden we zijn zonder **Peter**. Peter, je houdt het lab draaiende en je bent daarmee onmisbaar. Dat is geen gemakkelijke taak met zoveel mensen op zo'n klein oppervlak. Behalve belangrijke praktische dingen regel je ook de nog belangrijkere borrels en feestjes en de aanwezigheid van de allerbelangrijkste paaldans-paal!

In de categorie 'onmisbaar' mag **JanK** natuurlijk niet ontbreken. Jan, je weet niet alleen alles van computers en van statistiek, je weet het ook nog te combineren én uit te leggen. En dan ben je ook nog eens heel aardig en gezellig! Net als **Danny, Piet**, en **Richard**. Ik ga jullie allemaal wel een beetje missen. JanK omdat niemand zo vrolijk 'Fiekeeeeee!' kan roepen, Piet, vanwege je aanstekelijke lach en Danny, vanwege de gezellige meligheid tijdens de borrels. En Richard, jij blinkt uit met je ultiem (wel of niet bedoeld) lompe en daarmee hilarische opmerkingen. Helaas voor jou, gelukkig voor ons, krijg je soms (of eigenlijk best vaak) de hark (meestal onbedoeld) zelf tegen je kop. Gelukkig voor jou en gelukkig voor ons, kwam **Marloes** erbij, een ogenschijnlijk stille hoek waar vanuit zomaar ineens met tomaten gegooid kan worden.

En met **Timmetje** is het altijd lachen! Leuk om met jou een beetje herrie te schoppen op het lab, tijdens het labweekend of op Texel. En je tegenpool, **Peter** Stroeken, weet met z'n onverbeterlijke nuchterheid alles in perspectief te zetten. **Nurdan, Franciska, Nancy** en **Jennemiek**, met jullie was het altijd gezellig (dijen)kletsend te lunchen. En te dansen! Ik zal tijdens m'n co-schappen af en toe ontsnappen om nog eens te komen buurten. Als jullie me tenminste niet uitlachen vanwege m'n jas. **Bart**, jij haalde de stamcellen erbij, mogelijk de toekomst van het begrijpen (en behandelen?) van het neuroblastoom. Gelukkig krijg je daarbij hulp van Inge, met wie het altijd leuk kletsen is over paarden.

Also **Evan, Natalia, Laurel, Maria** and **Ksenia** are a real pleasure to have on the lab. Evan, you are one of the best persons to ask for critical feedback or interesting new theories. Natalia: we had such a fantastic idea together, too bad we couldn't prove it, but it has been a pleasure anyway. Laurel and Maria, I love giggling with you guys, I'll miss that! Ksenia, quiet and friendly, it is good to have you on the lab.

Monique en **Antoinet**, jullie hebben me ondersteund met praktische zaken zoals de ogenschijnlijk onoverkomelijke baal papierwerk die nodig is voor de totstandkoming van een promotie. Als ik bij jullie langskwam werd alles overzichtelijk en was er meteen gelegenheid voor een gezellige babbel.

Sommige collega's zijn in de loop van de tijd verhuisd en/of van baan gewisseld. Sommigen gingen ver weg, anderen bleven in de buurt. Voor ons een groot gemis, maar gelukkig zijn ze allemaal op een goede nieuwe plek gekomen. **Mireille**, je was één van de belangrijkste gangmakers van het lab. Gelukkig komen we elkaar zo nu en dan nog eens tegen op een borrel of spelletjesavond. **Lilith**, I am happy that you still live and work in Amsterdam, so we can still run into each other and give each other an update of life. **Marcel**, behalve je kritische vragen tijdens de werkbespreking, mis ik ook iemand die me leuke restaurantjes in het Oostelijk Havengebied kan adviseren. **Alvin** en **Gerben**, wat jammer dat jullie weg gingen! Graag hoor ik een keer wat nou de minst lelijke plek van Rotterdam is. **Dirk**, de man die antwoord heeft op al je vragen (echt AL je vragen), jij zet je nog altijd in voor kinderen met kanker, dus wij komen elkaar over een paar jaar in Utrecht wel weer tegen. **Hinco** en **Arjen** zijn al een tijdje weg. Ik heb niet alleen leuke herinneringen aan jullie als collega's, ik heb ook tijdens jullie promotie een beetje kunnen zien hoe het moet.

Ik heb ook hulp gehad van mensen van andere afdelingen en ziekenhuizen. **André, René** en **Odette**, het was leuk met jullie samenwerken. Bedankt voor al jullie advies met betrekking tot synergie assays en mitochondriën. **Kees**, de man die alles over muizen weet, en **Berend**, de man die alles over FACSen weet, jullie hebben me vaak geholpen en geadviseerd. Ook bij 'acute nood' stonden jullie klaar, en hebben daarmee menig experiment van de ondergang gered. En als jullie denken, goh wat is dit een mooi boekje! Het is ontworpen door **Eelco**. Hartelijk bedankt voor de layout. Ik ben heel blij met hoe het geworden is. **Ingrid Øra**, first you were a very nice collegue in our lab, later a very nice collegue in Sweden, who always takes the time to give some advice. It has been a good collaboration, I very much appreciated that.

I would also like to thank our collegues from TI Pharma, especially **Roger, Erno** and **Carla** for your collaboration and advice.

En waar zou ik zijn zonder mijn vrienden. Sommigen van hen zou ik in het bijzonder willen bedanken, voor hun steun en interesse.
'de 8': **Claudia, Laura, Heleen, Marloes, Wieteke, Saskia** en **Netta**, jullie zijn er al vanaf de middelbare school (of zelfs de basisschool) voor mij geweest. Ik ben dankbaar voor de talloze leuke herinneringen die we al hebben en nog zullen krijgen. **Caroline** en **Jouke**, bedankt voor jullie luisterend oor, en dat weekendje weg is voor herhaling vatbaar! **Frans**, bedankt voor 'het vlot' en alles wat daarna kwam. **Esther**, bedankt voor alle goede gesprekken tijdens de Voorschotense bos-, duin-, en strandwandelingen!

En tot slot wil ik mijn familie bedanken:
Eva en **Claus**, bedankt dat jullie altijd zoveel interesse hebben getoond en hebben meegeleefd.

Lieve **pap** en **mam**, jullie zijn er altijd voor mij geweest, door jullie durf ik ergens op af te stappen en dingen te ondernemen. Door jullie ben ik een optimist en is het leven voor mij een feest. Jullie hebben me opgevoed en gevormd op een manier die ik me niet beter heb kunnen wensen.

László, lieve schat, met jou is elke tegenslag overkomelijk en elke overwinning een dubbel zo groot feest. Bedankt dat je bij me bent.